Technische Universität München

WACKER-Lehrstuhl für Makromolekulare Chemie

New Methods for the Surface Functionalization of Photoluminescent Silicon Nanocrystals

Ignaz Malvin Dominik Höhlein

Vollständiger Abdruck der von der Fakultät für Chemie der Technischen Universität München zur Erlangung des akademischen Grades eines

Doktors der Naturwissenschaften

genehmigten Dissertation.

Vorsitzender:	Univ.-Prof. Dr.-Ing Kai-Olaf Hinrichsen
Prüfer der Dissertation	1. Univ.-Prof. Dr. Dr. h.c. Bernhard Rieger
	2. Univ.-Prof. Dr. Tom Nilges
	3. Univ.-Prof. Dr. Fritz E. Kühn (mündliche Prüfung)
	Prof. Jonathan Veinot, PhD, University of Alberta, Edmonton, Kanada (schriftliche Beurteilung)

Die Dissertation wurde am 22.04.2015 bei der Technischen Universität München eingereicht und durch die Fakultät für Chemie am 01.06.2015 angenommen.

Danksagung

Mein besonderer Dank gilt *Prof. Dr. Dr. h.c. Bernhard Rieger* für die Aufnahme an seinem Lehrstuhl und die interessante Themenstellung. Seinen Führungsstil des eigenverantwortlichen Arbeitens, verbunden mit richtungsweisenden Ratschlägen zum passenden Zeitpunkt, habe ich sehr schätzen gelernt.

Prof. Dr. Jonathan G. C. Veinot danke ich für seine fachliche Unterstützung und die herzliche Aufnahme in seinen Arbeitskreis während meiner Aufenthalte an der University of Alberta, Edmonton, Kanada.

Bedanken möchte ich mich bei *Dr. Carsten Troll* für seinen unermüdlichen Einsatz, um am Lehrstuhl die besten Arbeitsbedingungen zu schaffen.

Mein Dank gilt allen Mitgliedern des WACKER-Lehrstuhls für Makromolekulare Chemie. Insbesondere danke ich *Arzu Angı*, die während ihrer Zeit als Masterandin hervorragende Arbeit geleistet hat. In Erinnerung bleiben meine Kollegen *Benedikt Soller*, *Patrick Werz* und *Peter Altenbuchner* für die nie langweiligen Stunden im Labor. *Tobias Helbich* und *Julian Kehrle* danke ich für die vielen wertvollen Diskussionen.

Dem gesamten Arbeitskreis von Prof. Veinot danke ich für die Unterstützung und die freundliche Aufnahme bei meinen Forschungsaufenthalten.

Dem *Verband der Chemischen Industrie e. V.* (VCI), der meine Promotion großzügig über das Chemifonds-Stipendium unterstützt hat, bin ich sehr verbunden.

Besonderer Dank gilt meinen Eltern *Angelika* und *Prof. Dr. Günter Höhlein* sowie meinen Schwestern *Anna Maria* und *Luzia* für ihre fortwährende Unterstützung während meines Studiums und meiner Promotion.

Contents

1 Introduction 1

2 Applications of Photoluminescent Silicon Nanocrystals 3

2.1 Sensors 3

2.2 Solar Cells 4

2.3 Light Emitting Diodes 6

2.4 Photoluminescent Biological Markers 7

3 Theoretical Background 9

3.1 Properties of Photoluminescent Silicon Nanocrystals 9

3.2 Synthesis of Photoluminescent Silicon Nanocyrstals 10

3.2.1 Top-Down Approaches 11

3.2.2 Bottom-Up Approaches 11

3.3 Surface Functionalization of Photoluminescent Silicon Nanocrystals 16

3.3.1 Hydrosilylation Reaction 17

3.3.2 Reactions of Halogen Terminated SiNCs 20

3.3.3 Multi-Step Functionalization 20

4 Aim of This Work 22

5 Diazonium Salts as Grafting Agents and Efficient Radical-Hydrosilylation Initiators for Freestanding Photoluminescent Silicon Nanocrystals 23

6 Photoluminescent Silicon Nanocrystals with Chlorosilane Surfaces – Synthesis and Reactivity 39

7 Functionalization of Hydride-Terminated Photoluminescent Silicon Nanocrystals with Organolithium Reagents 53

8 Photoluminescent Silicon Nanocrystal-Polymer Hybrid Materials *via* Surface Initiated Reversible Addition-Fragmentation Chain Transfer (RAFT) Polymerization 68

9 Summary and Outlook 77

10 Publications beyond the Scope of this Thesis 80

10.1 Thermoresponsive and Photoluminescent Hybrid Silicon Nanoparticles by Surface-Initiated Group Transfer Polymerization of Diethyl Vinylphosphonate 81

10.2 Activation of silicon surfaces for H_2 evolution by electrografting of pyridine molecules 82

10.3 Catalytic C–F activation via cationic group IV metallocenes 83

10.4 A Robust Route towards Functionalized Pyrrolizidines as Precursors for *Daphniphyllum* Alkaloids 84

Bibliography 85

Table of Abbreviations

ATRP	atom transfer radical polymerization
4-BDB	4-bromobenzene diazonium tetrafluoroborate
2,6-Br-4DDB	2,6-dibromo-4-decyl-diazobenzene tetrafluoroborate
CB	conduction band
ClDMVS	chlorodimethyl(vinyl)silane
c-Si	crystalline silicon
d	days
d	diameter
DCC	N,N'-dicyclohexylcarbodiimide
4-DDB	4-decylbenzene diazonium tetrafluoroborate
DLS	dynamic light scattering
DMAP	4-dimethylaminopyridine
DMPA	2,2-dimethoxy-2-phenylacetophenone
DMF	dimethylformamide
DNA	deoxyribonucleic acid
DNT	dinitrotoluene
DOX	doxorubicin
EA	elemental analysis
EDX	energy-dispersive X-ray spectroscopy
EQE	external quantum efficiency
eq	equivalents
ESI	electrospray ionization
ESI	electronical supporting information
ETFE	ethylene tetrafluoroethylene
eV	electron volt
FTIR	fourier transform infrared
GPC	gel permeation chromatography

HAC	hexyl acrylate
HR-TEM	high-resolution transmission electron microscopy
HSQ	hydrogen silsesquioxane
IR	infrared
LED	light emitting diode
M	molar mass
M_n	number average molecular weight
M_w	weight average molecular weight
MALS	multiangle light scattering
mCPBA	*meta*-chloroperoxybenzoic acid
Me	methyl
MEG	multiple exciton generation
MMA	methyl methacrylate
MS	mass spectrometry
n-BuLi	n-butyllithium
4-NDB	4-nitrobenzene diazonium tetrafluoroborate
NIPAM	N-isopropylacrylamide
nm	nanometer
NMP	nitroxide mediated radical polymerization
NMR	nuclear magnetic resonance
2-NO_2-4-DDB	2-nitro-4-decyl-diazobenzene tetrafluoroborate
P3HT	poly(3-hexylthiophene)
%PD	normalized polydispersity
PDI	polydisperisity index
PETN	pentaerythritol tetranitrate
Ph	phenyl
PL	photoluminescence
PMAA	poly(methacrylic acid)
pSi	porous silicon
ppm	parts per million
QD	quantum dot

RAFT	reversible addition-fragmentation chain transfer
RDX	1,3,5-trinitroperhydro-1,3,5-triazine
SiNC	silicon nanocrystal
TEM	transmission electron microscope
TGA	thermogravimetric analysis
THF	tetrahydrofuran
TMS	trimethylsilyl
TNT	trinitrotoluene
TOAB	tetraoctylammonium bromide
UV	ultraviolet
VB	valence band
4-VBCl	4-vinylbenzyl chloride
VTMS	vinyltrimethylsilane
wt%	weight percent
XPS	X-ray photoelectron spectroscopy

1 Introduction

Nanotechnology covers the synthesis and manipulation of matter with the dimension of 1 to 100 nanometers. In this range, the properties of a material are not only determined by its composition but also by its size. This behavior is observed due to the increasingly large surface to volume ratio and by quantum mechanical effects that arise. Nanotechnology therefore offers access to materials with unprecedented properties and it is believed to be a key technology for the technological progress in the 21st century. Already nanotechnology products have possessed a global market value of $26 billion in 2014 and it is expected to reach $64 billion in 2019.[1]

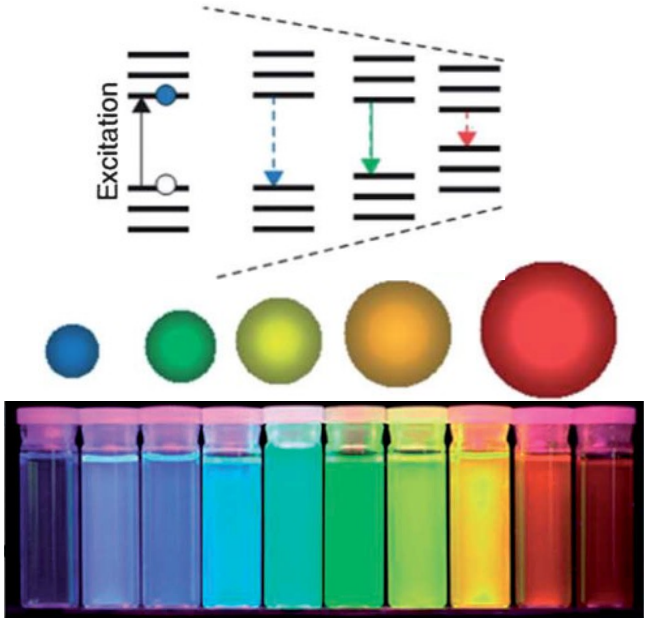

Figure 1.1: Top: Schematic drawing representing the changes in optical behavior of qantum dots depending on their size. Bottom: Quantum dots with varying sizes under UV radiation showing photoluminescence.[2]

A class of nanomaterials that has gained significant interest are semiconductor nanoparticles in the size range of a few nanometers, also called quantum dots (QD). In a QD, excitons (electron-hole pairs) are confined in all three spatial dimensions. This results in splitting of the

continuous energy-band structure, which is found in bulk-semiconductors, into discrete energy levels. As a result the band gap varies with the QD dimensions, increasing with declining particle sizes. The behavior offers the possibility to control the absorption and emission spectrum just by varying the size of the particles and quantum dots spanning the visible to the near-IR range of the electromagnetic spectrum have been synthesized (Figure 1.1). Extensive reports exist concerning compound semiconductor QDs like CdSe, InP and GaAs.[3] This is mainly due to their simple synthesis from solution precursors that yield particles in high purities, with narrow size distributions and therefore defined properties. A great variety of applications have been realized based on QDs including single electron transistors, light-emitting diodes, solar cells, liquid crystals and fluorescent labeling.[4–8] Recently also TV-displays with CdSe quantum dots as light emitting elements have hit the mass consumer market.[9] Many of these materials are made of comparably expensive precursors and contain toxic heavy metals such as lead and cadmium, therefore possessing a potential health hazard.

Silicon is a non-toxic semiconductor which is found abundantly in the form of SiO_2 on earth. Also it is extensively used in the microelectronic industry for decades, its properties are well investigated and it can be obtained in highest purities. Therefore silicon is a highly desirable material as basis of quantum dots. During the last decade, great efforts have been made towards synthesis and application of freestanding silicon nanocrystals (SiNCs).[10, 11] However, challenges remain to be solved concerning stability, processability, large scale synthesis and electronic as well as optical properties of SiNCs to be on even footing with the established compound quantum dots.

2 Applications of Photoluminescent Silicon Nanocrystals

Silicon nanocrystals have been tested for a great variety of applications including light emitting diodes,[12] batteries,[13] photovoltaics,[14] thermoelectrics,[15] sensoring materials[16] and biorelated applications.[17] Since this work focuses on photoluminescent SiNCs, only applications relying on quantum confined SiNCs will be discussed in this chapter.

2.1 Sensors

Due to their outstanding photoluminescence properties, compound quantum dots were intensively investigated as photoluminescent sensoring materials for metal ions, gases and organic molecules.[18,19] However, reports of SiNCs for this application are scarce in literature.

Veinot *et al.* reported that freestanding photoluminescent SiNCs can be applied for the detection of high-energy compounds bearing nitro-groups such as trinitrotoluene (TNT) and dinitrotoluene (DNT).[16] Regular filter paper was dip coated in a dispersion of SiNCs and followingly treated with solutions or solid residue of the respective nitrocompound, resulting in a photoluminescence (PL) quenching. Detection limits for DNT were found to be as low as 0.341 mM in solution or 18 ng of solid DNT. The quenching mechanism is suggested to occur *via* an electron transfer from the SiNCs to the nitro compounds.[16,20]

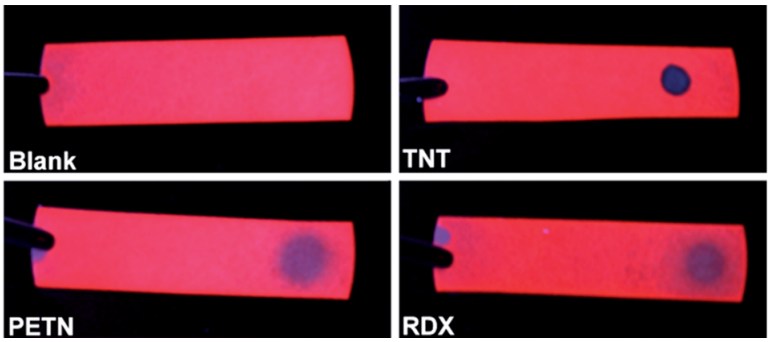

Figure 2.1: SiNC coated paper under UV radiation. Solutions of commonly used explosives induce a quenching of the PL.[16]

Chen *et al.* presented an approach to sense dopamine with water soluble SiNCs.[21] The detection limit was found to be as low as 0.3 nM which is below common physiological concentrations for dopamine (26-40 nM).[22] The PL quenching was found to occur with satisfying selectivity compared to other molecules commonly found in cells such as aminoacids and sugars. Förster resonance energy transfer was suggested as mechanism for the observed quenching.

2.2 Solar Cells

Current commercial production of solar cells almost entirely relies on silicon. Solar cells based on single- and polycrystalline silicon make up around 80 % and thin film solar cells from amorphous silicon around 20 % of the installed panels.[23] Photovoltaic cells of single crystal silicon show the best efficiencies (14 %) of commercially available solar cells, but they are comparably expensive in production. Development of low-cost and efficient designs therefore is an essential target.

The simplest setup for silicon based solar cells consists of a *n*-doped (electron conducting) and a *p*-doped (hole conducting) silicon layer (Figure 2.2 A). The layers stand in direct contact with each forming a *p*-*n* junction and are connected *via* an outer electrical circuit. Electrons leave the *n*-type region leaving behind positively charged donor ions. In the same way, holes diffuse into the *n*-type region creating negatively charged acceptor ions *p*-type region. This process continues until an equilibrium is reached establishing a potential difference across the junction, the built-in potential. If photons are absorbed by the photoelectric cell with energies higher than the band gap of the semiconductor, electron–hole pairs are generated. Electrons generated in the *p*-layer near the *p*-*n* junction are carried into the *n*-region by the built-in potential at the junction. Similarly, excess holes are transferred to the *p*-layer. The potential between the *p*- and *n*-layer decreases and a voltage appears in the external circuit. If the circuit is closed, the current generated by the light in the photovoltaic cell flows through it and an external load will match the power of this current to be used in various applications.

There are two major factors that hamper the efficiency of solar cells based on bulk silicon. For one, the band gap of silicon is fixed at around 1.1 eV, therefore limiting the energy that can be absorbed from the solar spectrum. Second, when photons with higher energies than 1.1 eV are absorbed, the excess energy is lost, since from each photon only one electron-hole pair

is generated. Additionally other energy losses by unwanted recombination of electron-hole pairs, limited electron and hole mobility in the material and blackbody radiation, contribute to a theoretical efficiency for crystalline silicon solar cells of around 29 %, the so called Shockley-Queisser limit.[24]

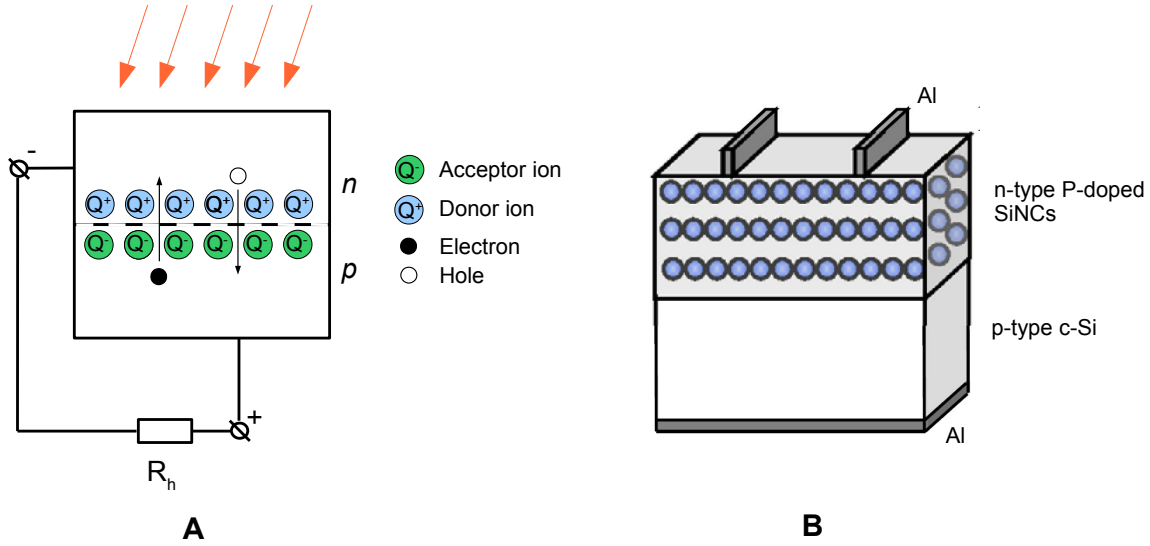

Figure 2.2: A: Schematic setup of a photovoltaic cell with a connected load R_h, B: dual-junction SiNCs solar cell by Green *et al.*[25]

Several strategies have been developed to overcome the Shockley-Queisser limit. One way is to build a solar cell that is made from multiple materials with varying band gaps that are stacked over each other to optimize light absorption, the multiple-junction solar cell. A theoretical efficiency up to 68.2 % or 86.8 % under concentrated sunlight has been calculated for this approach.[26] Currently the most efficient solar cells are based on this design with reported values up to 44.7 %.[27] The sophisticated design and need for a variety of materials with matching band gaps currently results in very high production costs for multi-junction solar cells.

The band gap of SiNCs can be tailored with their size. By this way, a multi-junction solar cell could be fabricated, consisting only of SiNCs with varying sizes, therefore reducing its cost. The feasibility of this approach was demonstrated by Green *et al.* (Figure 2.2 B) with a two-junction solar cell made from phosphorous doped SiNCs (band gap 1.7 eV) and crystalline silicon (c-Si) (band gap 1.1 eV).[25]

Another possible option to push the efficiency of solar cells beyond the Shockley-Queisser

limit is to take advantage of materials that show multiple exciton generation (MEG). Quantum dots made from various materials like PbSe, PbS and CdSe but also silicon have shown that excitation with photons with energies higher than twice their band gap can result in the generation of more than one exciton from one photon.[28–30] This effect could improve solar cells by more efficiently using part of the solar spectrum with higher energies. Still, to exploit this effect remains challenging since it is difficult to extract the charge carriers from a nanocrystal layer without losing most of them to recombination and no solar cells based on SiNCs have been reported so far that show MEG.

The external quantum efficiency (EQE) is defined as the ratio of electron-hole pairs generated from the photons reaching the surface of a solar cell. The EQE decreases in crystalline silicon solar cells at wavelengths below 400 nm and in multicrystalline silicon devices already below 500 nm due to unwanted interactions with the solar cell material and the high energy photons.[31] To avoid this problem, the solar cell can be coated with a material that absorbs light in the UV/blue region and converts it to higher wavelengths. SiNCs in the size range of a few nanometers show a strong absorption below 400 nm and photoluminescence at around 700 nm and are suitable for this task.[32] Yang *et al.* reported that a thin layer of SiNCs, applied *via* inkjet printing, indeed increased the efficiency of a commercially produced multicrystalline silicon solar cell from 17.2 to 17.5 %.[33]

2.3 Light Emitting Diodes

The basic working principle of a light emitting diode (LED) is equivalent to a reverse operated solar cell. An external current is applied to a *p*-*n* junction which induces charge carriers, electrons and holes, to flow from the electrodes to the junction. Upon the recombination of an electron with a hole, energy is released in form of a photon. The wavelength of the emitted light is dependent on the band gap of the semiconductor material. This offers the opportunity to build LEDs emitting light with different colors just by using quantum dots with varying sizes.

Several reports exist of SiNC-LEDs with emission wavelengths spanning from yellow to the near-IR region.[34–37] To build devices with high quantum yields remains challenging. The highest external quantum yield for SiNC-LEDs found in literature is 1.1 %,[38] compared to LEDs based on CdSe quantum dots with 18 %, which is close to the theoretical maximum for

planar thin film LEDs of 20 %.[39]

Up to this point, also no blue emitting SiNC-LEDs were reported. Blue emitting LEDs are of special interest, since they can be used for white light LEDs. This is commonly achieved by coating a blue LED with a phosphor, that partially absorbs the LED light and emits it at higher wavelengths to obtain a light spectrum that is sensed as white light by the human eye.[40]

2.4 Photoluminescent Biological Markers

Fluorescence techniques have developed to be a valuable tool for the understanding of biological processes for *in vitro* and *in vivo* studies. Applications include molecular and cellular imaging, cell tracking and labeling and DNA detection. Still, there is need for the development of more efficient fluorescent markers. An ideal marker should exhibit bright photoluminescence, be non toxic and it needs to be stable against photobleaching. Traditional dyes often do not possess the necessary stability for the use in biological systems. Quantum dots in contrast are known to be highly resistant against photobleaching, and their photoluminescence wavelength can be tuned with their size, which is particularly interesting for multicolor experiments.[41] Efforts have been made to apply quantum dots as photoluminescent biological markers.[42] However it needs to be considered that quantum dots often contain heavy metal ions like cadmium and lead and can be toxic to cells and organisms, even when encapsulated for example in core-shell structures.[43] Since silicon does not possess an inherent cytotoxicity, SiNCs are a promising alternative for biological applications.

As synthesized SiNCs mostly possess a hydrophobic surface such as Si–H groups and are not dispersible in aqueous environments. In the first reported application of SiNCs as fluorescent markers, Ruckenstein *et al.* functionalized SiNCs with poly(acrylic acid) to obtain water dispersible particles.[44] Cellular uptake of the thus treated SiNCs was confirmed with Chinese hamster ovary cells, additionally the particles showed good stability in water and no photobleaching was observed, in contrast to commonly used dyes. Several reports followed that used different methods to obtain water dispersible SiNCs.[45–48] However the particles had not been decorated with any bio-functional moieties, so no specific cell types or locations could be targeted, but the SiNCs were randomly distributed in the cells. This issue was addressed by Prasad *et al.* by coupling carboxyl terminated SiNCs to folate, antimesothelin

and transferrin.[49] Panc-1 cancer cells, in contrast to normal cells, possess a high amount of specific receptors for these molecules, therefore the cancer cells were selectively marked by the functionalized SiNCs.

SiNCs were also applied as photoluminescent drug carrier systems.[50] In this approach, hydride terminated SiNCs were coated with a poly(methacrylic acid) (PMAA) surface layer. In a second esterification step, the SiNCs were functionalized with polyethylene glycol monomethylether. The thus prepared core shell structures were loaded with doxorubicin (DOX) which is a common anti-cancer drug. DOX possesses a free amine group and ionically binds the acid groups of the PMAA layer. Release of the drug is selectively triggered under acidic conditions which are found in cancer cells. The uptake in the cells can be followed due to the photoluminescence of the SiNC core.

3 Theoretical Background

In this chapter, an introduction is given about the field of photoluminescent SiNCs. This includes a view at their physical properties, a summary of several synthetic methods to obtain SiNCs and an overlook about their surface functionalization.

3.1 Properties of Photoluminescent Silicon Nanocrystals

The properties of bulk silicon and its synthesis have been intensively investigated and are well understood. Silicon combines several unique features such as high purity, non-toxicity, availability of large single crystals and possibility of band gap engineering with dopant atoms. Therefore silicon was established as the most important semiconductor material for the microelectronics industry and it sustained the development of information technology during the past decades.

In contrast to the favorable electronical properties of bulk silicon, its use in optical applications is limited due to its band structure. The maximum-energy state of the valence band (VB) and the minimum-energy state of the conduction band (CB) are both characterized by a crystal momentum (k-vector) in the Brillouin zone. If the crystal momentum of the two energy states differs, like in the case of bulk silicon, the material possesses an indirect band gap. For a radiative recombination, an electron from the conduction band recombines with a hole in the valence band releasing its energy as a photon. In this process, both energy and crystal momentum need to be conserved. In an indirect band gap material, this transition can not occur directly but only under the involvement of a phonon, where the phonon momentum equals the difference between the electron and hole momentum (Figure 3.1 A). [51] Since this process is comparably unlikely to occur, radiative recombination is less efficient in indirect band gap materials compared to direct band gap ones.

In contrast to bulk silicon, SiNCs in the size range below 5 nm emit photoluminescence (PL) in the visible range when excited with UV light. Two possible approaches exist to explain this behavior. In the first, the PL is attributed to quantum confinement, that occurs in

the SiNCs when their size lies below the exciton bohr radius of silicon (4.2 nm). Quantum confinement induces a quantization of the energy levels and a widening of the band gap in the SiNCs. In addition, due to Heisenberg's uncertainty principle, the spacial restriction in the SiNCs increases the uncertainty for the k-vector, favoring the possibility for a direct transition without the involvement of a phonon (Figure 3.1 B). [51] The quantum confinement model is supported by observations such as size dependent emission wavelength, characteristic fast (nanosecond) decay times and pressure sensitivity of the PL. [52, 53]

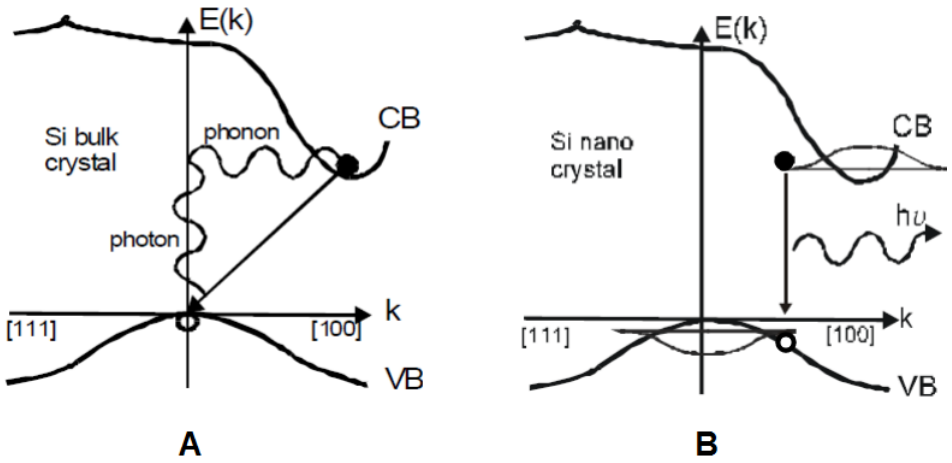

Figure 3.1: Schematic band structure for an electron-hole recombination process in bulk silicon (A) and nanocrystalline silicon (B). [51]

The second model attributes observed PL to surface states. Excited carriers rapidly relax into lower-lying defect states which then irradiate. This theory is supported e. g. by the observation that the PL is influenced by chemical treatments like oxidation or the functionalization with various surface groups. [54, 55]

Most likely, quantum confinement and surface state induced PL both are valid explanations for the PL. But in each case the SiNC properties need to be investigated to determine which mechanism applies. [56]

3.2 Synthesis of Photoluminescent Silicon Nanocyrstals

A great variety of methods have been developed to synthesize freestanding SiNCs. The procedures can roughly be categorized from which direction the nanoscopic dimension is

approached. In "top down" methods, larger pieces of silicon are broken up until nanoparticles are formed. "Bottom-up" methods rely on molecular precursors, that assemble in chemical reactions to form SiNCs.

3.2.1 Top-Down Approaches

Ball Milling

The most straight forward way to form SiNCs is to crush silicon pieces until nanoparticles are obtained. This approach was demonstrated by Muller *et al.* using ball milling.[57] The method is comparably cheap, allows the synthesis of SiNCs with a diameter of a few nanometers with narrow size distributions and the material is obtained in tangible amounts (∼10 g). But a partial phase transition from crystalline to amorphous silicon takes place during the milling process.[58,59] The amorphous defects act as source of nonradiative recombinations, reducing the PL intensity.

Etching of Bulk Silicon

Electrochemical etching of bulk silicon in HF electrolytes results in the formation of porous silicon (pSi). pSi possesses a very high surface area with nanostructured domains and therefore emits photoluminescence under UV radiation.[60,61] Sailor *et al.* showed that by ultrasonication of pSi, luminescent dispersions of SiNCs are obtained.[62] This was the first time that photoluminescent freestanding SiNCs were reported in literature. Due to its simplicity, this approach has been widely applied since.[63,64] A major drawback of this method is, that the amounts of obtained SiNCs are rather small and therefore the synthesis is costly.

3.2.2 Bottom-Up Approaches

Laser Pyrolysis

Silane gas (SiH_4) can be decomposed under high temperatures (up to 1000 °C), induced by a laser beam, forming SiNCs (Figure 3.2). This was first demonstrated by Cannon *et al.* and then successfully adopted by several other groups.[65–68] Initially the amount of material that could be obtained was only in the scale of a few milligrams per day, Swihart *et al.* advanced this method by using an aerosol-reactor with a CO_2 laser producing up to 200 mg of well

defined SiNCs per hour. [69] Controlled etching of the obtained particles with a mixture of HF and HNO_3 resulted in photoluminescent SiNCs, spanning the whole visible spectrum.

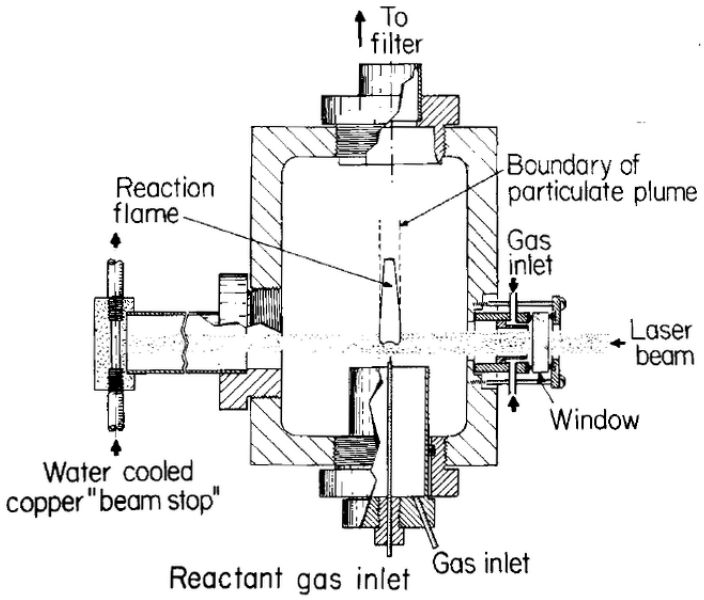

Figure 3.2: Experimental setup for the pyrolysis of SiH_4 gas to form silicon nanocrystals by Cannon *et al.*. [65]

Plasma Synthesis

Non-thermal plasma contains electrons with a much higher temperature compared to the heavy neutral particles and ions of the plasma. The hot electrons induce the dissociation of precursor molecules such as SiH_4 forming unsaturated silane clusters Si_nH_m. [70] These clusters have positive electron affinities and attach electrons to give negative ions which are electrostatically trapped in the plasma. [71] The ions then act as seeds for the particle nucleation and anion-molecule reactions allow the formation of a crystalline core. Since the particles are negatively charged in the plasma, the agglomeration of particles is hindered which results in narrower size distributions. [72] This is a significant advantage towards other gas phase syntheses, where no force prevents particle interactions and agglomeration is a common problem. [73] The plasma synthesis of SiNCs was performed by several groups and high quality SiNCs with PL quantum yields up to 60 % are reported in literature (Figure 3.3). [74–76]

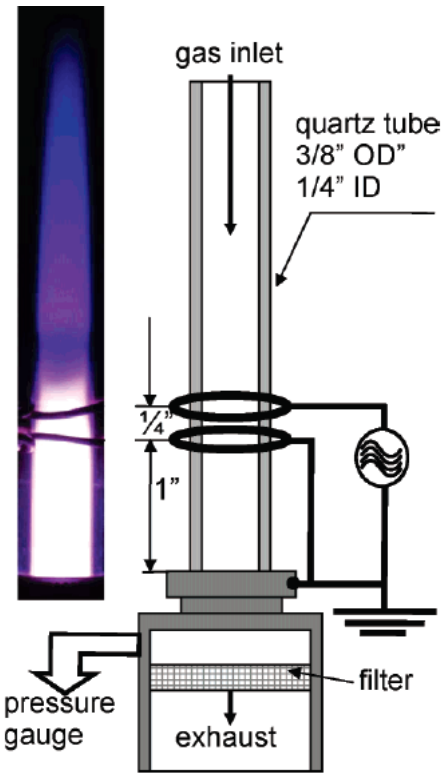

Figure 3.3: Scheme of a rector by Kortshagen *et al.* for the non-thermal plasma synthesis of SiNCs from an argon-silane plasma. The plasma is created *via* radio-frequency power transmission, applied through a matching network of two copper ring electrodes. [74]

Synthesis in Supercritical Fluids

SiNCs can be prepared by the decomposition of precursor molecules in supercritical solvents. This method was introduced by Korgel *et al.* who described the synthesis of alkoxy-coated SiNCs by the reaction of diphenyl silane with ocatanol under 345 bar and 500 °C in hexane. [52,77] The SiNCs are obtained in comparably good yields (0.5–5%), have a size of a few nanometers and emit photoluminescence.

Precursor Reduction in Solution

The reduction of silane precursors in solution to form silicon nanocrystals was first described by Heath *et al.*. [78] In his method, $SiCl_4$ and octyltrichlorosilane were reduced by sodium at high pressures and temperatures in hexane. This procedure was adapted by other groups and different reducing agents like sodium naphthalenide ($NaC_{10}H_8$) or silicon precursors e.g. tetraethyl orthosilicate were successfully applied. [79,80] To obtain SiNCs with narrow size

distribution remained challenging. This issue was resolved with the addition of a phase transfer agent and a surfactant like tetraoctylammonium bromide (TOAB). TOAB forms inverse micelles in the nonpolar reaction medium, stabilizing the halogenated silane precursor. [45,81] Addition of $LiAlH_4$ as reducing agent then yields hydride terminated SiNCs in the range of a few nanometers. The method was further improved by replacing the surfactant with silanes containing long carbon chains, therefore simplifying the purification process and giving additional surface moieties for further functionalization. [82,83] A major drawback of the precursor reduction method is, that up to this date, only blue photoluminescent SiNCs have been obtained.

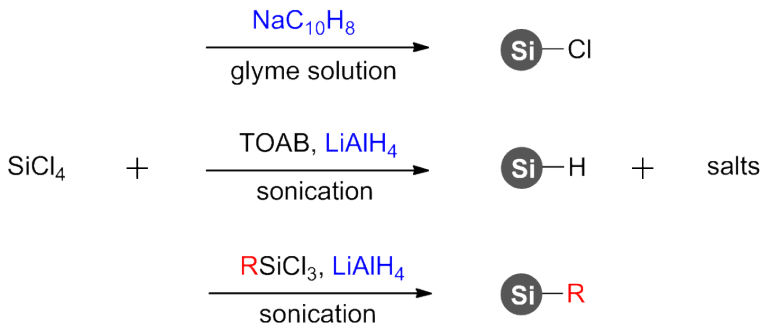

Scheme 3.1: Examples for the synthesis of SiNCs by reduction of $SiCl_4$. [84]

Zintl Salt Based Synthesis

Silicon Zintl salts like NaSi, KSi and Mg_2Si are known to form silicon nanocrystals either by metathesis-type reaction with silicon halides or oxidation with bromine (Scheme 3.2). [85,86] In a typical procedure by Kauzlarich *et al.*, heating of KSi and $SiCl_4$ in a boiling glyme solution for 48 h gives chlorine terminated SiNCs with comparably narrow size distributions. [85] However, similar to the SiNCs synthesized by precursor reduction in solution, only blue photoluminescent SiNCs are reported in literature so far. [84]

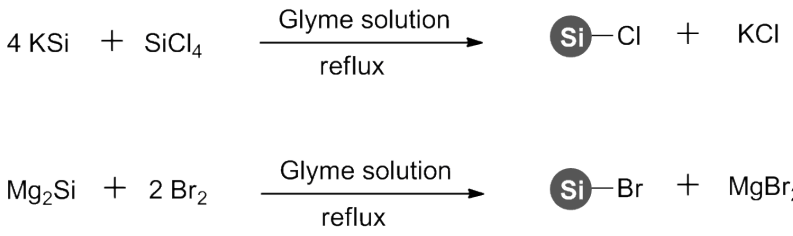

Scheme 3.2: Preparation of SiNCs from Zintl salts KSi and Mg_2Si by metathesis reaction with $SiCl_4$ or oxidation by Br_2. [85,86]

Disproportion of Silicon Rich Oxides

Silicon rich oxides (SiO_x, x < 2) can be used as precursor material for SiNCs. When heated to temperatures above 1000 °C under inert gas atmosphere, a disproportion reaction takes place and silicon nanoparticles are formed incorporated into a SiO_2 matrix. To obtain freestanding, hydride terminated SiNCs, the SiO_2 is removed by etching with hydrofluoric acid. Silicon rich oxides for the SiNCs synthesis can be prepared by various methods like co-sputtering of Si and SiO_2 or plasma enhanced vapor deposition. [87–89] Thin films of silicon rich oxides are formed on substrates which are tempered afterwards. By these procedures SiNCs are obtained only in very small quantities.

A more convenient precursor is polymeric hydrogen silsesquioxane (HSQ) with the molecular formula $(HSiO_{1.5})_n$. HSQ can be produced in large amounts and high purity by the controlled hydrolysis of $HSiCl_3$ or it is commercially available since HSQ is used as a spin-on dielectric in the microchip industry. [90,91] It has to be noted that HSQ for the SiNC synthesis sometimes erroneously is described as the cage like molecule $H_8Si_8O_{12}$ in literature, but in all cases the polymeric form was used.

The formation of SiNCs from HSQ has been investigated by Veinot *et al.*. [92] Thermal processing under inert gas first induces a rearrangement of the HSQ network at 250-350 °C (Scheme 3.3 A) and formation of SiH_4. [93] At higher temperatures (350-450 °C) in addition a thermal dissociation of Si–H bonds is observed which leads to the formation of elemental silicon. If the heating rate is high enough, ≥ 50 °C/min in a N_2 atmosphere or ≥ 10 °C/min in N_2 containing small percentages of H_2, thermally liberated SiH_4 is unable to escape the forming SiO_2 matrix before decomposing. The role of H_2 is not clear to this point, possibly it prevents dehydrogenation of HSQ and increases the SiH_4 available for thermal decomposition.

Nanocrystalline silicon domains are observed when HSQ is heated to over 1000 °C and the particle size increases with higher temperatures (Scheme 3.3 B). [92,94] The size can be tuned between 3 ± 0.3 nm and 13 ± 2.4 nm which requests a temperature of 1100 or 1350 °C respectively. [94] At even higher temperatures, the dispersity of the obtained SiNCs increases dramatically, possibly due to a softening of the SiO_2 matrix and higher diffusion of the Si atoms. By choosing heating time and temperature properly, also the shape of the obtained SiNCs can be influenced. Veinot *et al.* reported the formation cubic SiNCs by heating HSQ for 20 h at 1300 °C. [95] Photoluminescence for hydride terminated SiNCs obtained by the thermal disproportion of HSQ has been reported, spanning from yellow (600 nm) to the near infrared region (1060 nm). [92,94] Blue and green photoluminescent SiNCs could not be obtained so far without further surface functionalization.

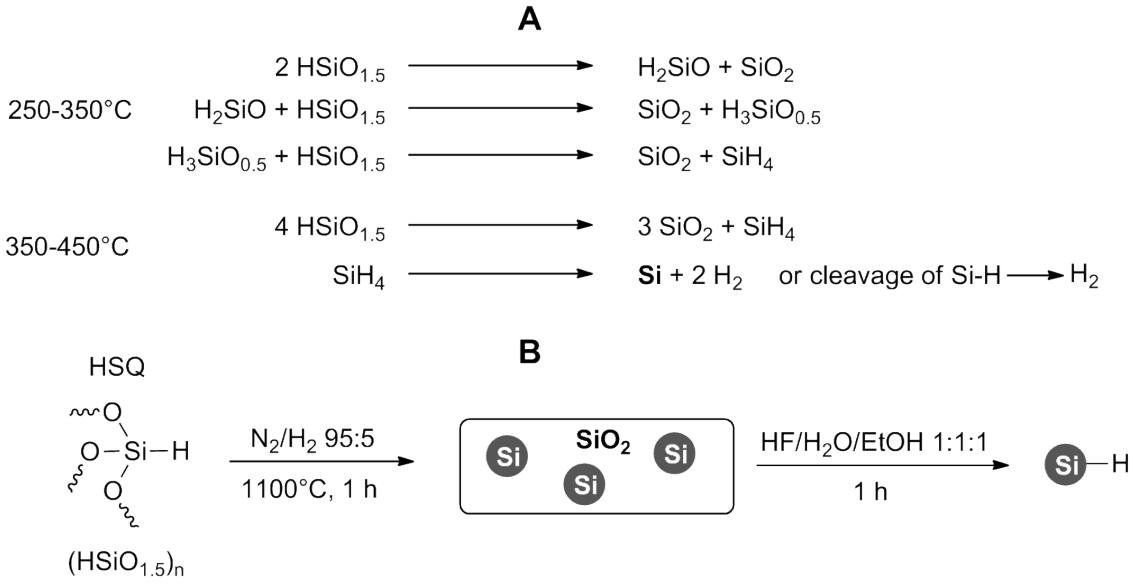

Scheme 3.3: A: Thermal decomposition of HSQ. [93] B: Synthesis of SiNCs with an average diameter of 3 nm from the thermal disproportion of polymeric hydrogen silsesquioxane (HSQ) and subsequent liberation to obtain freestanding, hydride terminated SiNCs by etching with HF. [92]

3.3 Surface Functionalization of Photoluminescent Silicon Nanocrystals

Silicon is easily oxidized by water or oxygen forming stable silicon dioxide. This is especially true for SiNCs since they possess a very high surface area and exhibit an even higher reactivity

than bulk silicon. Also SiNCs are not easily dispersible in solvents because they tend to form agglomerates. In addition, it has been established that control of the surface chemistry is necessary to influence the optical properties of SiNCs.[55] Therefore defined functionalization of the SiNC surface is of crucial importance to render SiNCs useful for applications.

3.3.1 Hydrosilylation Reaction

Si–H moieties react with unsaturated carbon compounds to form stable Si–C bonds. This so called hydrosilylation reaction is extensively used for molecular silanes and also for the functionalization of hydride terminated surfaces of bulk silicon.[96,97]

Since many of the previously described syntheses give Si–H terminated SiNCs, hydrosilylation is a versatile reaction to functionalize SiNCs.

Radical and Exciton Initiated Hydrosilylation

Applying suitable conditions, Si–H bonds can be homolytically cleaved forming silicon surface radicals (Scheme 3.4 A). This reaction was demonstrated under elevated temperature (190 °C) or in the presence of radical initiators.[95,98] The silicon surface radicals can react with olefins, forming a carbon centered radical that again abstracts a hydrogen radical from the surface. By this way, the hydrosilylation proceeds as a radical chain reaction.

The hydrosilylation of nanocrystalline silicon can also be initiated by UV and white light irradiation. For these conditions, an excitonic mechanism is proposed (Scheme 3.4 B).[99] An unbound exciton induced by light absorption leads to a positive surface charge which then reacts with an alkene under Si–C bond formation, giving a carbocation. The carbocation can abstract a hydride from an adjacent Si–H group yielding a covalently bound, neutral alkyl group on the surface. The mechanism is supported by the observation that SiNCs show size dependency for UV induced hydrosilylation.[100] Also hydrosilylation by white light irradiation should not be possible following a radical mechanism since the applied energy is not sufficient for a Si–H homolysis.[101]

Although widely applied due to its simplicity, thermal and UV irradiation initiated hydrosilylation has several drawbacks that need to be considered. UV radiation and high temperatures are not compatible with all alkenes since side reactions like cycloadditions or polymerizations can occur.[102,103] Also several functional groups like amines and nitro moieties compete for

the addition to a Si–H terminated surface. [104,105]

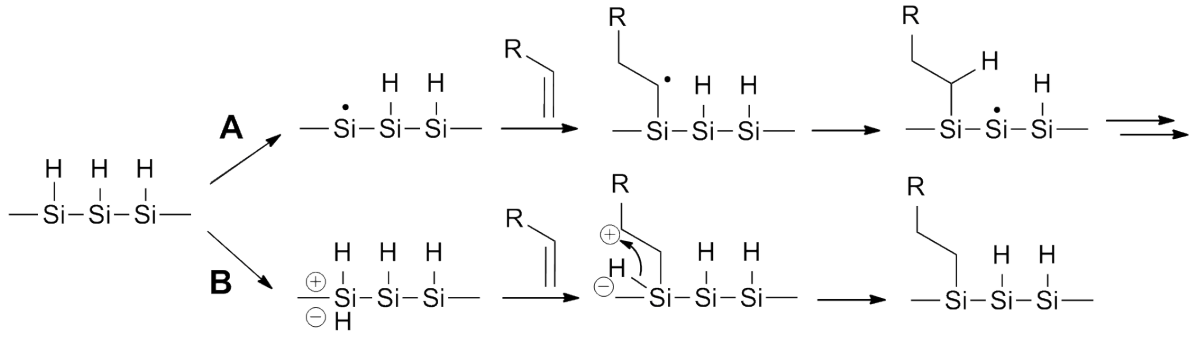

Scheme 3.4: Hydrosilylation mechanism on nanocrystalline silicon. A: radical initiated; B: exciton mediated. [100]

Metal Catalyzed Hydrosilylation

Platinum complexes are well known as hydrosilylation catalysts for molecular silanes and olefins. [106] Tilley *et al.* transfered this approach to hydride terminated SiNCs. Hexachloroplatinic acid (H_2PtCl_6) was used to obtain alkyl or watersoluble alkylamine capped SiNCs, however the precise reaction mechanism was not further investigated. [107,108] Although being a mild hydrosilylation method, the use of such catalysts always bears the risk of metal impurities that already in small concentrations can alter the SiNC properties, e.g. by quenching their photoluminescence. [109,110]

Lewis Acid Catalyzed Hydrosilylation

Another option to initiate hydrosilylation on nanocrystalline silicon is the catalysis by Lewis acids. This approach has been investigated on porous silicon with Lewis acids such as $EtAlCl_2$ and tris(pentafluorophenyl)borane by Canham *et al.*. [111] Recently Veinot *et al.* reported the room temperature functionalization of freestanding SiNCs by BH_3·THF. [112] Two possible mechanisms were proposed for the reaction. Either by formation of a hydroborated intermediate followed by the insertion in a Si–H bond (Figure 3.5 A) or through direct activation of the alkene/alkyne and subsequent reaction with the Si–H surface (Figure 3.5 B).

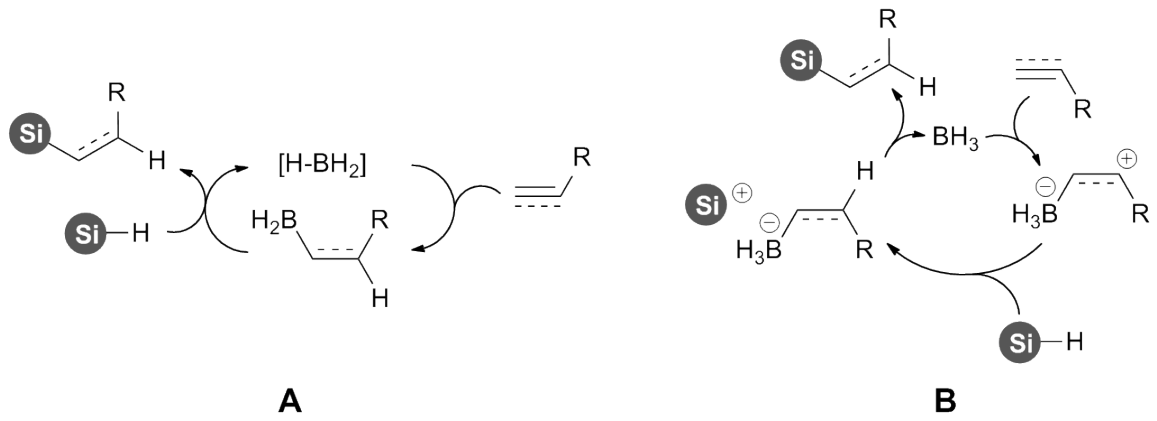

Scheme 3.5: Possible reaction mechanisms for the BH_3·THF induced hydrosilylation of SiNCs by Veinot *et al.*. [112]

Plasma Assisted Hydrosilylation

Plasma assisted gas-phase hydrosilylation of SiNCs has become a valuable alternative to the functionalization by a wet-chemical approach. A typical experimental setup consists of a two part system (Figure 3.4). [113]

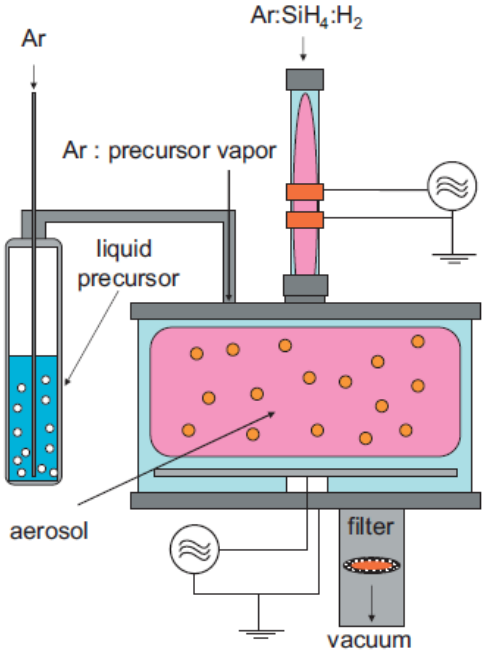

Figure 3.4: Experimental setup for the in-flight functionalization of SiNCs obtained by non-thermal plasma synthesis. [113]

In the first compartment, SiNCs are synthesized by the plasma induced decomposition of

silane gas. An argon stream transfers the particles in a second chamber which contains an aerosol of the desired unsaturated carbon compounds for the surface grafting. Also gaseous substrates like ethylene can be bound on the surface by this way. [114] An advantage over the wet chemical route is that at no stage of the functionalization the particles are exposed to air, therefore surface oxidation is prevented.

3.3.2 Reactions of Halogen Terminated SiNCs

Halogen terminated SiNCs offer a differing reactivity compared to H-terminated SiNCs due to the strong electrophilicity of the Si–X bond. Nucleophilic substitution reactions with various organometallic compounds, amines and alcohols have been reported (Figure 3.6). [115–117] The functionalization with organolithium and Grignard reagents forms Si–C bonds which are stable against hydrolysis in contrast to Si–O and Si–N bonds from the reaction with alcohols and amines.

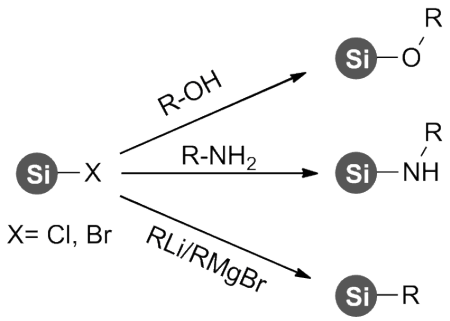

Scheme 3.6: Reaction of halogen terminated SiNCs with various nucleophiles.

3.3.3 Multi-Step Functionalization

Some synthetic goals for the functionalization of SiNC can not directly be achieved just by the formation of a molecular monolayer on the surface. This is e. g. the case when a very high stability against environmental influences is required, competitive reactive moieties on the reactant are present or expensive surface groups, e. g. in biomedicinal applications, need to be attached with lowest possible substrate concentration and highest possible yields. Multi-step approaches can then be favorable over a direct modification since they allow a greater variety in the functionalization.

Kauzlarich *et al.* reported the stepwise synthesis of highly stable SiNCs. [118] SiNCs with a

chlorine terminated surface were methoxylated followed by a hydrolysis step to obtain Si–OH surface groups. Finally, the reaction with alkyl trichlorosilane gave SiNCs with a crosslinked siloxane surface (Scheme 3.7 A). The obtained SiNCs showed steady blue PL over the course of weeks in contrast to chlorine or alkoxy terminated SiNCs, which lost their PL after a few days.

In a multi-step synthesis by Tilley *et al.*, hexa-1,5-diene was hydrosilylated on the surface of Si–H terminated SiNCs followed by an epoxidation step with m-CPBA (Scheme 3.7 B). Final hydrolysis gave hydroxy-terminated SiNCs. [119]

Thiol-ene click chemistry was applied by Zuilhof and Gooding *et al.*. First, alkene passivated SiNCs were prepared and in a second step, the terminal alkene group was reacted with various thiols to obtain SiNCs with ether, ester, hydroxy, carboxyl, amine and sulfonic acid endgroups (Scheme 3.7 C). The obtained SiNCs were dispersible in polar and nonpolar solvents depending on the surface functionality. [83, 120]

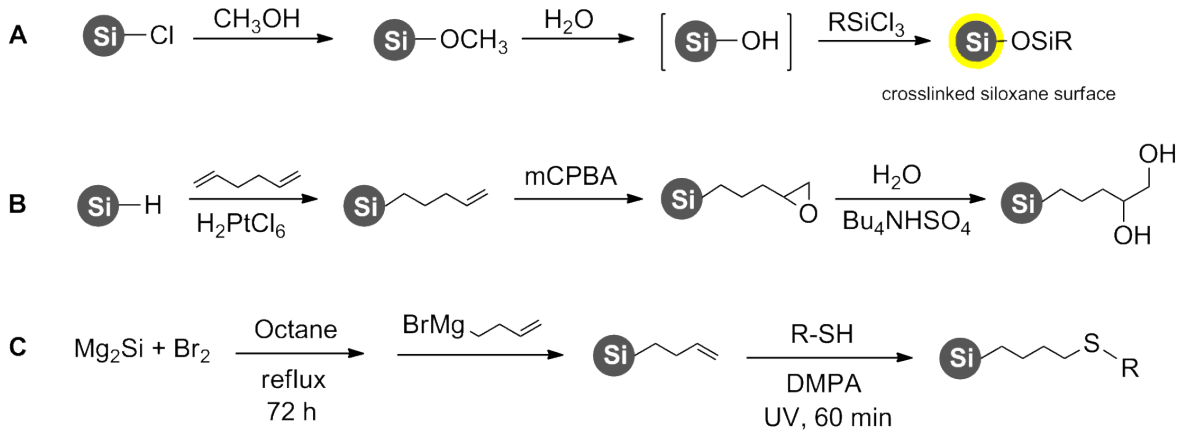

Scheme 3.7: Multi-step syntheses for the surface functionalization of SiNCs. [118–120]

4 Aim of This Work

Even though progress has been made to imply a great variety of different chemical approaches and functionalities on SiNCs, there is still the need for improvement in this field.

The hydrosilylation reaction, work horse for the surface functionalization of hydride terminated SiNCs, is mainly performed under harsh reaction conditions like high temperature or UV radiation. Since some functional groups are not compatible with this treatment, new hydrosilylation methods are needed that proceed at low temperatures and in absence of high energy radiation.

Hydride terminated SiNCs are widely studied since they are available in high purities and with good photoluminescent properties. However surface functionalization only is possible with alkenes and alkynes *via* hydrosilylation which limits the functional groups that can be bound on the surface. It is desirable to find new synthetic methods apart from hydrosilylation to functionalize hydride terminated SiNCs e. g. with nucleophiles.

Currently mostly alkyl chains are used to stabilize the SiNC surface against oxidation. This treatment forms an insulating layer on the SiNCs which possibly hampers their applicability in e. g. solar cells. Molecules with conjugated π-systems, covalently bound on the SiNCs, could diminish this problem by improving the charge transfer from and to the particles. However the possibilities to attach these compounds on SiNCs, especially with a hydride terminated surface, are limited to the hydrosilylation reaction. Therefore only alkene linker from the reaction with alkynes could be obtained. Establishing a route to directly bind aromatic groups and alkynes to SiNCs is an attractive target.

Finally, more complex structures like SiNC-polymer hybrids could enhance the stability and processability of SiNCs or introduce new properties to obtain functional materials.

5 Diazonium Salts as Grafting Agents and Efficient Radical-Hydrosilylation Initiators for Freestanding Photoluminescent Silicon Nanocrystals

Status	Published online: March 24, 2014
Journal	Chemistry - A European Journal, 2014, Volume 15, 4212-4216.
Publisher	Wiley-Blackwell
DOI	10.1002/chem.201400114
Authors	Ignaz M. D. Höhlein, Julian Kehrle, Tobias Helbich, Zhenyu Yang, Jonathan G. C. Veinot, Bernhard Rieger

Content

Diazonium salts are well known grafting agents for a variety of surfaces including metals and silicon. However reports of the reactivity from diazonium salts towards freestanding silicon nanocrystals were still missing to this date. In the first part of the communication, SiNCs are therefore reacted with various diazonium salts. It is observed that direct grafting takes place, however the surface coverage is insufficient and oxidation is a strongly observed side reaction. In the second part, diazonium salts are applied as radical initiators for hydrosilylation reactions. For this purpose, novel diazonium salts were synthesized which are soluble in nonpolar solvents. The diazonium salt initiated hydrosilylation was found to proceed efficiently with a variety of substrates at room temperature and with short reaction times.

JOHN WILEY AND SONS LICENSE TERMS AND CONDITIONS

Apr 07, 2015

This Agreement between Ignaz Hoehlein ("You") and John Wiley and Sons ("John Wiley and Sons") consists of your license details and the terms and conditions provided by John Wiley and Sons and Copyright Clearance Center.

License Number	3566101471603
License date	Feb 11, 2015
Licensed Content Publisher	John Wiley and Sons
Licensed Content Publication	Chemistry - A European Journal
Licensed Content Title	Diazonium Salts as Grafting Agents and Efficient Radical-Hydrosilylation Initiators for Freestanding Photoluminescent Silicon Nanocrystals
Licensed Content Author	Ignaz M. D. Höhlein,Julian Kehrle,Tobias Helbich,Zhenyu Yang,Jonathan G. C. Veinot,Bernhard Rieger
Licensed Content Date	Mar 24, 2014
Pages	5
Type of use	Dissertation/Thesis
Requestor type	Author of this Wiley article
Format	Print and electronic
Portion	Full article
Will you be translating?	No
Title of your thesis / dissertation	New Methods for the Surface Functionalization of Photoluminescent Silicon Nanocrystals
Expected completion date	Jun 2015
Expected size (number of pages)	100
Requestor Location	Ignaz Hoehlein Technische Universität München Lichtenbergstraße 4 Garching bei München, Germany 85747 Attn: Ignaz Hoehlein
Billing Type	Invoice
Billing Address	Ignaz Hoehlein Technische Universität München Lichtenbergstraße 4 Garching bei München, Germany 85747 Attn: Ignaz Hoehlein
Total	0.00 EUR

ChemPubSoc Europe

DOI: 10.1002/chem.201400114

CHEMISTRY
A European Journal
Communication

Diazo Compounds

Diazonium Salts as Grafting Agents and Efficient Radical-Hydrosilylation Initiators for Freestanding Photoluminescent Silicon Nanocrystals

Ignaz M. D. Höhlein,[a] Julian Kehrle,[a] Tobias Helbich,[a] Zhenyu Yang,[b] Jonathan G. C. Veinot,*[b] and Bernhard Rieger*[a]

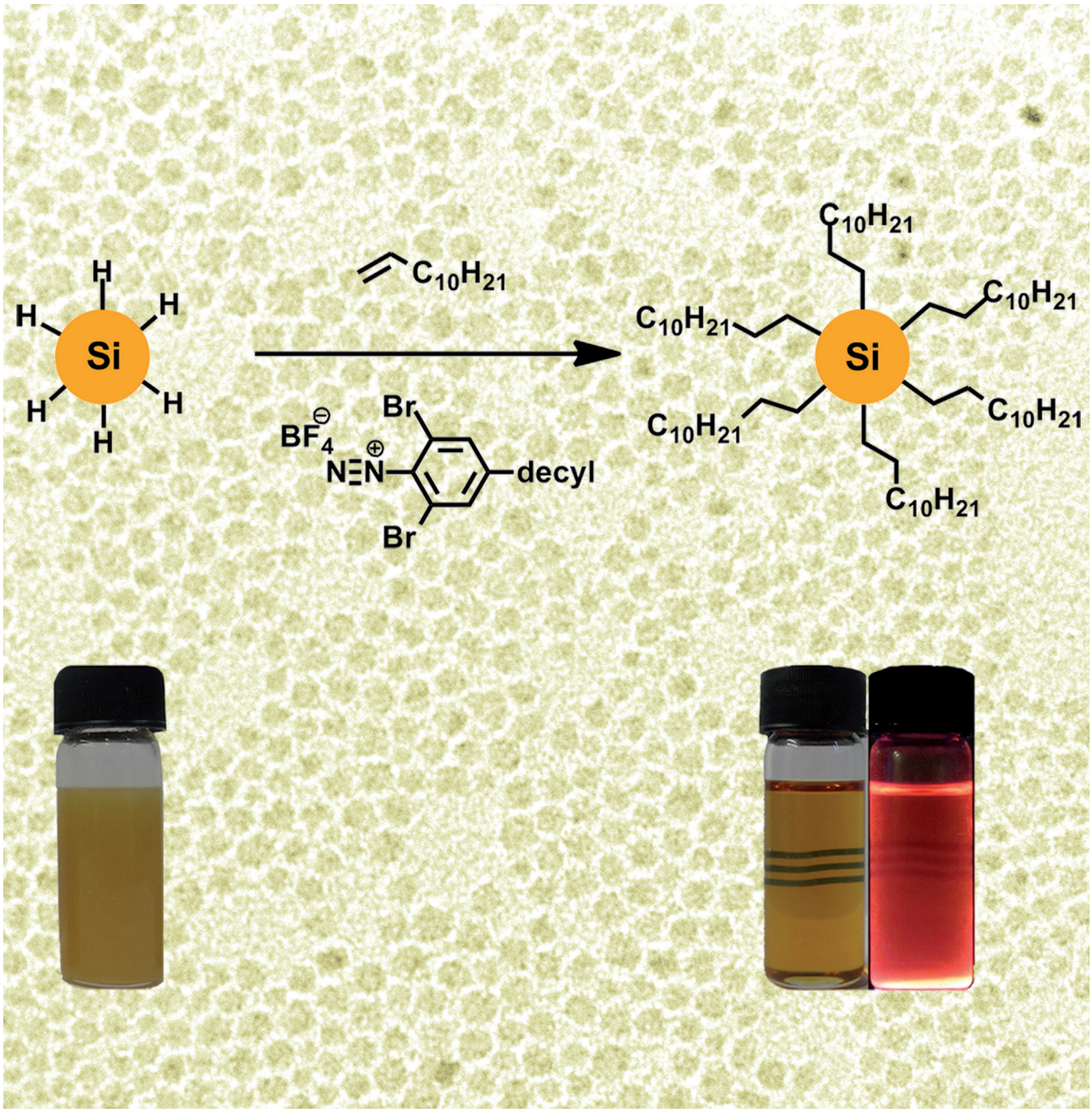

Abstract: The reactivity of diazonium salts towards freestanding, photoluminescent silicon nanocrystals (SiNCs) is reported. It was found that SiNCs can be functionalized with aryl groups by direct reductive grafting of the diazonium salts. Furthermore, diazonium salts are efficient radical initiators for SiNC hydrosilylation. For this purpose, novel electron-deficient diazonium salts, highly soluble in nonpolar solvents were synthesized. The SiNCs were functionalized with a variety of alkenes and alkynes at room temperature with short reaction times.

Silicon nanocrystals (SiNCs) exhibit properties that differ substantially from their bulk counterpart.[1–3] Their optoelectronic behavior (e.g., photoluminescence) is tunable with size and surface functionality. This, in combination with their low toxicity and biocompatibility, has garnered SiNCs much attention in wide ranging applications, such as solar cells, biological probes, and light-emitting diodes.[4–6]

Most syntheses yield freestanding SiNCs containing a reactive Si–H-terminated surface.[7–10] The surfaces of these particles must be modified, if they are to be useful, because SiNCs are sensitive toward oxidation and difficult to disperse in common solvents. In this context, a variety of hydrosilylation methods have been developed, involving reaction with unsaturated carbon-based compounds (i.e., terminal alkenes and alkynes). These methods generally require high temperatures, UV radiation, and/or metal-based catalysts.[9,11,12] Furthermore, these reactions can lead to multilayer and polymer surfaces that can passivate the SiNC surface.[13] The development of new, mild, and metal-free ways to functionalize SiNCs monolayers and other surface groups is, therefore, a timely and attractive target.

In part, because well-defined SiNCs have not been available, the surface chemistry of hydride-terminated bulk silicon has been more thoroughly investigated than for its nanocrystalline counterpart.[14] An attractive and widely applied method to obtain mono- and multilayers of aryl groups on silicon surfaces involves reductive grafting of diazonium compounds.[15] This assembly can be performed under electrochemically reducing or even at the open-circuit potential conditions.[16,17] The generally accepted reaction mechanism when no bias is applied proceeds by a one-electron reduction of the diazonium salt, release of nitrogen, generation of an aryl radical from the diazonium compound, and formation of a surface-silyl radical cation. After deprotonation, coupling of the two radicals gives a robust silicon–carbon bond (Scheme 1).[17] The formation of silicon-surface radicals during the diazonium reaction offers yet another path to NC surface modification through the attachment of a variety of surface groups—diazonium reagents could reasonably act as radical initiators to induce hydrosilylation reactions. Previously, porous silicon (p-Si), an electrochemically etched form of silicon that exhibits very high surface areas, was functionalized with various compounds in this way at room temperature with short reaction times.[18] In contrast to bulk silicon, reports about the reactivity of colloidal SiNCs with diazonium salts are scarce in literature. To date, only direct grafting was performed, or the diazonium salts were used as linking agents, and only comparably large SiNCs ($d \geq$ 50 nm) that do not exhibit size-dependent properties were investigated.[19–21]

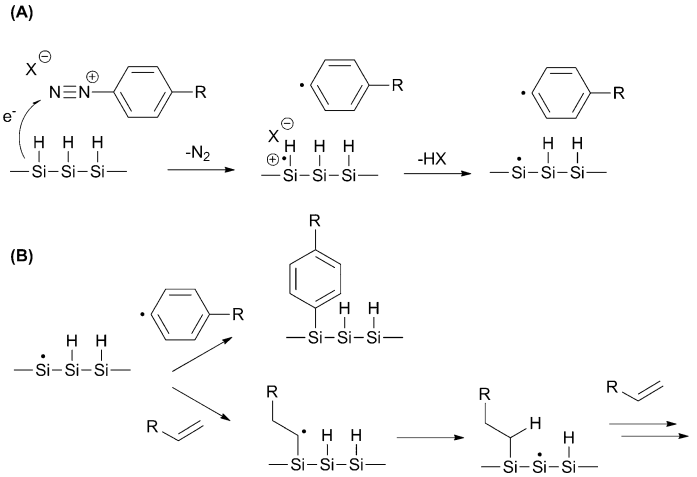

Scheme 1. Reaction mechanism of silicon surfaces with diazonium salts. A) Reduction of the diazonium salt and formation of an aryl radical with release of nitrogen and formation of Si-surface radical after deprotonation. B) Possible reactions of the Si-centered radical to form Si–C bonds.

Herein, we report the first investigation into the reactivity of several diazonium salts toward photoluminescent quantum confined SiNCs ($d = 3$ nm). We also demonstrate that the studied diazonium salts give direct, reductive surface grafting, as well as radical hydrosilylation initiation.

The H-terminated SiNCs used in this work were synthesized by following a known procedure through disproportion of hydrogen silsesquioxane (HSQ) giving SiNCs embedded in a silicon oxide matrix. The SiNCs were subsequently liberated by etching with hydrofluoric acid and final extraction in toluene.[7]

Direct reductive grafting of diazonium salts was first investigated by using commercially available 4-nitro (4-NDB) and 4-bromobenzene diazonium tetrafluoroborate (4-BDB). For these

[a] *I. M. D. Höhlein, J. Kehrle, T. Helbich, Prof. B. Rieger*
Wacker-Lehrstuhl für Makromolekulare Chemie
Technische Universität München
Lichtenbergstrasse 4, 85747 Garching (Germany)
Fax: (+49) 89-289-13562
E-mail: rieger@tum.de

[b] *Z. Yang, Prof. J. G. C. Veinot*
Department of Chemistry, University of Alberta
Edmonton, Alberta, T6G 2G2 (Canada)

Supporting information for this article is available on the WWW under http://dx.doi.org/10.1002/chem.201400114. It contains additional transmission electron microscope (TEM), X-ray photoelectron spectroscopy (XPS), photoluminescence (PL), and dynamic light scattering (DLS) data, as well as the experimental procedures.

grafting experiments, SiNCs (150 mg etched SiO_2/SiNC compound) were suspended in a dry and degassed 0.1 M solution (2 mL) of the diazonium salt in acetonitrile and stirred for 6 h. In each stage of the reaction, the SiNCs formed turbid suspensions, so the SiNCs could be separated and purified with several centrifugation and ultrasonication steps in acetonitrile, toluene, and dichloromethane. FTIR analyses confirmed surface modification with clear evidence of C–C ring-stretching bands (1400–1600 cm^{-1}), and in the case of 4-NDB, the spectral signature of the NO_2 moiety (1350, 1500 cm^{-1}; Figure 1 B and C). However, strong residual Si–H bands (2100 cm^{-1}) imply the coverage of the SiNCs is poor. Further supporting partial surface modification, surface oxidation evidenced by Si–O bands (1050 cm^{-1}), was observed for all samples. The present oxidation of SiNC surfaces is consistent with published reports of diazonium-based modification of p-Si.[18]

It is possible that the incomplete functionalization is a manifestation of the divergent solubility properties of the diazonium salts and the H-terminated SiNCs. Acetonitrile is commonly used solvent when manipulating diazonium compounds because of their solubility properties. Unfortunately, H-terminated SiNCs are hydrophobic/nonpolar and do not disperse well in this solvent system. In an effort to minimize the impact of solvent polarity and improve SiNC surface coverage, we turned to an organic-soluble diazonium salt (i.e., 4-decylbenzene diazonium tetrafluoroborate (4-DDB)) known to give toluene-dispersible hydrophobic aryl-grafted Au and Pt nanoparticles.[22] SiNC modification and product isolation were performed by using conditions identical to those described herein (see below) for the other diazonium salts. Unfortunately, the IR spectrum of the SiNCs showed evidence of limited functionalization, and Si–H and Si–O bands were dominant (Figure 1 D).

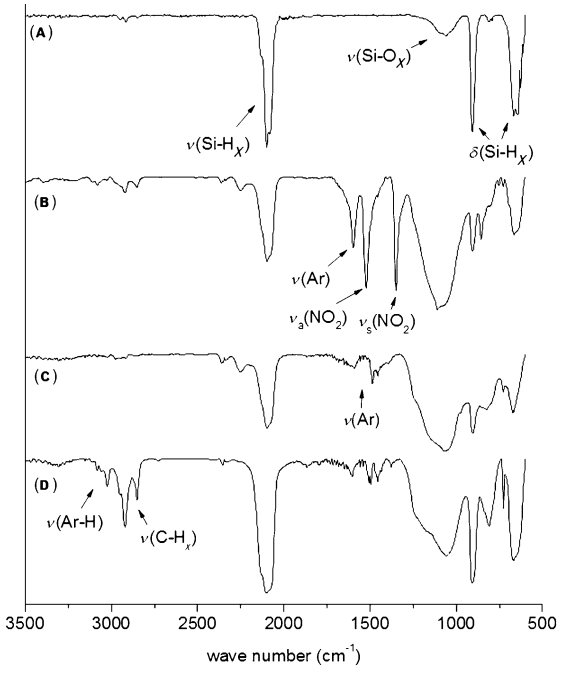

Figure 1. FTIR spectra of A) freshly etched hydride terminated SiNCs; B) reacted with 4-NDB; C) with 4-BDB; and D) with 4-DDB.

Clearly, an extensive surface modification of small SiNCs is not straightforward for this reaction system. It is reasonable that surface reactivity differences noted for bulk Si and SiNCs may result from the limited ability of the SiNC to support the required radical cation intermediate noted in Scheme 1.

Because the surface modification of colloidal SiNCs through direct reductive grafting of diazonium species is inefficient and led to substantial surface oxide that can influence the optoelectronic properties of SiNCs, we turned to the application of diazonium salts as radical initiators.

Diazonium salts have proven to be efficient radical initiators of hydrosilylation on p-Si surfaces.[18] It was illustrated above that reactions suitable for modifying bulk and p-Si are not always directly transferable to colloidal SiNCs. In this context, we explore the application of diazonium salts as radical initiators in the surface modification of freestanding SiNCs. Hydride-terminated SiNCs tend to agglomerate in solution giving turbid dispersions. Alkyl-surface modification achieved upon reaction with α-olefins (e.g., dodecene) gave clear colloidal dispersions.[5,23] For ease of comparison, dodecene was used for the present hydrosilylation experiments.

Diazonium salt induced hydrosilylation was achieved upon dispersing H-terminated SiNCs (150 mg etched SiO_2/SiNC compound) in 3 mL of a toluene solution of dodecene (3 mmol). The reaction at room temperature was initiated upon addition of 4-DDB (15 μmol; Note: diazonium salts without long alkyl chains, such as 4-NDB and 4-BDB, are ill-suited for reactions in toluene because of their limited solubility). After stirring for 2 h at room temperature and in complete darkness, the functionalized SiNCs were isolated and purified by established antisolvent precipitation with methanol. In contrast to the SiNCs containing Si–H surfaces, the present dodecyl-terminated SiNCs form a stable clear colloidal dispersion (Figure 2). The resulting SiNCs showed red photoluminescence (PL) with an emission maximum at approximately 700 nm, which is typical for their size.[24]

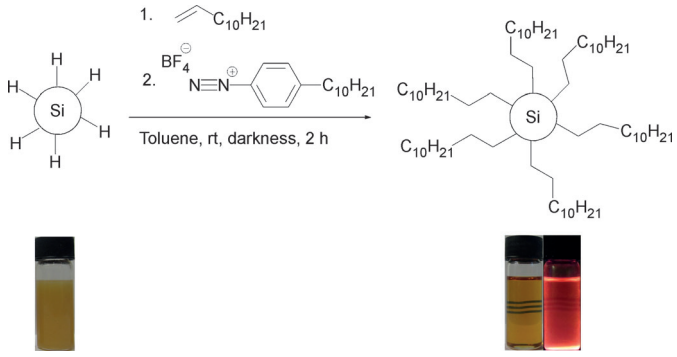

Figure 2. Unfunctionalized SiNCs in toluene (left), dodecyl functionalized SiNCs in toluene under visible light and UV radiation (right).

FTIR analysis showed clear evidence of dodecyl surface termination: the C–H stretching band (2900 cm^{-1}) dominates the spectrum, whereas substantially weaker features attributable to trace Si–H and Si–O bands are also present (Figure 3 A). In contrast, the reference sample without the addition of the di-

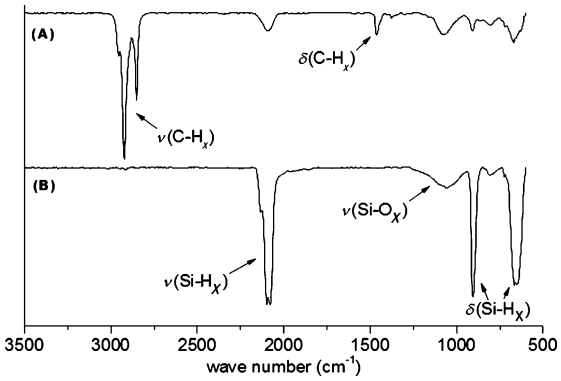

Figure 3. A) Dodecyl-functionalized SiNCs with 4-DDB as radical-hydrosilylation initiator; B) reference sample without the addition of 4-DDB.

azonium salt showed no evidence of functionalization (Figure 3 B).

Having established diazonium reagents do initiate surface modification of SiNCs, we explored the influence of the diazonium structure on the present reaction. Electron-deficient diazonium salts were reported to be more reactive towards homolytic dediazotation.[25] Thus, diazonium salts containing electron-withdrawing groups are expected to be even more effective initiators for the present reactions. To test this hypothesis, the heretofore unknown diazonium salts 2-nitro-4-decyl (2-NO_2-4-DDB) and 2,6-bromo-decyl-diazobenzene tetrafluoroborate (2,6-Br-4-DDB) were synthesized and applied as hydrosilylation radical initiators, and their reactivity was compared to that of 4-DDB and 4-BDB. Conveniently, because the reaction dispersions become non-opalescent upon functionalization, the progress of the reaction can be readily monitored qualitatively (Figure 4).

As was expected, the more electron-deficient 2-NO_2-4-DDB and 2,6-Br-4-DDB reacted faster than 4-DDB, as was evidenced by the transparency of the reaction mixture. With 2,6-Br-4-DDB being the most reactive, the suspension started to turn transparent after only 30 min. Compounds 2-NO_2-4-DDB and 4-DDB needed 60 or 90 min, respectively, to reach this point. No reaction, in comparison to the reference sample without diazonium salt, was observed with 4-BDB, presumably due to its low solubility in toluene.

If the present SiNC reactivity is to find wide application, it is necessary to demonstrate a broad applicability and functional group tolerance of the diazonium-salt-induced hydrosilylation. In this context, we explored reactions with dodecyne, vinyl laurate, methyl methacrylate (MMA), styrene, and ethinyltrimethylsilane (ethinyl-TMS) by using 2,6-Br-4-DDB as radical initiator (Figure 5).

The reaction times differ for each the compounds with dodecyne being the most reactive and turning transparent after only 10 min, whereas vinyl laurate showed the lowest reactivity and needed 6 h until reaching this point. These differences are possibly due to different stabilities of the carbon-centered radicals, which are formed during hydrosilylation (Scheme 1 B) and are subject of ongoing investigations. We also noted that alkenes containing acidic protons, such as alcohols and amines,

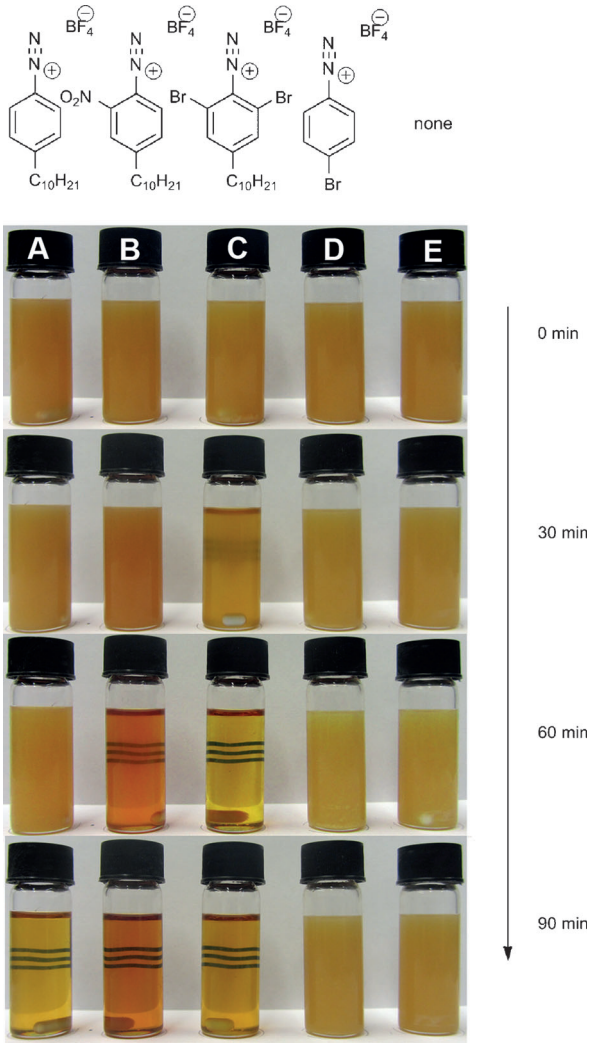

Figure 4. Functionalization of SiNCs with dodecene by using A) 4-DDB; B) 2-NO_2-4-DDB; C) 2,6-Br-4-DDB; and D) 4-BDB as radical-hydrosilylation initiators; and E) without addition of a diazonium salt.

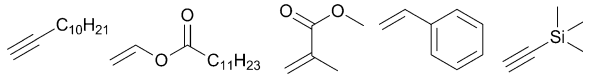

Figure 5. Alkenes and alkynes that were used for the hydrosilylation reactions from left to right: dodecyne, vinyl laurate, MMA, styrene, and ethinyl-TMS.

seem to hamper the hydrosilylation reaction. This issue will be addressed in future work.

All given alkenes/alkynes provided stable colloidal dispersions that showed photoluminescence with a maximum at approximately 700 nm. The FTIR spectra of the functionalized SiNCs are given in Figure 6 and show the expected bands arising from the surface groups in question, as well as trace Si–H and Si–O bands.

The functionalized SiNCs were further analyzed by using dynamic light scattering (DLS) method. Table 1 lists the hydrodynamic radii of the SiNCs. The values are in accordance with the size of the SiNCs and literature results.[11]

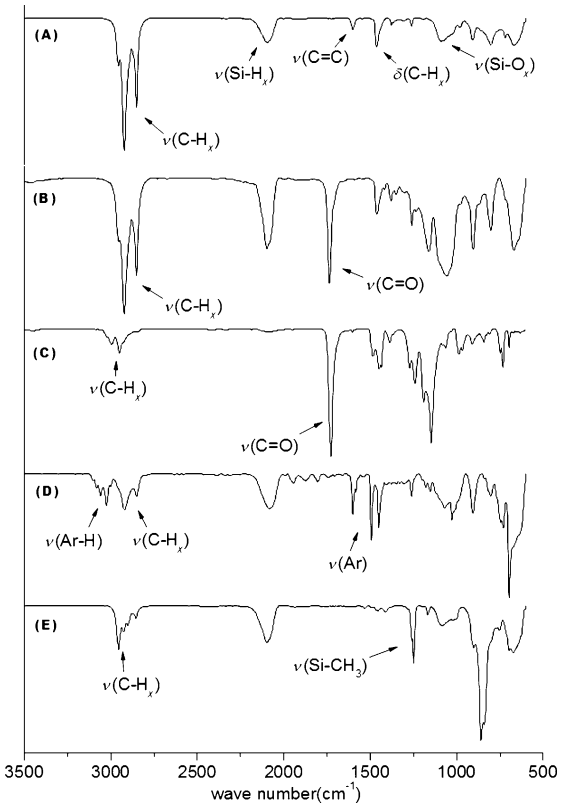

Figure 6. FTIR spectra of the hydrosilylated SiNCs with A) dodecyne; B) vinyl laurate; C) MMA; D) styrene; and E) ethinyl-TMS.

Table 1. Hydrodynamic radii with polydispersities of the functionalized SiNCs by diazonium salt initiated hydrosilylation determined with DLS.

Reagent	Hydrodynamic radius [nm]	Polydispersity [%]
dodecene	3.8	30.3
dodecyne	4.4	32.3
ethinyl-TMS	3.6	38.9
vinyl laurate	3.5	38.4
MMA	2.5	70.2
styrene	5.3	62.6

In summary, we have shown that SiNCs can be functionalized with aryl groups by direct reductive grafting of diazonium salts. However, the coverage of the SiNCs is incomplete, and oxidation is a strongly occurring side reaction. More effective is the application of diazonium salts as radical initiators for hydrosilylation reactions. For this purpose, new toluene-soluble diazonium salts were synthesized. Those with electron-withdrawing groups, such as 2,6-bromo-4-decyl-diazobenzene tetrafluoroborate, have shown to be the most reactive. Several alkenes and alkynes were hydrosilylated on the SiNCs using this method. In all cases, photoluminescent stable colloidal SiNC dispersions were obtained within reaction times of a few hours. Most importantly, we have demonstrated that the application of diazonium salts offers a new, mild, and fast way to initiate hydrosilylation reactions on SiNCs and opens the door to convenient and predictable surface modification.

Acknowledgements

Z.Y. and J.G.C.V. acknowledge funding from the Natural Sciences and Engineering Research Council of Canada (NSERC), Canada Foundation for Innovation (CFI), Alberta Science and Research Investment Program (ASRIP), and University of Alberta, Department of Chemistry. G. Popowich is thanked for assistance with TEM. The staff at the Alberta Centre for Surface Engineering and Sciences (ACSES) are thanked for XPS analysis. B. S. Soller and S. Kissling are thanked for valuable discussions. I.M.D.H. is grateful for a generous scholarship from the Fonds der Chemischen Industrie.

Keywords: diazo compounds · hydrosilylation · silicon nanocrystals · surface grafting

[1] L. Brus, *J. Phys. Chem.* **1994**, *98*, 3575 – 3581.
[2] Z. Ding, B. M. Quinn, S. K. Haram, L. E. Pell, B. A. Korgel, A. J. Bard, *Science* **2002**, *296*, 1293 – 1297.
[3] J. Heitmann, F. Müller, M. Zacharias, U. Gösele, *Adv. Mater.* **2005**, *17*, 795 – 803.
[4] C. Liu, Z. C. Holman, U. R. Kortshagen, *Nano Lett.* **2009**, *9*, 449.
[5] K.-Y. Cheng, R. Anthony, U. R. Kortshagen, R. J. Holmes, *Nano Lett.* **2010**, *10*, 1154 – 1157.
[6] J. Liu, F. Erogbogbo, K.-T. Yong, L. Ye, J. Liu, R. Hu, H. Chen, Y. Hu, Y. Yang, J. Yang, *ACS Nano* **2013**, *7*, 7303 – 7310.
[7] C. M. Hessel, E. J. Henderson, J. G. C. Veinot, *Chem. Mater.* **2006**, *18*, 6139 – 6146.
[8] X. Li, Y. He, S. S. Talukdar, M. T. Swihart, *Langmuir* **2013**, *29*, 8490 – 8496.
[9] R. D. Tilley, J. H. Warner, K. Yamamoto, I. Matsui, H. Fujimori, *Chem. Commun.* **2005**, 1833 – 1835.
[10] J. L. Heinrich, C. L. Curns, G. M. Credo, K. L. Kavanagh, M. J. Sailor, *Science* **1992**, *255*, 66 – 68.
[11] J. A. Kelly, J. G. C. Veinot, *ACS Nano* **2010**, *4*, 4645 – 4656.
[12] X. Li, Y. He, M. T. Swihart, *Langmuir* **2004**, *20*, 4720 – 4727.
[13] Z. Yang, M. Dasog, A. R. Dobbie, R. Lockwood, Y. Zhi, A. Meldrum, J. G. C. Veinot, *Adv. Funct. Mater.* **2014**, *24*, 1345 – 1353.
[14] J. M. Buriak, *Chem. Rev.* **2002**, *102*, 1271 – 1308.
[15] J. Pinson, *Aryl Diazonium Salts: New Coupling Agents in Polmyer and Surface Science*, WILEY-VCH, Weinheim, **2012**.
[16] C. H. De Villeneuve, J. Pinson, M. C. Bernard, P. Allongue, L. De Physique, *J. Phys. Chem. B* **1997**, *101*, 2415 – 2420.
[17] M. P. Stewart, F. Maya, D. V. Kosynkin, S. M. Dirk, J. J. Stapleton, C. L. McGuiness, D. L. Allara, J. M. Tour, *J. Am. Chem. Soc.* **2004**, *126*, 370 – 378.
[18] D. Wang, J. M. Buriak, *Langmuir* **2006**, *22*, 6214 – 6221.
[19] J. M. Chem, S. Yang, G. Li, Q. Zhu, Q. Pan, *J. Mater. Chem.* **2012**, *22*, 3420 – 3425.
[20] S. Yang, Q. Pan, J. Liu, *Electrochem. commun.* **2010**, *12*, 479 – 482.
[21] C. Martin, O. Crosnier, R. Retoux, D. Bélanger, D. M. Schleich, T. Brousse, *Adv. Funct. Mater.* **2011**, *21*, 3524 – 3530.
[22] F. Mirkhalaf, J. Paprotny, D. J. Schiffrin, *J. Am. Chem. Soc.* **2006**, *128*, 7400 – 7401.
[23] Z. Yang, A. R. Dobbie, K. Cui, J. G. C. Veinot, *J. Am. Chem. Soc.* **2012**, *134*, 13958 – 13961.
[24] M. Dasog, Z. Yang, S. Regli, T. M. Atkins, A. Faramus, M. P. Singh, E. Muthuswamy, S. M. Kauzlarich, R. D. Tilley, J. G. C. Veinot, *ACS Nano* **2013**, *7*, 2676 – 2685.
[25] C. Galli, *Chem. Rev.* **1988**, *88*, 765 – 792.

Received: January 10, 2014

CHEMISTRY
A European Journal

Supporting Information

Diazonium Salts as Grafting Agents and Efficient Radical-Hydrosilylation Initiators for Freestanding Photoluminescent Silicon Nanocrystals

Ignaz M. D. Höhlein,[a] Julian Kehrle,[a] Tobias Helbich,[a] Zhenyu Yang,[b] Jonathan G. C. Veinot,*[b] and Bernhard Rieger*[a]

chem_201400114_sm_miscellaneous_information.pdf

General information

All reactants and reagents were purchased from Sigma-Aldrich and used without further purification if not stated otherwise. Vinyl laurate, dodecene, dodecyne and ethinyltrimethylsilane were degassed via several freeze-pump-thaw cycles prior to use. In addition to this treatment, methyl methacrylate and styrene were purified by passing through a basic alumina column. Toluene and acetonitrile were dried over CaH_2, distilled, degassed via several freeze-pump-thaw cycles and stored in an argon filled glove box prior to use.
Nuclear magnetic resonance (NMR) spectra were measured on a *ARX*-300 from Bruker in deuterated chloroform at 300 K. FTIR spectra were measured with a *Bruker Vertex 70 FTIR* using a *Platinum ATR* from *Bruker* for the hydrosilylated SiNCs and a *Spectratech 0030-011* for the SiNCs functionalized *via* direct grafting. Electrospray ionization mass spectroscopy (ESI-MS) was performed on a *Finnigan LCQ classic.* Dynamic light scattering measurements were made with a *Dyna Pro NanoStar* from *Wyatt* with toluene as solvent. Photoluminescence (PL) spectra were taken with a *AVA-Spec 2048* from *Avantes* using a *Prizmatix (LED Current controller)* as light source. Transmission electron microscopy was performed using a *JEOL-2010* (LaB 6 fi lament) electron microscope with an accelerating voltage of 200 keV. TEM samples of SiNCs were drop-casted onto a holey carbon coated copper grid (SPI supplies) and the solvent was evaporated in vacuum. XPS analyses were performed using a *Kratos Axis Ultra* instrument operating in energy spectrum mode at 210 W. A monochromatic Al Kα source (λ = 8.34 Å) was used to irradiate the samples, and the spectra were obtained with an electron takeoff angle of 90°.

Synthesis of Hydrogen Silsesquioxane (HSQ)

The HSQ was prepared following a literature procedure.[1] To a mixture of sulfuric acid (22.7 g) and fuming sulfuric acid (13.9 g), Toluene (45 ml) was added via a dropping funnel for 10 min and stirred for additional 20 min. To the yellow, biphasic solution, $HSiCl_3$ (21.5 g, 0.16 mol) dissolved in 110 ml Toluene was added over the course of several hours. Subsequently, the upper layer was separated, washed thrice with sulfuric acid 50 % (w/w) and stirred over night over $MgSO_4$ and $CaCO_3$. After filtration, the solvent was removed *in vacuo* giving a colorless solid.

EA: calculated Si: 52.90%, H: 1.90% found Si: 51.18 %, H: 1.88%

Preparation of oxide-embedded silicon nanocrystals (d = 3 nm)

HSQ (7 g) was placed in a quartz reaction boat, transferred to a *Nabertherm RD 30/200/11* oven with quartz working tube and heated from ambient to a peak processing temperature of 1100 °C at 18 °C min in a slightly reducing atmosphere (5% H_2/95% Ar).The sample was maintained at the peak processing temperature for 1 h. Upon cooling to room temperature, the resulting amber solid was ground into a fine brown powder using mortar and pestle to remove large particles. Further grinding was achieved via shaking the powder for 12 h with high-purity silica beads using a *WAB Turbula mixer.* The resulting SiNC/SiO_2 composite powder was stored in standard glass vials.

Liberation of SiNCs.

Hydride-terminated SiNCs were liberated from the SiNC/SiO_2 composites using HF etching. First, 0.15 g of the ground SiNC/SiO_2 composite was transferred to a ethylene-tetrafluoroethylene (ETFE) beaker equipped with a Teflon-coated stir bar. Ethanol (3 mL) and water (3 mL) were then added under mechanical stirring to form a brown suspension, followed by 3 mL of 49% HF aqueous solution. After 1 h of etching in subdued light, the suspension appeared yellow. Hydride-terminated SiNCs were subsequently extracted from the aqueous layer into ca. 30 mL of toluene by multiple (i.e., 3 × 10 mL)

extractions. The SiNC toluene suspension was transferred ETFE-centrifuge tubes, and the SiNCs were isolated by centrifugation at 5000 rpm.

Reaction of diazonium salts with H-terminated SiNCs

1. Reductive grafting

150 mg of the SiNC/SiO_2 composite was etched according the described procedure. After extraction and centrifugation, the resulting H-terminated SiNCs were dried, transferred into an argon filled glovebox and resuspended in 2 ml dried and degassed acetonitrile. The respective diazonium salt (0.2 mmol) was added and the dispersion was stirred overnight. Afterwards, the reaction mixture was transferred to a centrifugation vial and the SiNCs were isolated by centrifugation at 9000 rpm for 5 min. The precipitate was following washed with acetonitrile, toluene and CH_2Cl_2 using ultrasonication and centrifugation, before analytic studies were performed.

2. Diazonium salt induced hydrosilylation

150 mg of the SiNC/SiO_2 composite was etched according the described procedure. After extraction and centrifugation, the resulting H-terminated SiNCs were dried, transferred into an argon filled glovebox and resuspended in 3 ml dried and degassed toluene. The respective alkene/alkyne (3 mmol) was added and the mixture was stirred for 2 minutes before the 4-decyl diazonium salt (0.015 mmol) was added. After a typical reaction time between 20 min to 6 h, depending on the time the dispersion took to turn clear, the SiNCs were precipitated via addition of methanol or in the case of MMA with pentane. The precipitate was separated by centrifugation at 9000 rpm for 15 min, resuspended in a minimal amount of toluene and precipitated again. Finally, the functionalized SiNCs were resuspended in toluene, filtered through a 200 µm PTFE-filter and stored in vials for further use.

Synthesis of the diazonium salts

N-(4-decyl-2-nitrophenyl)acetamide

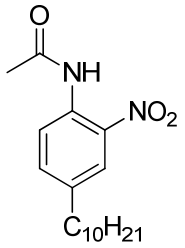

For the synthesis, a literature procedure was adapted.[2] 4-decylaniline (0.85 g, 4.5 mmol, 1 eq) was dissolved in a mixture of acetic acid (10 ml) and acetic acid anhydride (15 ml) and slowly added to a solution of $Cu(NO_3)_2 \cdot 3H_2O$ (1.08 g, 4.5 mmol, 1 eq) in acetic acid (3 ml) and acetic acid anhydride (6 ml). The solution was stirred for 1 h and poured into water. 4-decyl-2-nitroaniline formed as a yellow solid which was recrystallized from ethanol.

Yield 65 %, 940 mg, 2.9 mmol

^{1}H NMR (300 MHz, $CDCl_3$): δ[ppm]: 10.23 (br, 1 H), 8.63 (d, 1 H), 8.00 (d, 1 H), 7.46 (dd, 1 H), 2.85-2.77 (m, 2 H), 2.28 (s, 3 H), 1.62-1.54 (m, 2 H) 1.34-1.19 (m, 14 H), 0.91-0.84 (m, 3 H).

^{13}C NMR (75 MHz, $CDCl_3$): δ[ppm]: 169.1 (s), 138.7 (s), 136.4 (s), 132.7 (s), 125.0 (s) 122.3 (s), 35.0 (s), 32.0 (s), 31.2 (s), 29.7 (s), 29.7 (s), 29.5 (m), 29.5 (s), 29.2 (s), 25.8 (s), 22.8 (s), 14.3 (s)

ESI-MS: $M+H^+$ calculated: 321.2 found: 321.2

4-decyl-2-nitroaniline

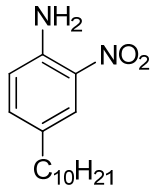

N-(4-decyl-2-nitrophenyl)acetamide (920 mg, 2.87 mmol, 1 eq) was suspended in a solution of acetic acid (20 ml) and concentrated hydrochloric acid (15 ml) and the dispersion was was heated to 80 °C. After 2 h, the now clear solution was poured into ice water and the 4-decyl-2-nitroaniline precipitates in quantitative yield as an orange solid.

^{1}H NMR (300 MHz, $CDCl_3$): δ[ppm]: 7.90 (d, 1 H), 7.19 (dd, 1 H), 6.74 (d, 1 H), 5.86 (br, 2 H) 2.55-2.48 (m, 2 H), 1.51-1.62 (m, 2 H) 1.32-1.22 (m, 14 H),0.91-0.85 (m, 3 H).

^{13}C NMR (75 MHz, CDCl3): δ[ppm]: 143.0 (s), 136.7 (s), 132.0 (s), 132.0 (s), 124.8 (s), 118.9 (s), 34.6 (s), 32.0 (s), 31.3 (s), 29.7 (s), 29.7 (s), 29.6 (s), 29.4 (s), 29.2 (m), 22,8 (s), 14.3 (s)

ESI-MS: $M+H^+$ calculated: 279.2 found: 279.3

2,6-dibromo-4-decylaniline

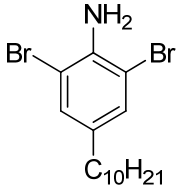

For the synthesis, a literature procedure was adapted.[3] 4-decylaniline (1.30 g, 5.6 mmol, 1 eq) was dissolved in a mixture of CH_2Cl_2 (50 ml) and methanol (20 ml). Benzyltrimethylammonium tribromide (6.51 g, 16.7 mmol, 3 eq) and $CaCO_3$ (2.00 g) were added. The suspension was stirred for 3 h, afterwards filtered and the solvent evaporated *in vacuo*. Water (20 ml) was added to the residue, the mixture was transferred into a separatory funnel and extracted three times with Et_2O (40 ml). The organic phases were combined and dried over $MgSO_4$. After evaporation of the solvent, the residue was recrystallized from EtOH giving 2,6-dibromo-4-decylaniline as colorless crystals.

Yield: 86 %, 1.88 g, 4.8 mmol

^{1}H NMR (300 MHz, $CDCl_3$): δ[ppm]: 7.19 (s, 2 H), 2.25 (br, 2 H) 2.48-2.40 (m, 2 H), 1.58-1.47 (m, 2 H) 1.31-1.22 (m, 14 H), 0.92-0.84 (m, 3 H).

^{13}C NMR (75 MHz, $CDCl_3$): δ[ppm]: 139.7 (s), 134.8 (s), 131.7 (s), 108.9 (s), 34.6 (s), 32.1 (s), 31.6 (s), 29.8 (s), 29.7 (s), 29.6 (m), 29.5 (s), 29.2 (s), 14.3 (s)

ESI-MS: $M+H^+$ calculated: 392.0 found: 392.2

4-decyldiazobenzene tetrafluoroborates

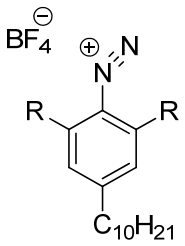

R = H;H, H;NO_2, Br;Br

For the synthesis, a literature procedure was adapted.[4] The respective 4-decylaniline (4.5 mmol, 1 eq) was suspended in a mixture of acetic acid (8 ml) and propanoic acid (8 ml) and HBF_4 50 wt% (6 ml). The suspension was cooled to 0 C and $NaNO_2$ (0.47 g, 6.6 mmol, 1.5 eq) was added in 4 portions. After 1 h, the solution was poured into ice water and the product precipitated as a white to slightly yellow or red solid which was filtered off, washed with water and dried *in vacuo*.

4-decyldiazobenzene tetrafluoroborate

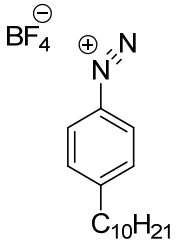

Yield: 86 %, 1.29 g, 3.9 mmol

^{1}H NMR (300 MHz, $CDCl_3$): δ[ppm]: 8.56-8.50 (m, 2 H), 7.64-7.57 (m, 2 H), 2.85-2.77 (m, 2 H), 1.72-1.58 (m, 2 H) 1.37-1.20 (m, 14 H), 0.91-0.84 (m, 3 H).

^{13}C NMR (75 MHz, $CDCl_3$): δ[ppm]: 159.7 (s), 133.0 (s), 131.7 (s), 110.6 (s), 37.2 (s), 32.0 (s), 30.6 (s), 29.7 (s), 29.6 (s), 29.5 (s), 2.94 (s), 29.4 (s), 22. 8 (s), 14.3 (s)

IR: ν(N≡N) 2279 cm^{-1}

ESI-MS: M – N_2, BF_4 calculated: 217.2 found: 217.2

2-nitro-4-decyldiazobenzene tetrafluoroborate

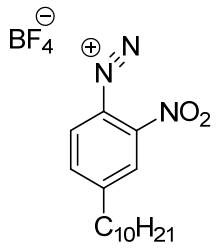

Yield: 65 %, 1.10 g, 2.9 mmol

^{1}H NMR (300 MHz, $CDCl_3$): δ[ppm]: 9.00 (d, 1 H), 8.39 (d, 1 H), 8.03 (dd, 1H), 3.00-2.93 (m, 2 H), 1.72-1.58 (m, 2 H) 1.44-1.20 (m, 14 H), 0.91-0.84 (m, 3 H).

^{13}C NMR (75 MHz, $CDCl_3$): δ[ppm]: 161.5 (s), 144.8 (s), 137.6 (s), 136.3 (s), 127.8 (s) 106.4 (s), 37.2 (s), 32.0 (s), 30.4 (s), 29.7 (s), 29.6 (s), 2.95 (m), 2.94 (s), 2.94 (s) 22.8 (s), 14.3 (s)

IR: ν(N≡N) 2285 cm^{-1}

ESI-MS: M – BF_4 calculated: 290.2 found: 290.2

2,6-bromo-4-decyldiazobenzene tetrafluoroborate

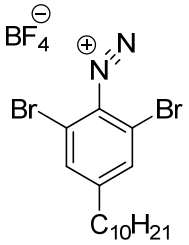

Yield: 93 %, 2.05 g, 4.2 mmol

^{1}H NMR (300 MHz, $CDCl_3$): δ[ppm]: 7.76 (s, 2 H), 2.84-2.75 (m, 2 H), 1.72-1.60 (m, 2 H) 1.78-1.66 (m, 14 H), 0.92-0.84 (m, 3 H).

^{13}C NMR (75 MHz, $CDCl_3$): δ[ppm]: 161.8 (s), 134.5 (s), 127.7 (s), 116.0 (s), 37.2 (s), 32.0 (s), 30.3 (s), 29.7 (s), 29.6 (s), 29.5 (s), 29.4 (s), 29.4 (s), 22.8 (s), 14.3 (s)

IR: ν(N≡N) 2259 cm^{-1}

ESI-MS: M –BF_4 calculated: 403.0 found: 403.0

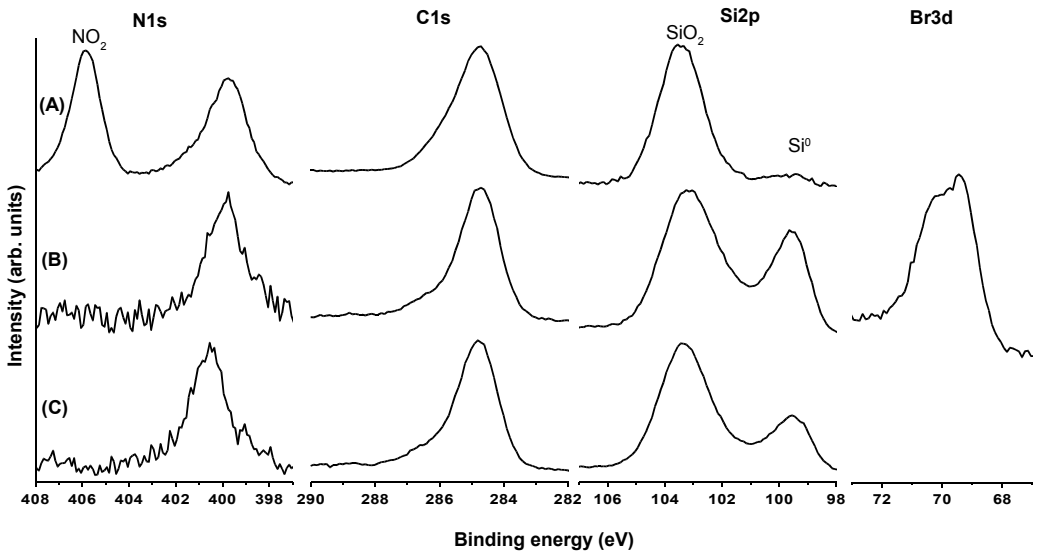

Figure S 1: XPS data of SiNCs after direct grafting with (A) 4-NDB, (B) 4-BDB and (C) 4-DDB. The nitrogen signal at 400 eV has been observed by several other groups while grafting diazonium salts and is believed to be due to formation of azo-linkages.[5]

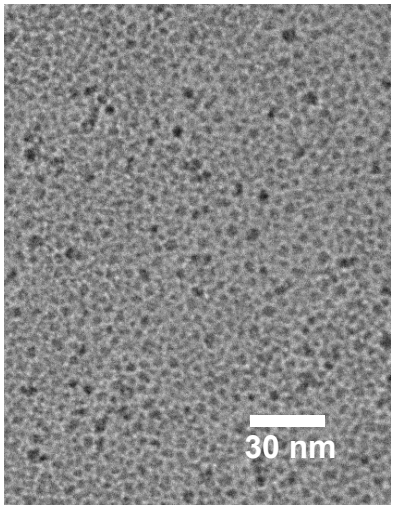

Figure S 2: TEM-picture of SiNCs functionalized with dodecene using 4-DBD as radical initiator.

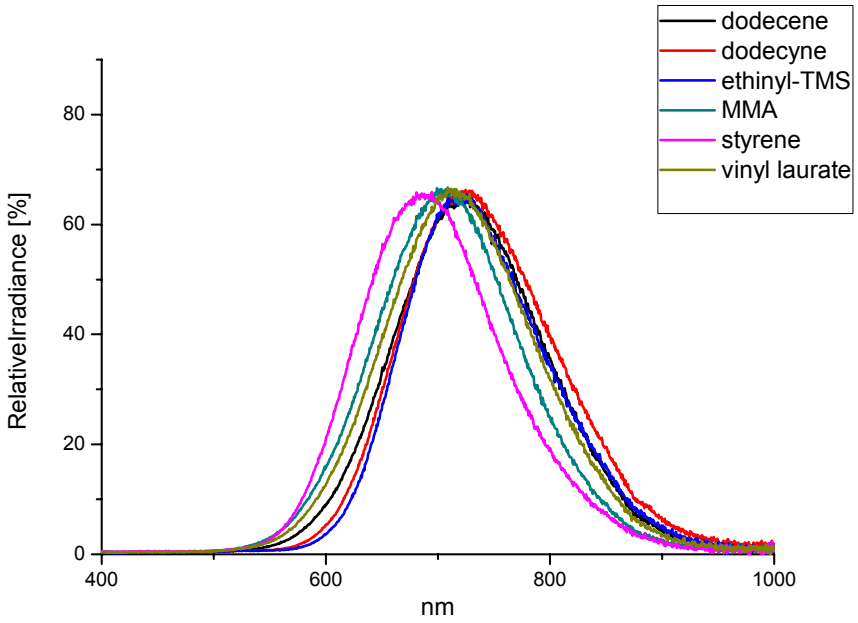

Figure S 3: PL-spectra of the functionalized SiNCS.

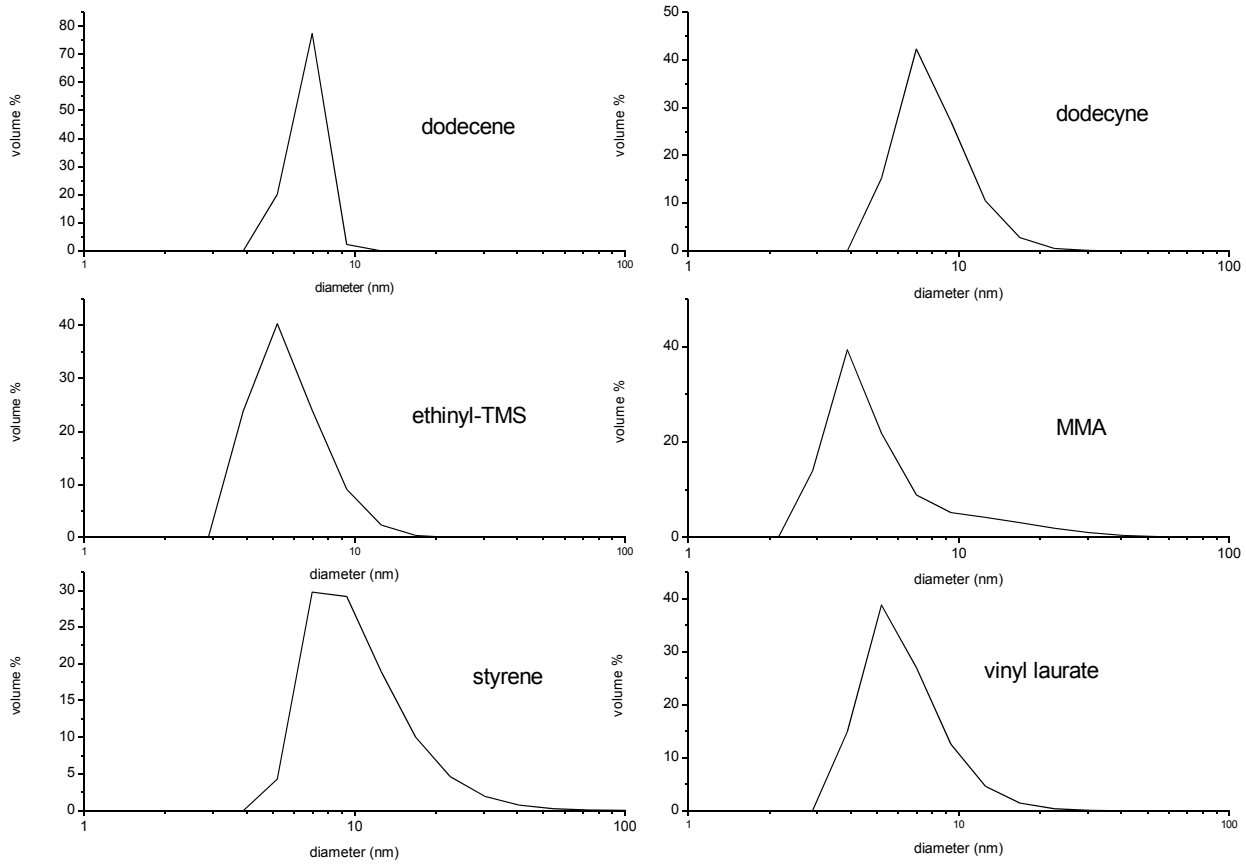

Figure S 4: DLS data of the functionalized SiNCs.

[1] H. M. Bank, M. E. Cifuentes, E. M. Theresa, *United States Pat.* **1991**, *5.010.159*.

[2] T. Part, *J. Am. Chem. Soc* **1927**, *40*, 1522–1527.

[3] H. Kajigaeshi, T. Kakinami, K. Inoue, M. Kondo, H. Nakamura, M. Fujikawa, T. Okamoto, *Bull. Chem. Soc. Jpn.* **1988**, *61*, 597–599.

[4] F. Mirkhalaf, J. Paprotny, D. J. Schiffrin, *J. Am. Chem. Soc.* **2006**, *128*, 7400–1.

[5] P. Doppelt, J. Pinson, F. Podvorica, S. Verneyre, V. Koso, R. V January, V. Re, M. Recei, V. May, *Chem. Mater* **2007**, *19*, 4570–4575.

6 Photoluminescent Silicon Nanocrystals with Chlorosilane Surfaces – Synthesis and Reactivity

Status	Published online: November 17, 2014
Journal	Nanoscale, 2015, Volume 7, 914-918.
Publisher	RSC Publishing
DOI	10.1039/C4NR05888G
Authors	Ignaz M. D. Höhlein, Julian Kehrle, Tapas K. Purkait, Jonathan G. C. Veinot, Bernhard Rieger

Höhlein et al. *Nanoscale* **2015**, *7*, 914-918. – Reproduced by permission of The Royal Society of Chemistry.

Content

The functionalization of SiNCs with nucleophiles is a challenging task. Commonly halogen terminated SiNCs are used for this purpose, however the halogen surface influences their optical properties and only blue photoluminescent SiNCs could be obtained so far. In this paper a straight forward two-step approach is presented to enable the reaction of hydride terminated SiNCs with nucleophiles. First, a reactive chlorosilane binding layer is formed on the SiNCs *via* hydrosilylation of chlorodimethyl(vinyl)silane. In the second step the terminal chlorosilane surface groups are used to bind various alcohols, silanols and organolithium reagents. As a side reaction, it is observed that organolithium compounds can also directly react with the silicon surface to a certain extend.

Nanoscale

COMMUNICATION

View Article Online
View Journal | View Issue

CrossMark click for updates

Cite this: *Nanoscale*, 2015, **7**, 914

Received 7th October 2014,
Accepted 10th November 2014

DOI: 10.1039/c4nr05888g

www.rsc.org/nanoscale

Photoluminescent silicon nanocrystals with chlorosilane surfaces – synthesis and reactivity†

Ignaz M. D. Höhlein,[a] Julian Kehrle,[a] Tapas K. Purkait,[b] Jonathan G. C. Veinot[b] and Bernhard Rieger*[a]

We present a new efficient two-step method to covalently functionalize hydride terminated silicon nanocrystals with nucleophiles. First a reactive chlorosilane layer was formed *via* diazonium salt initiated hydrosilylation of chlorodimethyl(vinyl)silane which was then reacted with alcohols, silanols and organolithium reagents. With organolithium compounds a side reaction is observed in which a direct functionalization of the silicon surface takes place.

Recently, silicon nanocrystals (SiNCs) have attracted great attention due to their unique properties such as size dependent photoluminescence and low toxicity.[1,2] Several applications including solar cells, LEDs, and photoluminescent biological probes have been realized based on SiNCs.[3–5]

Most common synthetic methods form SiNCs with either a hydride- or halogen terminated surface.[6–10] These reactive surfaces render SiNCs prone to oxidation under ambient conditions and they agglomerate in solution. To address these stability issues, the SiNCs need to be further functionalized. For hydride terminated SiNCs, the hydrosilylation reaction is abundantly used, where unsaturated carbon compounds react with the surface to form stable silicon–carbon bonds. However, conditions like high temperatures, UV radiation, radical initiators or the use of metal catalysts limit the possible molecules that can be bound on the surface and side reactions *e.g.*, oligomerizations need to be considered.[11–14]

Halogen terminated SiNCs react with nucleophiles such as alcohols as well as Grignard and organolithium reagents and therefore offer an alternative approach to functionalize SiNCs.[15,16] However, the halogen terminated surface alters the SiNC properties (*i.e.*, photoluminescence is quenched). Until now, only blue photoluminescent SiNCs have been reported based on halogen terminated SiNCs in contrast to the full optical spectrum with hydride terminated SiNCs.[17]

An alternative approach that contrasts direct functionalization of the SiNC surface is to first introduce reactive sites on the SiNCs that allow subsequent surface reactions. Gooding and Shiohara *et al.* showed this type of approach with bifunctional alkenes that were attached to SiNC surfaces *via* hydrosilylation.[18,19] For their NCs, the distal alkene moieties were reacted *via* thiol–ene "Click" chemistry or epoxidation and hydrolysis. This approach expands the scope of available reactions for derivatization, potentially limits any adverse effects that surface modification procedures may have on SiNC surfaces (*e.g.*, oxidation) and by extension preserves SiNC optical and electronic properties.

To prepare functionalized SiNCs, 100 mg of an etched $SiNC/SiO_2$ composite are reacted with ClDMVS (0.2 ml, 1.5 mmol) in 1 ml of dry and degassed toluene with the 4-decylbenzene diazonium tetrafluoroborate (1.5 mg, 4.6 μmol) radical initiator at room temperature for two hours (Scheme 1).[20] Afterward, the solvent and excess ClDMVS were removed *in vacuo*, giving SiNCs bearing chloro(dimethylethyl)-silane surfaces (*i.e.*, SiNC–SiCl) as an orange solid. In light of the sensitivity of SiNC–SiCl toward hydrolysis, no further purification was performed. The SiNC–SiCl were subsequently resuspended in 1 mL of dry toluene and reacted with

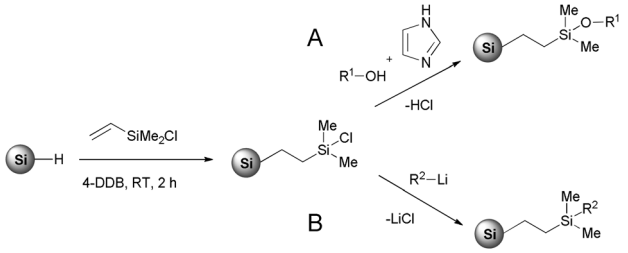

Scheme 1 Preparation of SiNCs with a chlorosilane surface *via* 4-decylbenzene diazonium tetrafluoroborate (4-DDB) induced hydrosilylation of chlorodimethyl(vinyl)silane (ClDMVS) and following reactions with (A) alcohols and silanols or (B) organolithium reagents.

[a]*Wacker-Lehrstuhl für Makromolekulare Chemie, Technische Universität München, Lichtenbergstraße 4, 85747 Garching, Germany. E-mail: rieger@tum.de*
[b]*Department of Chemistry, University of Alberta, Edmonton, Alberta T6G 2G2, Canada*

†Electronic supplementary information (ESI) available: Detailed experimental procedures and additional NMR, PL, EDX, DLS and TEM data. See DOI: 10.1039/C4NR05888G

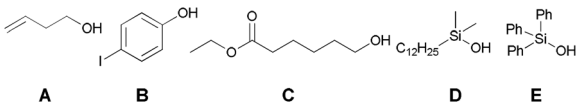

Fig. 1 Alcohols and silanols used for SiNC–SiCl functionalization. (A) 3-Buten-1-ol; (B) 4-iodophenol; (C) ethyl 6-hydroxy hexanoate; (D) dodecyldimethylsilanol; (E) triphenylsilanol.

0.5 mmol of the respective alcohol or silanol overnight. A small quantity of imidazole (*i.e.*, 2.0 mg, 29.4 μmol) was added to the reaction mixture to function as a base to trap the released HCl and as a nucleophilic catalyst for the reaction.[21] Finally, the particles were purified *via* three anti-solvent precipitation/centrifugation steps from acetonitrile.

SiNC–SiCl, reacted with 3-buten-1-ol (Fig. 1A), were analyzed using Fourier transform infrared (FTIR) spectroscopy. Unfunctionalized, hydride terminated SiNCs show only strong Si–H bands at 665, 906 and 2099 cm^{-1} and a small Si–O band at around 1050 cm^{-1} (Fig. 2A). Neat 3-buten-1-ol exhibits next to C–H bands at 1400 and 2900 cm^{-1} and the typical C=C–H and C=C bands at 3080 and 1642 cm^{-1}, respectively, a broad band at 3300 cm^{-1} from the C–OH functionality (Fig. 2B). For the functionalized SiNC–SiCl a strong IR band at 1258 cm^{-1} is found which can be attributed to the Si–Me groups of the silane. Also the C=C–H and C=C bands from the endstanding double bond are still visible (Fig. 2C). The C–OH band at 3300 cm^{-1} disappears and a strong Si–O band at 1050 cm^{-1} rises due to the formation of a silyl ether. Residual hydride is present in every case but this is expected since the hydrosilylation of ClDMVS cannot be complete due to steric hindrance.[22] These findings are also supported by NMR measurements of the functionalized SiNC–SiCl (ESI Fig. S1†).

SiNC–SiCl were reacted with 4-iodophenol, ethyl 6-hydroxy hexanoate, dodecyldimethylsilanol and triphenylsilanol

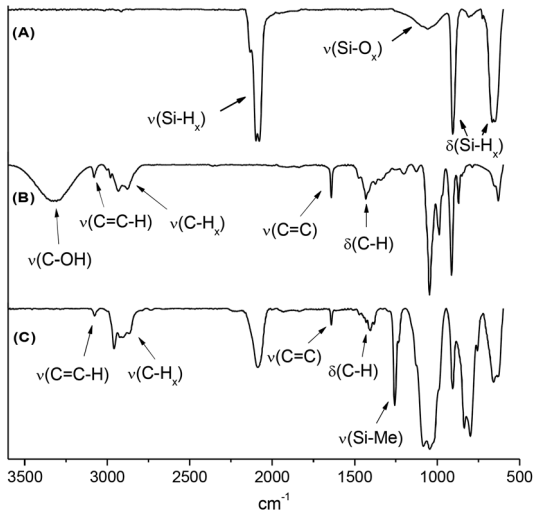

Fig. 2 FTIR spectra of (A) unfunctionalized, hydride terminated SiNCs; (B) neat 3-buten-1-ol; (C) SiNC–Cl reacted with 3-buten-1-ol.

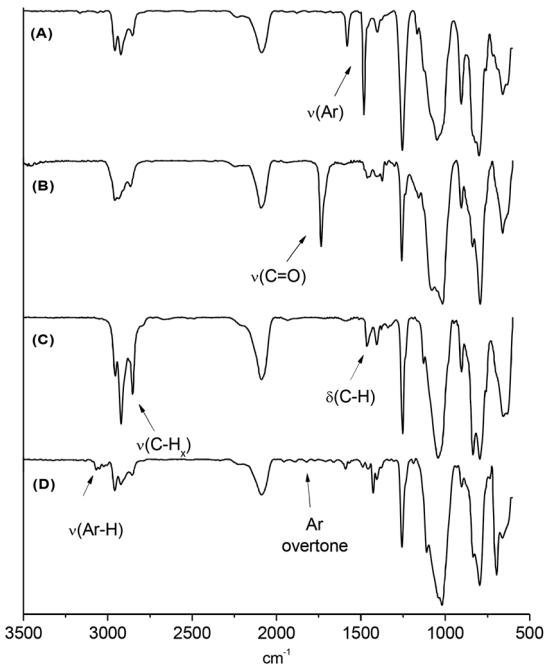

Fig. 3 FTIR spectra of SiNC–SiCl reacted with (A) 4-iodophenol; (B) ethyl 6-hydroxy hexanoate; (C) dodecyldimethylsilanol; (D) triphenylsilanol.

(Fig. 1B–E) to prove the versatility of the reaction procedure. In all cases the characteristic FTIR bands for each bound surface group are visible (Fig. 3A–D) and the absence of the R–OH bands shows that the separation from unreacted alcohols or silanols was successful.

All functionalized SiNC–SiCl show photoluminescence (PL) upon exposure to UV excitation with a maximum at *ca.* 690 nm (ESI Fig. S3†). A representative PL spectrum of SiNC–SiCl functionalized with 3-buten-1-ol is shown in Fig. 4. The hydrodynamic radii of the functionalized SiNC–SiCl determined by dynamic light scattering (DLS) vary between 2.6 and 4.0 nm (ESI Table S3†) indicating that no crosslinking or agglomeration of the SiNC–SiCl occurs.

To functionalize SiNC–SiCl using organolithium reagents (Scheme 1B), a procedure analogous to that used for alcohol

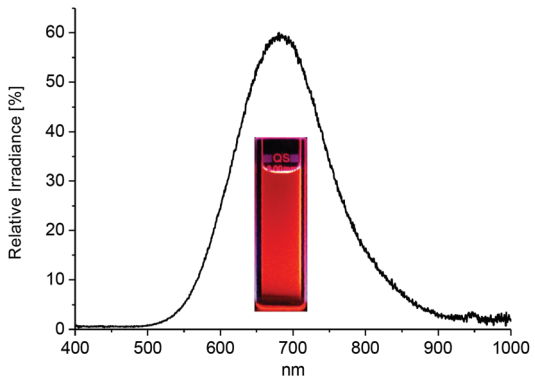

Fig. 4 PL spectrum of SiNC–SiCl functionalized with 3-buten-1-ol.

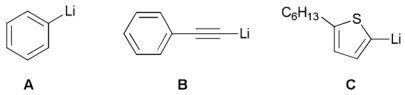

Fig. 5 Organolithium reagents that were used for the reaction with SiNC–SiCl and SiNC–SiMe. (A) Phenyllithium; (B) lithium phenylacetylide; (C) (5-hexyl-2-thienyl)lithium.

and silanol modification was employed. The organolithium reagents of choice (Fig. 5) were reacted with SiNC–SiCl overnight and precipitation was performed using acidified methanol.

Absorptions arising from Si–Me and C–H structural units of the silane binding layer are obvious in the FTIR spectra of SiNC–SiCl functionalized with phenyllithium, lithium phenylacetylide, and (5-hexyl-2-thienyl)lithium (Fig. 6A1–C1). The Si–O region at 1050 cm^{-1} is less dominant compared to that of the products from the reactions with alcohols; this difference is reasonably attributed to the linkage now being a Si–C bond. The IR spectra also show evidence of absorption bands arising from the respective surface groups introduced during derivatization (*e.g.*, C≡C at 2250 cm^{-1} from phenylacetylene and aromatic C–H bands at 3100 cm^{-1}).

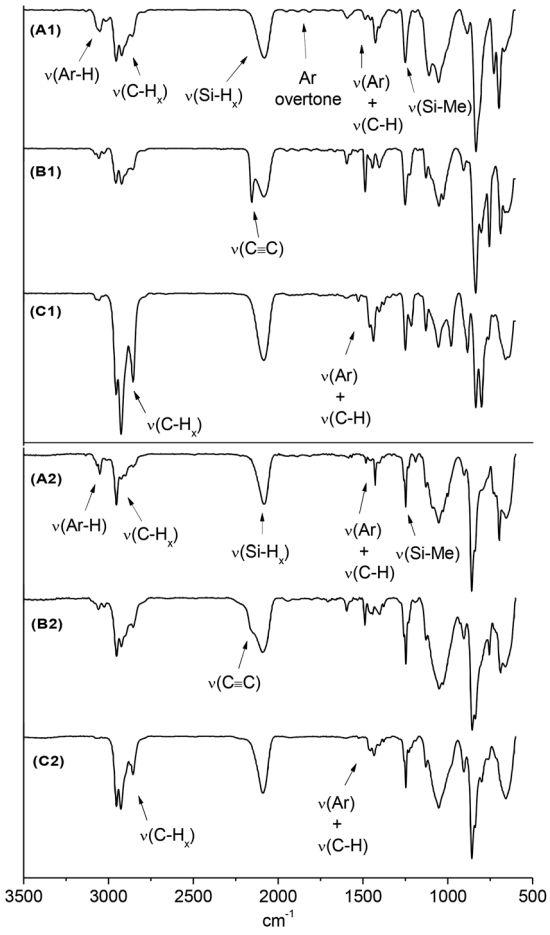

Fig. 6 FTIR spectra of SiNC–SiCl reacted with (A1) phenyllithium, (B1) lithium phenylacetylide, (C1) (5-hexyl-2-thienyl)lithium; (A2–C2) show the FTIR spectra of the same organolithium compounds reacted with SiNC–SiMe.

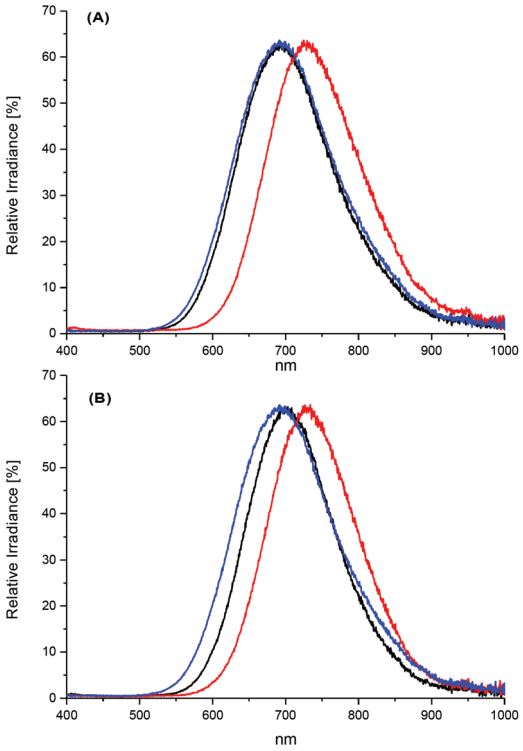

Fig. 7 (A) PL spectra of SiNC–SiCl reacted with phenyllithium (black), (5-hexyl-2-thienyl)lithium (blue) and lithium phenylacetylide (red); (B) PL spectra of SiNC–SiMe reacted with the same organolithium compounds.

The PL spectra for the hexylthiophene and phenyl functionalized SiNC–SiCl show PL maxima at *ca.* 690 nm, similar to the alcohol and silanol functionalized SiNC–SiCl (Fig. 7A). The PL from phenylacetylene functionalized SiNCs is less intense and is shifted to lower energy at *ca.* 740 nm (ESI Fig. S4†). The origin of the observed red-shift and decreased PL intensity is not obvious. Recent reports from our group show that the impact of surface chemistry on the SiNC optical and electronic response can be dramatic and complex.[23,24] While it is known that the direct attachment of phenylacetylene to SiNCs *via* hydrosilylation results in complete PL quenching, we had reasonably anticipated that the ethylsilyl layer on the SiNC–SiCl would isolate the SiNC core from the electronic effects of the phenylacetylene – clearly this is not the case.[12]

In light of our earlier observations involving PL quenching upon direct functionalization with phenylacetylene one possibility is the direct reaction of the organolithium reagents with the SiNC surface.[12] Reactions of this type are known for nanocrystalline porous silicon surfaces and aryllithium and Grignard reagents.[25,26] It is reasonable that SiNCs will react in a similar fashion. To explore this option, SiNCs were hydrosilylated with vinyltrimethylsilane (VTMS) as noted above to yield an ethyltrimethyl silyl surface (*i.e.*, SiNC–SiMe). The sub-

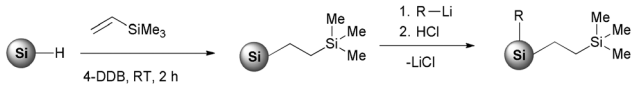

Scheme 2 Preparation of SiNC with a ethyl(trimethyl)silane surface and reaction with organolithium compounds.

sequent reaction of these SiNC–SiMe particles with organolithium compounds (Fig. 5) will provide a direct probe for the reaction of organolithium reagents at the SiNC surface (Scheme 2).

In all cases, the FTIR spectra of the SiNC–SiMe treated with the organolithium compounds show features consistent with the direct surface reaction as noted in Fig. 6A2–C2.

To obtain a semi-quantitative understanding of the present reaction, EDX measurements were performed for the hexylthiophene functionalized SiNC–SiCl and SiNC–SiMe. With SiNC–SiCl a Si : Si weight ratio of approx. 0.16 is found whereas for SiNC–SiMe it is only 0.06 (ESI Table S2†). These data are consistent with the reaction of the organolithium reagent occurring primarily at the chlorosilane moieties and to a lesser extent at the SiNC surface.

Consistent with the proposal that a direct reaction between lithium phenylacetylide and the underlying SiNC surface is occurring, the PL spectra of phenyl and hexylthiophene functionalized SiNC–SiMe show the expected PL maximum at *ca*. 690 nm whereas those reacted with lithium phenylacetylide show a red-shifted PL at 740 nm (Fig. 7B). Ongoing studies are aimed at elucidating the origin of these spectral changes.

To our knowledge, this is the first report that freestanding SiNCs with a non-halogenated surface can directly be functionalized with organometallic reagents and that the photoluminescence of the SiNCs is influenced in this way. This discovery offers new interesting options to alter the properties of SiNCs and will be studied more thoroughly in future work.

Regarding the stability of the prepared SiNCs, no degradation of the PL over a timeframe of months is observed for all functionalized SiNCs. Also no agglomeration is visible for SiNCs functionalized with organolithium reagents and silanols. When SiNC–SiCl functionalized with alcohols are dispersed in solvents that are not dried prior to use, formation of agglomerates can be observed over the course of weeks. This is possibly due to the slow hydrolysis of the Si–O–C bonds which are less stable than the Si–C or Si–O–Si bonds.

Conclusions

In summary, we report a new method for functionalizing SiNC surfaces with nucleophiles *via* a two-step process. First a chlorosilane layer is introduced to the SiNCs by hydrosilylation of chlorodimethyl(vinyl)silane. The surface bonded chlorosilane moieties are then subsequently reacted with nucleophiles such as alcohols and silanols. In contrast to the equivalent reaction of chloride terminated SiNCs, the PL properties of the SiNCs are not altered by the chlorosilane binding layer. Subsequent reaction with organolithium compounds provides further surface tailorability. Of important note, a side reaction between the underlying SiNC surface and organolithium reagents leads to direct functionalized SiNCs. These results open new opportunities for surface functionalization of SiNCs which is an important step to incorporate SiNCs in future applications.

Notes and references

1 A. Gupta, M. T. Swihart and H. Wiggers, *Adv. Funct. Mater.*, 2009, **19**, 696–703.
2 R. D. Tilley and K. Yamamoto, *Adv. Mater.*, 2006, **18**, 2053–2056.
3 K.-Y. Cheng, R. Anthony, U. R. Kortshagen and R. J. Holmes, *Nano Lett.*, 2010, **10**, 1154–1157.
4 C. Liu, Z. C. Holman and U. R. Kortshagen, *Nano Lett.*, 2009, **9**, 449.
5 J. Liu, F. Erogbogbo, K.-T. Yong, L. Ye, J. Liu, R. Hu, H. Chen, Y. Hu, Y. Yang, J. Yang, *et al.*, *ACS Nano*, 2013, **7**, 7303–7310.
6 C. M. Hessel, E. J. Henderson and J. G. C. Veinot, *Chem. Mater.*, 2006, **18**, 6139–6146.
7 J. L. Heinrich, C. L. Curns, G. M. Credo, K. L. Kavanagh and M. J. Sailor, *Science*, 1992, **255**, 66–68.
8 X. Li, Y. He, S. S. Talukdar and M. T. Swihart, *Langmuir*, 2013, **19**, 8490–8496.
9 R. K. Baldwin, K. a. Pettigrew, E. Ratai, M. P. Augustine and S. M. Kauzlarich, *Chem. Commun.*, 2002, 1822–1823.
10 C. Yang, R. A. Bley, S. M. Kauzlarich, H. W. H. Lee and G. R. Delgado, *J. Am. Chem. Soc.*, 1999, **121**, 5191–5195.
11 R. D. Tilley, J. H. Warner, K. Yamamoto, I. Matsui and H. Fujimori, *Chem. Commun.*, 2005, 1833–1835.
12 J. A. Kelly and J. G. C. Veinot, *ACS Nano*, 2010, **4**, 4645–4656.
13 J. Nelles, D. Sendor, A. Ebbers, F. M. Petrat, H. Wiggers, C. Schulz and U. Simon, *Colloid Polym. Sci.*, 2007, **285**, 729–736.
14 Z. Yang, M. Iqbal, A. R. Dobbie and J. G. C. Veinot, *J. Am. Chem. Soc.*, 2013, **135**, 17595–17601.
15 C. Yang, R. A. Bley, S. M. Kauzlarich and H. W. H. Lee, *J. Am. Chem. Soc.*, 1999, **121**, 5191–5195.
16 J. Zou, R. K. Baldwin, K. a. Pettigrew and S. M. Kauzlarich, *Nano Lett.*, 2004, **4**, 1181–1186.
17 X. Cheng, S. B. Lowe, P. J. Reece and J. J. Gooding, *Chem. Soc. Rev.*, 2014, **43**, 2680–2700.
18 X. Cheng, R. Gondosiswanto, S. Ciampi, P. J. Reece and J. J. Gooding, *Chem. Commun.*, 2012, **48**, 11874–11876.
19 A. Shiohara, S. Hanada, S. Prabakar, K. Fujioka, T. H. Lim, K. Yamamoto, P. T. Northcote and R. D. Tilley, *J. Am. Chem. Soc.*, 2010, **132**, 248–253.

20 I. M. D. Höhlein, J. Kehrle, T. Helbich, Z. Yang, J. G. C. Veinot and B. Rieger, *Chem. – Eur. J.*, 2014, **20**, 4212–4216.
21 S. Rubinsztajn, *J. Org. Chem.*, 1989, **367**, 27–37.
22 L. Scheres, B. Rijksen, M. Giesbers and H. Zuilhof, *Langmuir*, 2011, **27**, 972–980.
23 O. Wolf, M. Dasog, Z. Yang, I. Balberg, J. G. C. Veinot and O. Millo, *Nano Lett.*, 2013, **13**, 2516–2521.
24 M. Dasog, G. B. De Los Reyes, L. V. Titova, F. A. Hegmann and J. G. C. Veinot, *ACS Nano*, 2014, **8**, 9636–9648.
25 N. Y. Kim and P. E. Laibinis, *J. Am. Chem. Soc.*, 1998, **120**, 4516–4517.
26 J. H. Song and M. J. Sailor, *J. Am. Chem. Soc.*, 1998, **120**, 2376–2381.

Supplementary Information

Photoluminescent Silicon Nanocrystals with Chlorosilane Surfaces – Synthesis and Reactivity

Ignaz M. D. Höhlein, Julian Kehrle, Tapas K. Purkait, Jonathan G. C. Veinot and Bernhard Rieger*

Table of contents

Experimental Procedures 2
General Information 2
Preparation of oxide-embedded silicon nanocrystals 2
Liberation of SiNCs 2
Hydrosilylation of SiNCs with chlorodimethyl(vinyl)silane or trimethylvinylsilane 2
Functionalization of SiNC-SiCl with alcohols and silanols 3
Functionalization of SiNC-SiCl and SiNC-SiMe with organolithium reagents 3
Synthesis of (5-hexyl-2-thienyl)lithium 3
Synthesis of lithium phenylacetylide 3
Analytical Data 4
Nuclear Magnetic Resonance Spectroscopy (NMR) 4
Energy Dispersive X-ray Spectroscopy (EDX) 5
Photoluminescence Spectroscopy (PL) 6
Dynamic Light Scattering (DLS) 7
Transmission Electron Microscopy (TEM) 7

Experimental Procedures

General Information

All reactants and reagents were purchased from Sigma-Aldrich and used without further purification if not stated otherwise. 1-Butenol and ethyl 6-hydroxyhexanoate and dodecyldimethylsilanol were dried over activated molecular sieve (3Å) prior to use. Dry toluene was obtained from a MBraun SPS 800 solvent purification system. Fourier transform infrared (FTIR) spectra were measured with a *Bruker Vertex 70 FTIR* using a *Platinum ATR* from *Bruker*. Nuclear magnetic resonance (NMR) spectra were measured on a *ARX*-300 from Bruker in deuterated chloroform at 300 K. Dynamic light scattering measurements were made with a *Dyna Pro NanoStar* from *Wyatt* with toluene as solvent. Photoluminescence (PL) spectra were taken with a *AVA-Spec 2048* from *Avantes* using a *Prizmatix (LED Current controller)* as light source. Electron dispersive X-ray spectra (EDX) were measured with an *Oxford Instruments SwiftED-TM* coupled to a *Hitachi Tabletop Microscope TM-1000*. Transmission electron microscopy was performed using a *JEOL-2010* (LaB 6 fi lament) electron microscope with an accelerating voltage of 200 keV. TEM samples of SiNCs were drop-casted onto a holey carbon coated copper grid (SPI supplies) and the solvent was evaporated in vacuum. X-ray photoelectron spectroscopy (XPS) analyses were performed using a *Kratos Axis Ultra* instrument operating in energy spectrum mode at 210 W. A monochromatic Al Kα source (λ = 8.34 Å) was used to irradiate the samples, and the spectra were obtained with an electron takeoff angle of 90°.

Preparation of oxide-embedded silicon nanocrystals

Polymeric hydrogen silsesquioxane (HSQ) was prepared following a literature procedure.[1]
HSQ (7 g) was placed in a quartz reaction boat, transferred to a *Nabertherm RD 30/200/11* oven with quartz working tube and heated from ambient to a peak processing temperature of 1100 °C at 18 °C min in a slightly reducing atmosphere (5% H_2/95% N_2). The sample was maintained at the peak processing temperature for 1 h. Upon cooling to room temperature, the resulting amber solid was ground into a fine brown powder using mortar and pestle to remove large particles. Further grinding was achieved via shaking the powder for 12 h with high-purity silica beads using a *WAB Turbula mixer*. The resulting SiNC/SiO_2 composite powder was stored in standard glass vials.

Liberation of SiNCs

Hydride-terminated SiNCs were liberated from the SiNC/SiO_2 composites using HF etching. First, 100 mg of the ground SiNC/SiO_2 composite was transferred to an ethylene-tetrafluoroethylene (ETFE) beaker equipped with a Teflon-coated stir bar. Ethanol (1.0 mL) and water (1.0 mL) were then added under mechanical stirring to form a brown suspension, followed by 1.0 mL of 49% HF aqueous solution. After 1 h of etching in subdued light, the suspension appeared yellow. Hydride-terminated SiNCs were subsequently extracted from the aqueous layer into ca. 30 mL of toluene by multiple (i.e., 3 × 10 mL) extractions. The SiNC toluene suspension was transferred to ETFE-centrifuge tubes, and the SiNCs were isolated by centrifugation at 5000 rpm.

Hydrosilylation of SiNCs with chlorodimethyl(vinyl)silane or trimethylvinylsilane

SiNC/SiO_2 composite (100 mg) was etched according the described procedure. After extraction and centrifugation, the resulting H-terminated SiNCs were resuspended in a mixture of 1 ml of dried toluene and chlorodimethyl(vinyl)silane (0.2 ml, 1.5 mmol) or trimethylvinylsilane (0.3 ml, 1.5 mmol) respectively. The dispersion was degassed via three freeze-pump-thaw cycles. Afterwards 4-

decylbenzene diazonium tetrafluoroborate (1.5 mg, 4.6 µmol) was added to start the hydrosilylation. After two hours, solvent and excess silane was removed *in vacuo* to give the functionalized SiNC-SiCl/SiNC-SiMe. Since SiNC-SiCl are very sensitive towards hydrolysis and agglomeration via crosslinking in this state, they were used without further purification.

Functionalization of SiNC-SiCl with alcohols and silanols

The SiNC-SiCl were resuspended in toluene (1.0 ml) and the respective alcohol or silanol (0.5 mmol) was added followed by imidazole (2.0 mg, 0.03 mmol) and the reaction mixture was allowed to stir over night. Afterwards, the solution was filtered through a 0.45 µm Teflon-syringe filter and the functionalized SiNC-SiCl were precipitated with acetonitrile and centrifuged at 9000 rpm. The centrifugate was resuspended in a minimal amount of toluene and precipitated again with acetonitrile. This procedure was repeated three times in total. Finally, the functionalized SiNCs were suspended in toluene and stored in vials for further use.

Functionalization of SiNC-SiCl and SiNC-SiMe with organolithium reagents

The SiNC-SiCl or SiNC-SiMe respectively were resuspended in toluene (1 ml) and the organolithium reagents, phenyllithium (~1.9 M in dibutylether, 0.2 mmol, 0.1 ml), lithium phenylacetylide or 5-hexyl-2-thienyl)lithium respectively (~1 M in THF/hexane, 0.2 mmol, 0.2 ml) were added to the reaction mixture and allowed to stir over night. Afterwards the functionalized SiNC were precipitated with MeOH, acidified with conc. HCl and centrifuged, followed by two precipitation/centrifugation steps with pure methanol. The functionalized SiNCs were suspended in toluene, filtered through a 0.45 µm Teflon-syringe filter and stored in vials for further use.

Synthesis of (5-hexyl-2-thienyl)lithium

2-hexylthiophene was prepared following literature procedures.[2]
2-hexylthiophene (0.84 g, 5.0 mmol) was dissolved in dry THF (2.1 ml) and cooled to -78°C. Afterwards *n*-BuLi (2.5 M in hexanes, 2 ml, 5.0 mmol) was added slowly. The solution was warmed to room temperature and used without further purification.

Synthesis of lithium phenylacetylide

Phenylacetylene (0.51 g, 5.0 mmol) was dissolved in dry THF (2.1 ml) and cooled to -78°C. Afterwards *n*-BuLi (2.5 M in hexanes, 2 ml, 5.0 mmol) was added slowly. The solution was warmed to room temperature and used without further purification.

Analytical Data

Nuclear Magnetic Resonance Spectroscopy (NMR)

NMR measurements of SiNC-SiCl functionalized with 3-buten-1ol were conducted (Figure S1). The intermediate product, SiNCs functionalized only with dimethyl(vinyl)chlorosilane, is very instable towards hydrolysis and could therefore not be isolated.
The protons from the double bond of dimethyl(vinyl)chlorosilane (X, Y, Z) around 6 ppm are not found in the functionalized SiNC-SiCl since the double bond reacts in the hydrosilylation reaction. The two formed silicon bound methylene groups (M, N) should appear at around 0.5 ppm, however in this region, no signal is present.[3] This observation was made by several other groups that worked with SiNCs in the size range of a few nanometers.[4–6] A possible explanation is that the signals cannot be detected due to a broadening induced by the anisotropic surrounding and a prolonged relaxation time since the movement of the molecules is hindered on the SiNC surface. The protons of the two Si–Me groups of dimethyl(vinyl)chlorosilane at 0.5 ppm (A) are shifted upfield towards 0.1 ppm at the functionalized SiNC-SiCl, due to the absence of the electron withdrawing chlorine atom on the silicon. The proton signals of 3-buten-1-ol (B-E) are all present when bound on the SiNC-SiCl with the exception of the OH-Proton (G) at 2.0 ppm which is consumed during the reaction with the chlorosilane surface.

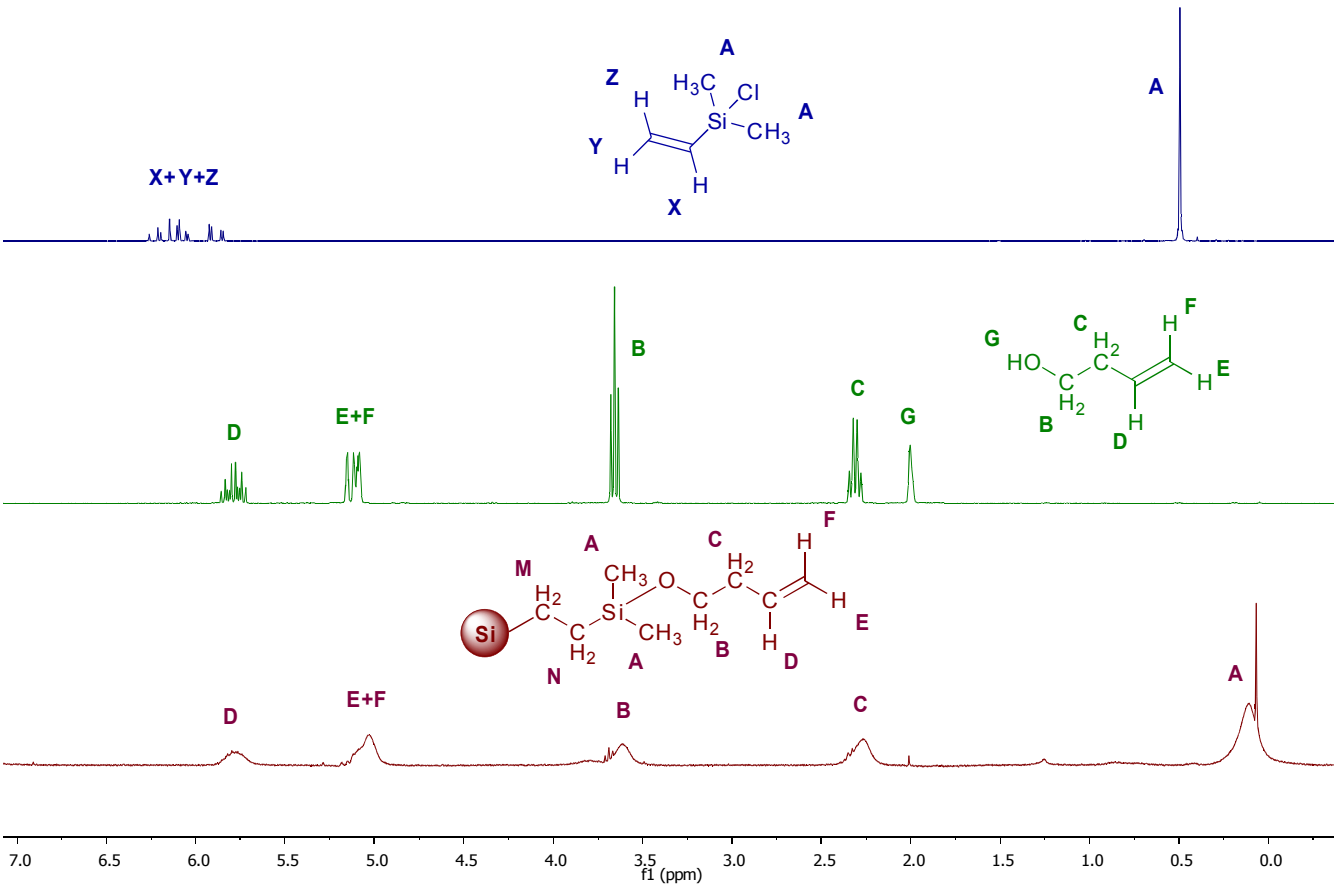

Figure S1: NMR spectrum of dimethyl(vinyl)chlorosilane (top, blue), 3-buten-1-ol (middle, green) and SiNC-SiCl reacted with 3-buten-1-ol (bottom, red).

Energy Dispersive X-ray Spectroscopy (EDX)

EDX analysis of the functionalized SiNC-SiCl shows only small amounts of residual chlorine left on the particles (Table S 1).

Table S 1: EDX data of the functionalized SiNC-SiCl. The values are given as weight percent and were averaged from at least five different measuring spots. Only elements with a molecular weight higher than ^{11}Na can be detected with the *Oxford Instruments SwiftED-TM*, therefore carbon and oxygen are not listed

Nucleophile	Si [wt%]	Cl [wt%]	I [wt%]
3-buten-1-ol	99.1	0.9	
4-iodophenol	73.6	1.2	25.2
ethyl 6-hydroxy hexanoate	99.2	0.8	
triphenylsilanol	98.2	1.8	
dodecyldimethylsilanol	97.7	2.3	
phenyllithium	99.6	0.4	
lithium phenylacetylide	97.7	2.3	

EDX results from SiNC-SiCl and SiNC-SiMe, functionalized with (5-hexyl-2-thienyl)lithium give with 0.16 to 0.06 a considerably higher silicon to sulphur ratio for the chlorosilane terminated SiNCs (Table S2).

Table S 2: EDX data of the functionalized SiNC-SiCl and SiNC-SiMe, functionalized with (5-hexyl-2-thienyl)lithium in weight percent.

Silane	Si [wt%]	S [wt%]	Cl [wt%]	S:Si (weight ratio)
ClVDMS	86.0	13.8	0.2	0.16
VTMS	94.1	5.9		0.06

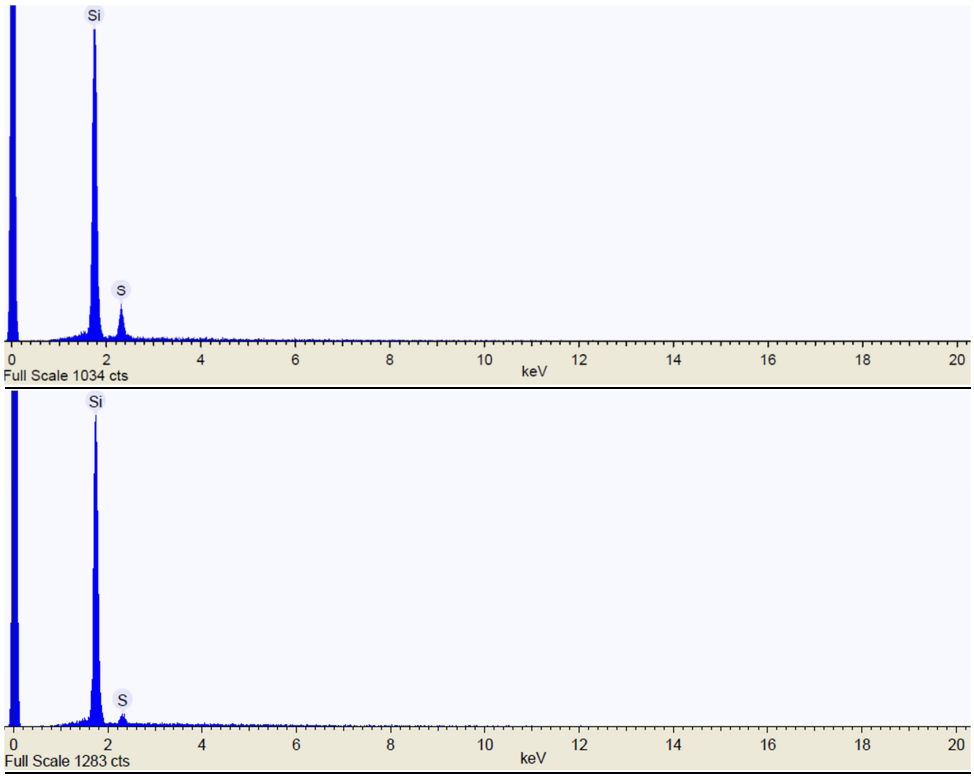

Figure S 2: EDX spectrum of SiNC-SiCl (top) and SiNC-SiMe (bottom) functionalized with (5-hexyl-2-thienyl)lithium.

Photoluminescence Spectroscopy (PL)

PL spectra of SiNC-SiCl functionalized with various alcohols and silanols all have an intensity maximum around 690 nm (Figure S3)

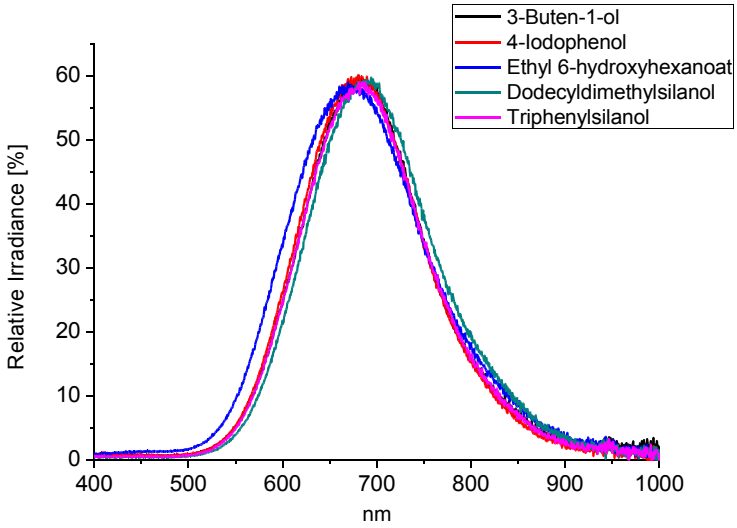

Figure S 3: PL spectra of SiNC-SiCl under 365 nm UV radiation, functionalized with 3-buten-1-ol, 4-iodophenol, ethyl 6-hydroxyhexanoat, dodecyldimethylsilanol and triphenylsilanol.

SiNC-SiCl reacted with lithium phenylacetylide show PL with a lesser intensity (Figure S4 B) than SiNC-SiCl functionalized with phenyllithium and (5-hexyl-2-thienyl)lithium (Figure S4 A, C).

Figure S 4: Solutions of SiNC-SiCl functionalized with phenyllithium (A), lithiuim phenylacetylide (B) and (5-hexyl-2-thienyl)lithium (C) under 365 nm UV radiation.

Dynamic Light Scattering (DLS)

The hydrodynamic radii of the functionalized SiNC are all in a size range for freestanding SiNCs therefore it can be assumed that no agglomeration of the SiNC takes place.[7]

Table S 3: DLS data of the functionalized SiNC-SiCl and SiNC-SiMe.

Silane	Nucleophile	Hydrodynamic radius [nm]	Polydispersity %
ClDMVS	3-buten-1-ol	2.6	42.1
ClDMVS	4-iodophenol	4.2	45.7
ClDMVS	ethyl 6-hydroxy hexanoate	4.0	46.9
ClDMVS	triphenylsilanol	3.4	41.1
ClDMVS	dodecyldimethylsilanol	3.0	37.0
ClDMVS	phenyllithium	2.6	26.2
ClDMVS	lithium phenylacetylide	2.9	30.4
ClDMVS	(5-hexyl-2-thienyl)lithium	2.9	15.4
VTMS	phenyllithium	1.9	29.5
VTMS	lithium phenylacetylide	2.6	41.4
VTMS	(5-hexyl-2-thienyl)lithium	1.8	37.2

Transmission Electron Microscopy (TEM)

A TEM picture of SiNC-SiCl functionalized with (5-hexyl-2-thienyl)lithium shows the single SiNCs (Figure S6).

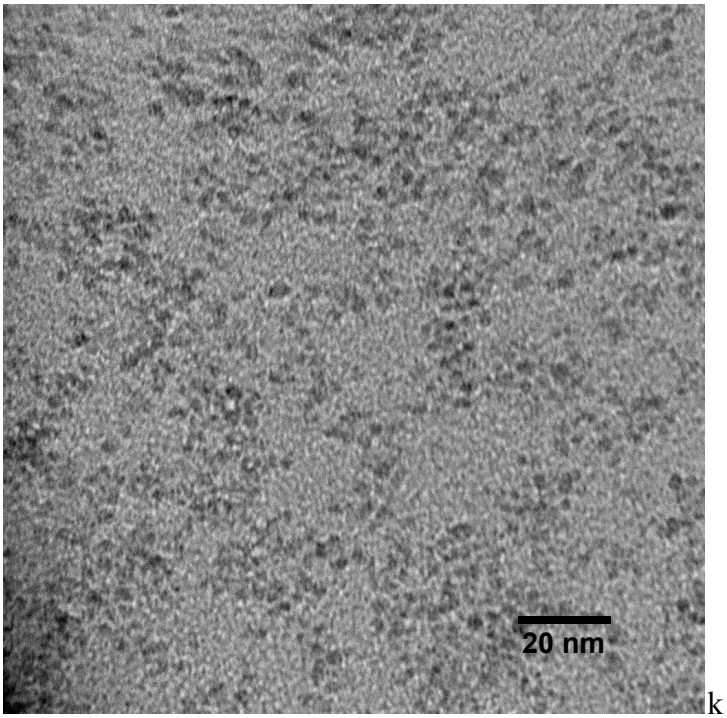

k

Figure S 5: TEM-picture of SiNCs-SiCl functionalized with (5-hexyl-2-thienyl)lithium.

References

(1) Bank, H. M.; Cifuentes, M. E.; Theresa, E. M. *United States Pat.* **1991**, *5.010.159*.

(2) Xia, C.; Fan, X.; Locklin, J.; Advincula, R. C. *Org. Lett.* **2002**, *4*, 2067.

(3) Biesta, W.; van Lagen, B.; Gevaert, V. S.; Marcelis, A. T. M.; Paulusse, J. M. J.; Nielen, M. W. F.; Zuilhof, H. *Chem. Mater.* **2012**, *24*, 4311.

(4) Shirahata, N.; Linford, M. R.; Furumi, S.; Pei, L.; Sakka, Y.; Gates, R. J.; Asplund, M. C. *Chem. Commun. (Camb).* **2009**, 4684.

(5) Ahire, J. H.; Wang, Q.; Coxon, P. R.; Malhotra, G.; Brydson, R.; Chen, R.; Chao, Y. *ACS Appl. Mater. Interfaces* **2012**, *4*, 3285.

(6) Shiohara, A.; Hanada, S.; Prabakar, S.; Fujioka, K.; Lim, T. H.; Yamamoto, K.; Northcote, P. T.; Tilley, R. D. *J. Am. Chem. Soc.* **2010**, *132*, 248.

(7) Kelly, J. A.; Veinot, J. G. C. *ACS Nano* **2010**, *4*, 4645.

7 Functionalization of Hydride-Terminated Photoluminescent Silicon Nanocrystals with Organolithium Reagents

Status	Published online: December 22, 2014
Journal	Chemistry - A European Journal, 2015, Volume 21, 2755-2758.
Publisher	Wiley-Blackwell
DOI	10.1002/chem.201405555
Authors	Ignaz M. D. Höhlein, Arzu Angı, Regina Sinelnikov, Jonathan G. C. Veinot, Bernhard Rieger

Content

The hydrosilylation reaction is the most common synthetical approach to functionalize hydride terminated SiNCs. However, since an alkene or alkyne group is necessary, restrictions apply concerning the molecules that can be bound on the surface. In this communication the reaction of hydride terminated SiCNs with organolithium reagents is presented. Using this method, SiNCs with a variety surface moieties, including covalently bound alkynes and aromatic groups are accessible. The reaction is proposed to proceed *via* cleavage of Si–Si bonds and the formation of a reactive Si–Li surface species. In a second step, the Si–Li groups can be quenched with electrophiles such as protons, epoxides or alkylbromides to obtain SiNCs with mixed surface functionalities. Also since the Si–H of the SiNC surface are not consumed in the reaction, subsequent hydrosilylation can be applied.

JOHN WILEY AND SONS LICENSE TERMS AND CONDITIONS

Apr 07, 2015

This Agreement between Ignaz Hoehlein ("You") and John Wiley and Sons ("John Wiley and Sons") consists of your license details and the terms and conditions provided by John Wiley and Sons and Copyright Clearance Center.

License Number	3566110308214
License date	Feb 11, 2015
Licensed Content Publisher	John Wiley and Sons
Licensed Content Publication	Chemistry - A European Journal
Licensed Content Title	Functionalization of Hydride-Terminated Photoluminescent Silicon Nanocrystals with Organolithium Reagents
Licensed Content Author	Ignaz M. D. Höhlein,Arzu Angı,Regina Sinelnikov,Jonathan G. C. Veinot,Bernhard Rieger
Licensed Content Date	Dec 22, 2014
Pages	4
Type of use	Dissertation/Thesis
Requestor type	Author of this Wiley article
Format	Print and electronic
Portion	Full article
Will you be translating?	No
Title of your thesis / dissertation	New Methods for the Surface Functionalization of Photoluminescent Silicon Nanocrystals
Expected completion date	Jun 2015
Expected size (number of pages)	100
Requestor Location	Ignaz Hoehlein Technische Universität München Lichtenbergstraße 4 Garching bei München, Germany 85747 Attn: Ignaz Hoehlein
Billing Type	Invoice
Billing Address	Ignaz Hoehlein Technische Universität München Lichtenbergstraße 4 Garching bei München, Germany 85747 Attn: Ignaz Hoehlein
Total	0.00 USD

ChemPubSoc Europe

DOI: 10.1002/chem.201405555

CHEMISTRY
A European Journal
Communication

Surfaces and Interfaces |Hot Paper|

Functionalization of Hydride-Terminated Photoluminescent Silicon Nanocrystals with Organolithium Reagents

Ignaz M. D. Höhlein,[a] Arzu Angı,[a] Regina Sinelnikov,[b] Jonathan G. C. Veinot,[b] and Bernhard Rieger*[a]

Abstract: Hydride-terminated photoluminescent silicon nanocrystals (SiNCs) were functionalized with organolithium compounds. The reaction is proposed to proceed through cleavage of Si–Si bonds and formation of a Si–Li surface species. The method yields colloidally stabilized SiNCs at room temperature with short reaction times. SiNCs with mixed surface functionalities can be prepared in an easy two-step reaction by this method by quenching of the Si–Li group with electrophiles or by addressing free Si–H groups on the surface with a hydrosilylation reaction.

Nanomaterials have gained great interest in recent years due to differing properties in contrast to their bulk material counterparts, such as size-dependent optical properties, for example, photoluminescence. Silicon nanocrystals (SiNCs) are of special interest, because they are comparably non-toxic in contrast to often used heavy metal-containing materials and therefore biocompatible.[1] In addition, the abundance of silicon makes it a promising precursor for the production of low-cost nanomaterials. A variety of applications have been realized by using SiNCs including solar cells, photoluminescent biomarkers, and light-emitting diodes (LEDs).[1–3]

Due to the high surface-to-volume ratio of nanomaterials, the control over their surface chemistry is of crucial importance. This is especially true for SiNCs, because silicon is oxidized under ambient conditions by water or oxygen. Also, different surface groups influence the photoluminescence of SiNCs.[4,5] In addition, a surface functionalization is needed to render the SiNCs soluble in various solvents. Finding new ways to modify and protect the surface of SiNCs is therefore an attractive target.

The most common synthetic ways form SiNCs with a silicon hydride (Si–H)-terminated surface.[6–9] To functionalize these SiNCs, the hydrosilylation reaction is normally used. A compound with a double or triple bond forms a covalent Si–C bond through addition reaction with the Si–H surface group. The hydrosilylation can be induced thermally, by UV irradiation, radical initiators, or Lewis acids.[8,10–12] A drawback of the hydrosilylation reaction is that no aryl- or alkinyl-groups can be bound directly to the SiNCs surface. However, these groups with conjugated π-systems could be promising for application in electronic devices, because they might offer the possibility of charge transfer from or to the SiNCs.

SiNCs can be synthesized with a halogen (Si–X, X = Br, Cl) instead of a hydrogen-terminated surface as well.[13,14] These SiNCs offer a different reactivity, because the Si–X bond can be attacked by nucleophiles including organometallic compounds. This reaction path allows the functionalization of SiNCs with conjugated molecules, such as phenyl groups. The halogen-terminated surface itself, however, alters the properties of the SiNCs, and up to date, only blue photoluminescent SiNCs have been reported in contrast to the full visible spectrum with hydride-terminated SiNCs.[15]

Organolithium compounds and Grignard reagents can also react directly with silicon surfaces, without the presence of hydrolyzable groups. This was shown on porous silicon (p-Si), a form of silicon with a very high, nanostructured surface area.[16,17] The mechanism is believed to proceed by breaking of Si–Si bonds and therefore formation of a Si–C bond and a Si–Li surface species (Scheme 1). The reactive Si–Li group is quenched during the workup with electrophiles, such as protons or deuterons.

Herein, we report that hydride-terminated SiNCs react with organolithium compounds at room temperature by breaking of Si–Si bonds. The SiNCs were functionalized with a variety of organolithium reagents and form colloidally stabilized disper-

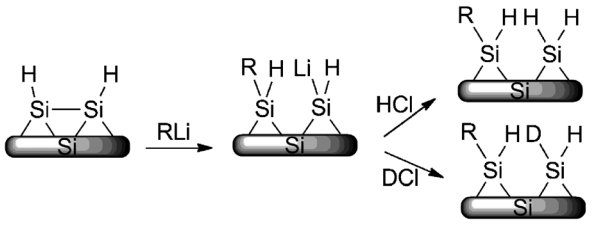

Scheme 1. Reactivity of organolithium reagents towards nanostructured silicon surfaces.

[a] I. M. D. Höhlein,[+] A. Angı,[+] Prof. B. Rieger
Wacker-Lehrstuhl für Makromolekulare Chemie
Technische Universität München
Lichtenbergstrasse 4, 85747 Garching (Germany)
E-mail: rieger@tum.de

[b] R. Sinelnikov, Prof. J. G. C. Veinot
Department of Chemistry, University of Alberta
Edmonton, Alberta, T6G 2G2 (Canada)

[+] These authors contributed equally to this work.

Supporting information for this article is available on the WWW under http://dx.doi.org/10.1002/chem.201405555. It contains detailed experimental procedures, as well as further FTIR, DLS, PL, TGA, NMR, and HR TEM data.

sions. Also, SiNCs with mixed surface functionalities are formed by quenching of the reaction with various electrophiles or by addressing free Si–H groups through hydrosilylation reaction with 1-dodecene.

The H-terminated SiNCs used in this work have an average diameter of around 3-4 nm and were prepared by pyrolysis of hydrogen silsesquioxane (HSQ) at 1100 °C for 1 h in an atmosphere consisting of 5% hydrogen and 95% nitrogen.[6] Under these conditions, SiNCs were formed incorporated into a silica matrix. The SiNCs were liberated by etching the composite with HF and final extraction in toluene.

SiNCs obtained by etching 300 mg Si/SiO_2 composite were dispersed in a 0.1 M solution of *n*-hexylltihium in toluene and stirred at room temperature for 2 h (Figure 1 A). The reaction was quenched by methanol, acidified with HCl, and the functionalized SiNCs were further purified by two antisolvent precipitation steps from toluene with methanol.

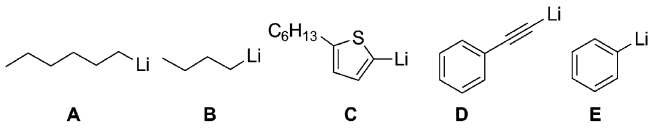

Figure 1. Organolithium reagents used for the functionalization of SiNCs. A) *n*-hexyllithium; B) *n*-butyllithium; C) (5-hexyl-2-thienyl)lithium; D) lithium phenylacetylide; and E) phenyllithium.

The unfunctionalized, hydride-terminated SiNCs form a turbid yellow dispersion in toluene and showed only the distinctive Si–H bands at 2099, 906, and 665 cm^{-1} in the IR spectrum (Figure 2 A). After reaction with *n*-hexyllithium, additional strong C–H bands at 2900 and 1450 cm^{-1} from surface-bound alkyl chains were visible (Figure 2 B). The functionalization was sufficient to stabilize the SiNCs colloidally, which is apparent by the formation of a clear SiNCs dispersion. Minor surface oxidation of the SiNCs was observed, evident from the Si–O band at 1050 cm^{-1}.

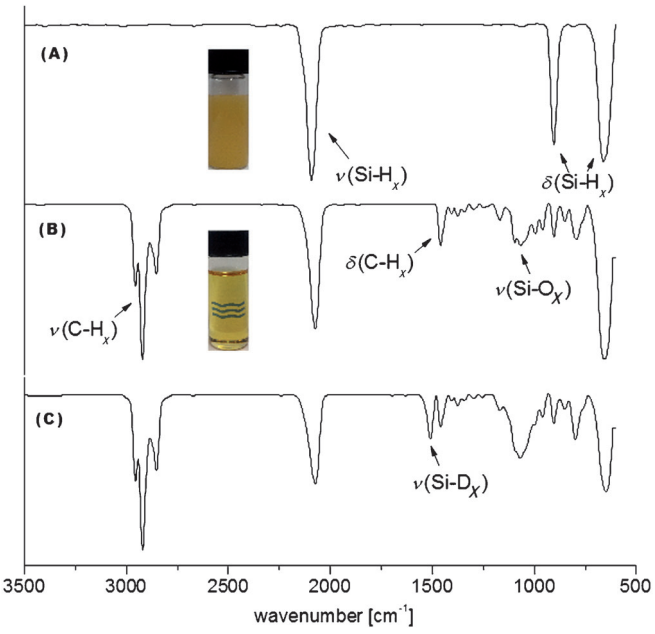

Figure 2. FTIR spectra of A) freshly etched SiNCs; B) functionalized with *n*-hexyllithium and HCl used for workup; C) functionalized with *n*-hexyllithium and DCl used for workup.

To prove the postulated mechanism by formation of a Si–Li group is also accurate for SiNCs, the quenching was also performed with deuterated methanol, acidified with DCl. A FTIR band at 1510 cm^{-1} was observed after this reaction, which can be assigned to a Si–D bond (Figure 2 C). A control experiment, in which unfunctionalized SiNCs were treated with DCl, did not indicate any formation of Si–D bonds (Figure S2 in the Supporting Information).

Hexylmagnesiumbromide was also tested to check the reactivity of Grignard reagents towards SiNCs. The same reactivity compared to organolithium compounds was found, but the surface coverage seems to be lower, because only comparably weak alkyl bands were visible in the FTIR spectra (Figure S3 in the Supporting Information), and the functionalized SiNCs were poorly dispersible in toluene. Therefore, further reactions were conducted only with organolithium reagents.

To show a broad applicability of the reaction, the organolithium reagents *n*-butyllithium, (5-hexyl-2-thienyl)lithium, lithium phenylacetylide, and phenyllithium (Figure 1 B–E) were tested for the functionalization of SiNCs. The reaction procedure was the same as that described with *n*-hexyllithium. In every case, colloidally stabilized dispersions were formed, and the functionalized SiNCs showed IR bands of the respective surface groups (Figure 3 A–D).

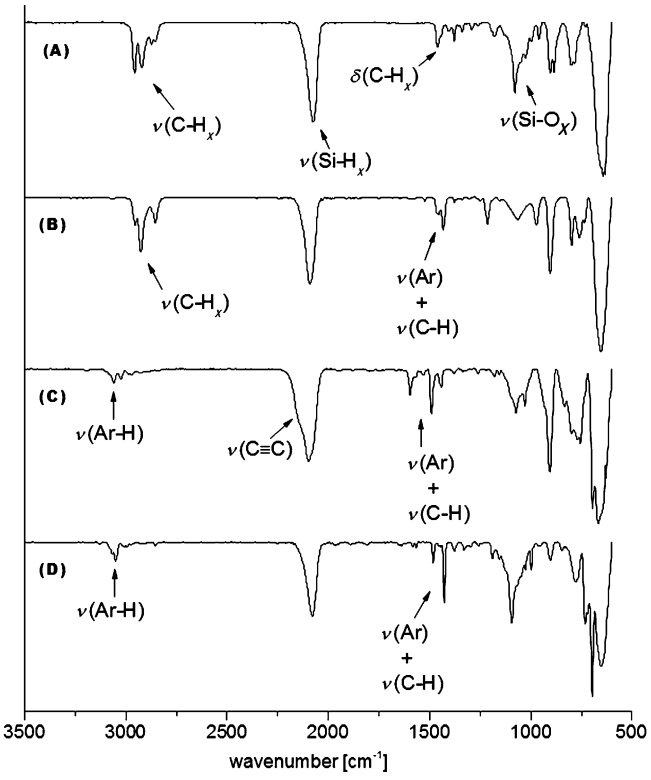

Figure 3. FTIR spectra of SiNCs functionalized with A) *n*-butyllithium; B) (5-hexyl-2-thienyl)lithium; C) lithium phenylacetylide; and D) phenyllithium.

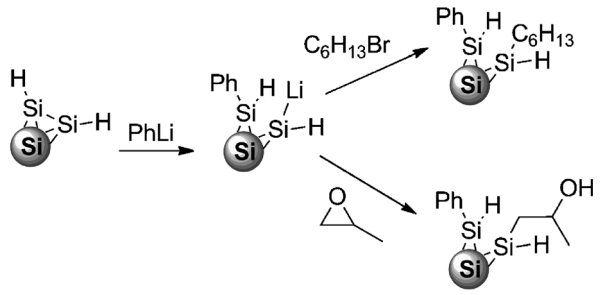

Scheme 2. Reaction of SiNCs with phenyllithium and quenching of the surface Si–Li group with 1-bromohexane (top) and propylene oxide (bottom).

For the quenching of the silyl anions during the workup, other electrophiles than protons can be used. This was shown by Kim and Laibinis and Song and Sailor, for example, with acyl chlorides on porous silicon.[16,17] We wanted to determine whether less reactive electrophiles are also suitable for this reaction. Therefore, 1-bromohexane and propylene oxide were used as quenching reagents (Scheme 2).

The SiNCs were functionalized with phenyllithium in the described way and the reaction mixture was cooled to −78 °C before adding 20 equivalents of the respective quenching reagent. The dispersion was then warmed to room temperature, and the following purification was performed by three precipitation/centrifugation cycles from toluene and methanol. In the FTIR spectra additional C–H bands were visible for the 1-bromohexane-functionalized SiNCs (Figure 4A), and a broad C–OH band at 3400 cm^{-1} for the SiNCs reacted with propylene oxide, which indicates that the quenching was successful (Figure 4B).

Because the Si–H groups of the SiNCs are not consumed during the reaction with organolithium reagents, they should be available for further functionalization, such as hydrosilylation reactions (Scheme 3). This hypothesis was tested with SiNCs that were first reacted with phenyl lithium and after the workup resuspended in 3 mL of a 1 M solution of 1-dodecene in toluene. The hydrosilylation reaction was started with the addition of 4-decylbenzene diazonium tetrafluoroborate (4-DDB) as radical initiator and stirred overnight.[12] Purification of the functionalized SiNCs was performed by three antisolvent precipitations from toluene with methanol/ethanol. The FTIR spectrum clearly showed additional C–H bands from surface-bound dodecyl groups next to the aromatic bands from the phenyl rings on the surface (Figure 4C). Bands of Si–H were still present; however, this is expected, because a complete coverage by hydrosilylation cannot be achieved due to steric hindrance.[18]

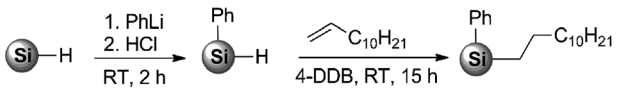

Scheme 3. Functionalization of SiNCs with PhLi followed by 4-decylbenzene diazonium tetrafluoroborate (4-DDB) initiated hydrosilylation of dodecene.

Dynamic light scattering (DLS) measurements were conducted of the functionalized SiNCs (Table 1). Hydrodynamic radii between 2.1 and 3.2 nm are consistent with values reported in literature of SiNCs functionalized by hydrosilylation, and indicate that the SiNCs do not agglomerate in the solvent.[10] The only exception are SiNCs functionalized with penyllithium and quenched with propylene oxide, which have a hydrodynamic radius over 300 nm. The free hydroxide groups on the surface could render the SiNC surface more polar, which then would be reasonable to cause the formation of agglomerates in toluene.

Table 1. DLS data of the SiNCs with different surface functionalities dispersed in toluene.

Reagent	Hydrodynamic radius [nm]	Polydispersity [%]
n-butyllithium	2.2	41.1
n-hexyllithium	2.3	35.9
(5-hexyl-2-thienyl)lithium	3.2	42.1
lithium phenylacetylide	2.5	41.5
phenyllithium	2.1	22.4
phenyllithium and 1-dodecene	2.8	34.4
phenyllithium and 1-bromohexane	2.3	16.5
phenyllithium and propylene oxide	362.8	20.6

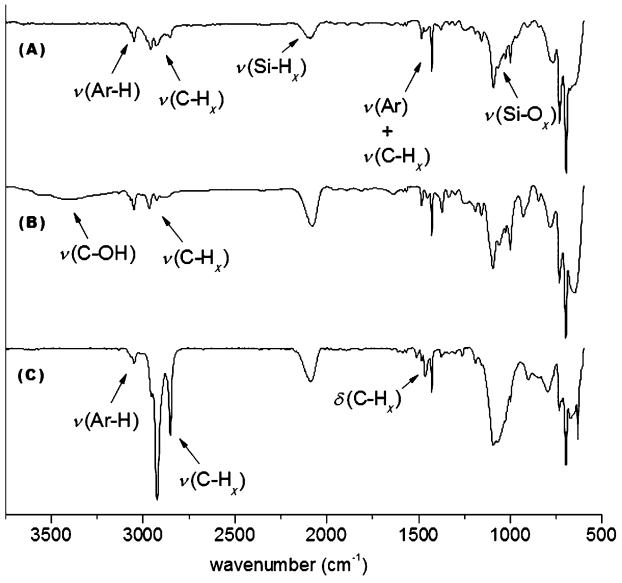

Figure 4. FTIR spectra of SiNC functionalized with A) phenyllithium and quenched with 1-bromohexane; B) phenyllithium and quenched with propylene oxide; and C) phenyllithium followed by hydrosilylation of 1-dodecene initiated with 4-DDB.

The photoluminescence (PL) maxima of the functionalized SiNCs were found at $\lambda = 690$ nm except for SiNCs with phenylacetylene surface groups, in which it is redshifted to 740 nm (Figure 5). The cause of this shift is not known to us, but it has been reported before that the photoluminescence of porous silicon is influenced by covalently bound phenylacetylene groups.[17] However, Song et al. described only a weakening of the photoluminescence, not a shift of the emission wavelength. This matter will be subject to further investigations.

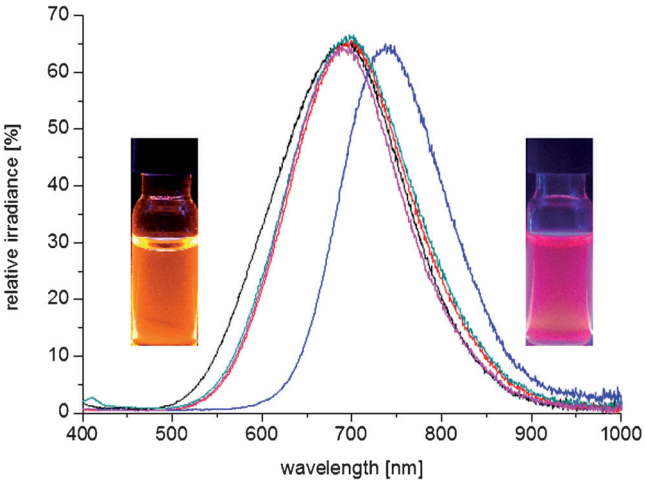

Figure 5. PL spectra of SiNCs functionalized with *n*-hexyllithium (green), (5-hexyl-2-thienyl)lithium (black), phenyllithium (red), *n*-butyllithium (magenta), and lithium phenylacetylide (blue). Dispersion of SiNC with hexyl surface groups (left) and phenylacetylene surface groups (right) under $\lambda = 365$ nm UV radiation.

In summary, we report that SiNCs with a hydride surface can be functionalized with organolithium compounds. The reaction was performed at room temperature with short reaction times and the functionalized SiNCs form colloidally stable dispersions. The proposed mechanism proceeds through breaking of Si–Si bonds and formation of surface Si–Li species. SiNCs with mixed surface functionalities can be obtained when the Si–Li groups are quenched with various electrophiles or if free Si–H groups on the SiNC are addressed through hydrosilylation reaction in a following step.

Acknowledgements

R.S. and J.G.C.V. acknowledge funding from the Natural Sciences and Engineering Research Council of Canada (NSERC), Canada Foundation for Innovation (CFI), Alberta Science and Research Investment Program (ASRIP), and University of Alberta Department of Chemistry. Kai Cui from the National Institute for Nanotechnologie (NINT) is thanked for HR TEM measurements. I.M.D.H., A.A., and R.S. are grateful for scholarships from the Fonds der Chemischen Industrie (FCI), the Deutscher Akademischer Austauschdienst (DAAD) & Turkish Education Foundation (TEV) and Alberta Innovates Technology Futures (AITF), respectively.

Keywords: nanoparticles · organometallic compounds · silicon · surface chemistry

[1] J. Liu, F. Erogbogbo, K.-T. Yong, L. Ye, J. Liu, R. Hu, H. Chen, Y. Hu, Y. Yang, J. Yang, *ACS Nano* **2013**, *7*, 7303 – 7310.
[2] K.-Y. Cheng, R. Anthony, U. R. Kortshagen, R. J. Holmes, *Nano Lett.* **2010**, *10*, 1154 – 1157.
[3] C. Liu, Z. C. Holman, U. R. Kortshagen, *Nano Lett.* **2009**, *9*, 449.
[4] K. Dohnalová, T. Gregorkiewicz, K. Kůsová, *J. Phys. Condens. Matter* **2014**, *26*, 173201.
[5] M. Dasog, G. B. De Los Reyes, L. V. Titova, F. Hegmann, J. G. C. Veinot, *ACS Nano* **2014**, 8, 9636-9648.
[6] C. M. Hessel, E. J. Henderson, J. G. C. Veinot, *Chem. Mater.* **2006**, *18*, 6139 – 6146.
[7] X. Li, Y. He, S. S. Talukdar, M. T. Swihart, *Langmuir* **2013**, *29*, 8490 – 8496.
[8] R. D. Tilley, J. H. Warner, K. Yamamoto, I. Matsui, H. Fujimori, *Chem. Commun.* **2005**, 1833 – 1835.
[9] J. L. Heinrich, C. L. Curns, G. M. Credo, K. L. Kavanagh, M. J. Sailor, *Science* **1992**, *255*, 66 – 68.
[10] J. A. Kelly, J. G. C. Veinot, *ACS Nano* **2010**, *4*, 4645 – 4656.
[11] J. Nelles, D. Sendor, A. Ebbers, F. M. Petrat, H. Wiggers, C. Schulz, U. Simon, *Colloid Polym. Sci.* **2007**, *285*, 729 – 736.
[12] I. M. D. Höhlein, J. Kehrle, T. Helbich, Z. Yang, J. G. C. Veinot, B. Rieger, *Chem. Eur. J.* **2014**, *20*, 4212 – 4216.
[13] C. Yang, R. A. Bley, S. M. Kauzlarich, H. W. H. Lee, G. R. Delgado, *J. Am. Chem. Soc.* **1999**, *121*, 5191 – 5195.
[14] J. Zou, R. K. Baldwin, K. a. Pettigrew, S. M. Kauzlarich, *Nano Lett.* **2004**, *4*, 1181 – 1186.
[15] X. Cheng, S. B. Lowe, P. J. Reece, J. J. Gooding, *Chem. Soc. Rev.* **2014**, *43*, 2680 – 2700.
[16] N. Y. Kim, P. E. Laibinis, *J. Am. Chem. Soc.* **1998**, *120*, 4516 – 4517.
[17] J. H. Song, M. J. Sailor, *J. Am. Chem. Soc.* **1998**, *120*, 2376 – 2381.
[18] L. Scheres, B. Rijksen, M. Giesbers, H. Zuilhof, *Langmuir* **2011**, *27*, 972 – 980.

Received: October 7, 2014
Published online on December 22, 2014

CHEMISTRY
A European Journal

Supporting Information

Functionalization of Hydride-Terminated Photoluminescent Silicon Nanocrystals with Organolithium Reagents

Ignaz M. D. Höhlein,[a] Arzu Angı,[a] Regina Sinelnikov,[b] Jonathan G. C. Veinot,[b] and Bernhard Rieger*[a]

chem_201405555_sm_miscellaneous_information.pdf

Table of Contents

1 General information 2
2 Synthetic procedures 2
2.1 Synthesis of Hydrogen Silsesquioxane (HSQ) 2
2.2 Preparation of oxide-embedded silicon nanocrystals 2
2.3 Liberation of SiNCs 2
2.4 Synthesis of lithium phenylacetylide and (5-hexyl-2-thienyl)lithium 3
2.5 Functionalization of SiNCs with organometallic reagents 3
2.6 Quenching with 1-bromohexane 3
2.7 Quenching with propylene oxide 3
2.8 Two-step functionalization of SiNCs via hydrosilylation 3
3 Analytical data 4
3.1 Nuclear Magnetic Resonance Spectroscopy (NMR) 4
3.2 Fourier Transform Infrared Spectroscopy (FTIR) 5
3.3 Photoluminescence Spectra (PL) 6
3.4 Thermogravimetric analysis (TGA) 6
3.5 Dynamic light scattering (DLS) 7
3.6 High Resolution Transmission Electron Microscopy (HR-TEM) 8

1 General information

All reactants and reagents were purchased from Sigma-Aldrich and used without further purification if not stated otherwise. Phenyllithium was bought as a 1.8 M solution in dibutyl ether, hexyllithium as 2.3 M solution in hexane, butyllithium as 2.5 M solution in hexane and hexylmagnesiumbromide as 2.0 M solution in diethylether. Dry toluene and THF was obtained from a MBraun SPS 800 solvent purification system.
FTIR spectra were measured with a *Bruker Vertex 70 FTIR* using a *Platinum ATR* from *Bruker*. . Nuclear magnetic resonance (NMR) spectra were measured on a *ARX*-300 from Bruker in deuterated chloroform at 300 K. Photoluminescence (PL) spectra were taken with an *AVA-Spec 2048* from *Avantes* using a *Prizmatix (LED Current controller)* as light source. Dynamic light scattering measurements were made with a *Dyna Pro NanoStar* from *Wyatt* with toluene as solvent. TGA-analysis was performed with a *Netzsch TG 209 F1 Libramachine* at a heating rate of 10 K/min in an argon flow of 20 mL/min (Ar 4.8) in platinum pans. HR-TEM measurements were performed on a JEM-2200FS TEM with 200kV field emission gun.

2 Synthetic procedures

2.1 Synthesis of Hydrogen Silsesquioxane (HSQ)

The HSQ was prepared following a literature procedure.[1] To a mixture of sulfuric acid (22.7 g) and fuming sulfuric acid (13.9 g), Toluene (45 ml) was added via a dropping funnel for 10 min and stirred for additional 20 min. To the yellow, biphasic solution, $HSiCl_3$ (21.5 g, 0.16 mol) dissolved in 110 ml Toluene was added over the course of several hours. Subsequently, the upper layer was separated, washed thrice with sulfuric acid 50 % (w/w) and stirred over night over $MgSO_4$ and $CaCO_3$. After filtration, the solvent was removed *in vacuo* giving a colorless solid.

EA: calculated Si: 52.90%, H: 1.90% found Si: 51.18 %, H: 1.88%

2.2 Preparation of oxide-embedded silicon nanocrystals

HSQ (7 g) was placed in a quartz reaction boat, transferred to a *Nabertherm RD 30/200/11* oven with quartz working tube and heated from ambient to a peak processing temperature of 1100 °C at 18 °C/min in a slightly reducing atmosphere (5% H_2/95% N_2).The sample was maintained at the peak processing temperature for 1 h. Upon cooling to room temperature, the resulting amber solid was ground into a fine brown powder using mortar and pestle to remove large particles. Further grinding was achieved via shaking the powder dispersed in ethanol for 24h with high-purity silica beads using a *WAB Turbula mixer*. The resulting SiNC/SiO_2 composite was dried *in vacuo* and the powder stored in glass vials.

2.3 Liberation of SiNCs

Hydride-terminated SiNCs were liberated from the SiNC/SiO_2 composites using HF etching. First, 0.30 g of the ground SiNC/SiO_2 composite was transferred to a ethylene-tetrafluoroethylene (ETFE) beaker equipped with a Teflon-coated stir bar. Ethanol (3 mL) and water (3 mL) were then added under mechanical stirring to form a brown suspension, followed by 3 mL of 49% HF aqueous solution. After

1 h of etching in subdued light, the suspension appeared yellow. Hydride-terminated SiNCs were subsequently extracted from the aqueous layer into ca. 30 mL of toluene by multiple (i.e., 3 × 10 mL) extractions. The SiNC toluene suspension was transferred to ETFE-centrifuge tubes, and the SiNCs were isolated by centrifugation at 5000 rpm.

2.4 Synthesis of lithium phenylacetylide and (5-hexyl-2-thienyl)lithium

2-hexylthiophene was synthesized following literature procedures.[2] Phenyllithium or 2-hexylthiophene respectively (15 mmol) is dissolved in 9 ml THF and *n*-butyllithium (2.5 M in hexanes, 6 ml, 15 mmol) is added to the reaction flask dropwise in 1 hour at -78°C. Upon the completion of the addition the reaction mixture is stirred for 15 more minutes, then it is brought to room temperature. The product is obtained as a clear black or yellow solution. The solution is degassed and stored in the schlenk flask in a cool place.

2.5 Functionalization of SiNCs with organometallic reagents

Hydride terminated Si-NCs, obtained by etching 300 mg Si/SiO_2 composite, are dispersed in 2 ml of a degassed solution of the organolithium reagents. The organolithium reagents used for this study are diluted with toluene to form 0.1 M solutions. The mixture is stirred for 2 h and afterwards poured into methanol (5 ml) acidified with HCl conc. (0.2 ml) or deuterated methanol and DCl conc. respectively. The formed precipitate is centrifuged at 9000 rpm for 10 min and the sediment is redispersed in minimal amount of toluene. The precipitation-centrifugation-redispersion step is performed two more times from methanol and toluene. Finally the functionalized SiNCs are dispersed in toluene, filtered through a 0.45 µm PTFE syringe filter and stored in vials for further use.
For the functionalization with hexylmagnesiumbromide, the same procedure was used but the solvent was changed to a 1:1 mixture of toluene and diethyl ether.

2.6 Quenching with 1-bromohexane

SiNCs from 300 mg etched Si/SiO_2 are reacted with phenyllithium as described above. After 5 h, the reaction mixture is cooled to -78 °C and 1-bromohexane (0.56 ml, 4.0 mmol) is added. After 10 min, the dispersion is warmed to room temperature and stirred for further 2.5 h. Subsequently, the functionalized SiNCs are purified by three precipitation/centrifugation/redispersion steps with 1:1 ethanol/methanol and toluene. Finally the functionalized SiNCs are dispersed in toluene, filtered through a 0.45 µm PTFE syringe filter and stored in vials for further use.

2.7 Quenching with propylene oxide

SiNCs from 300 mg etched Si/SiO_2 are reacted with phenyllithium as described above. After 5 h, the reaction mixture is cooled to -78 °C and propylene oxide (0.28 ml, 4.0 mmol) is added. After 30 min, the dispersion is warmed to room temperature and stirred for further 90 min. Subsequently, the solvent and excess propylene oxide is evaporated *in vacuo* and the residue redispersed in 1 ml of toluene. Purification is performed *via* three precipitation/centrifugation/redispersion steps with 1:1 ethanol/methanol and toluene. Finally the functionalized SiNCs are dispersed in toluene, filtered through a 0.45 µm PTFE syringe filter and stored in vials for further use.

2.8 Two-step functionalization of SiNCs via hydrosilylation

Dry phenyllithium functionalized Si-NCs are resuspended in a mixture of toluene (3 ml) and 1-dodecene (0.66 ml, 3.0 mmol). The clear dispersion is degassed three times *via* freeze-pump-thaw cycles. 4-decylbenzene diazonium tetrafluoroborate (5 mg, 15.3 µmol) is added to start the

hydrosilylation and the reaction is stirred overnight. Purification of the functionalized SiNCs is performed by precipitation from a 1:1 mixture of ethanol and methanol (5 ml), centrifugation and redispersion in toluene. This cycle is repeated three times and the SiCNs are filtered afterwards through a 0.45 µm PTFE syringe filter and stored in vials for further use.

3 Analytical data

3.1 Nuclear Magnetic Resonance Spectroscopy (NMR)

NMR spectra of SiNCs functionalized with *n*-hexyllithium are in accordance with published spectra of SiNCs functionalized with alkyl chains via hydrosilylation.[3] The CH_2-group directly bound to SiNC surface (F) is expected to appear around 0.5 ppm.[4] However with SiNCs in the size range of a few nanometers, this group is commonly not observed.[3,5,6] A possible explanation is that the signals cannot be detected due to a broadening induced by anisotropic effects and a prolonged relaxation time since the molecules cannot move freely on the SiNC surface.

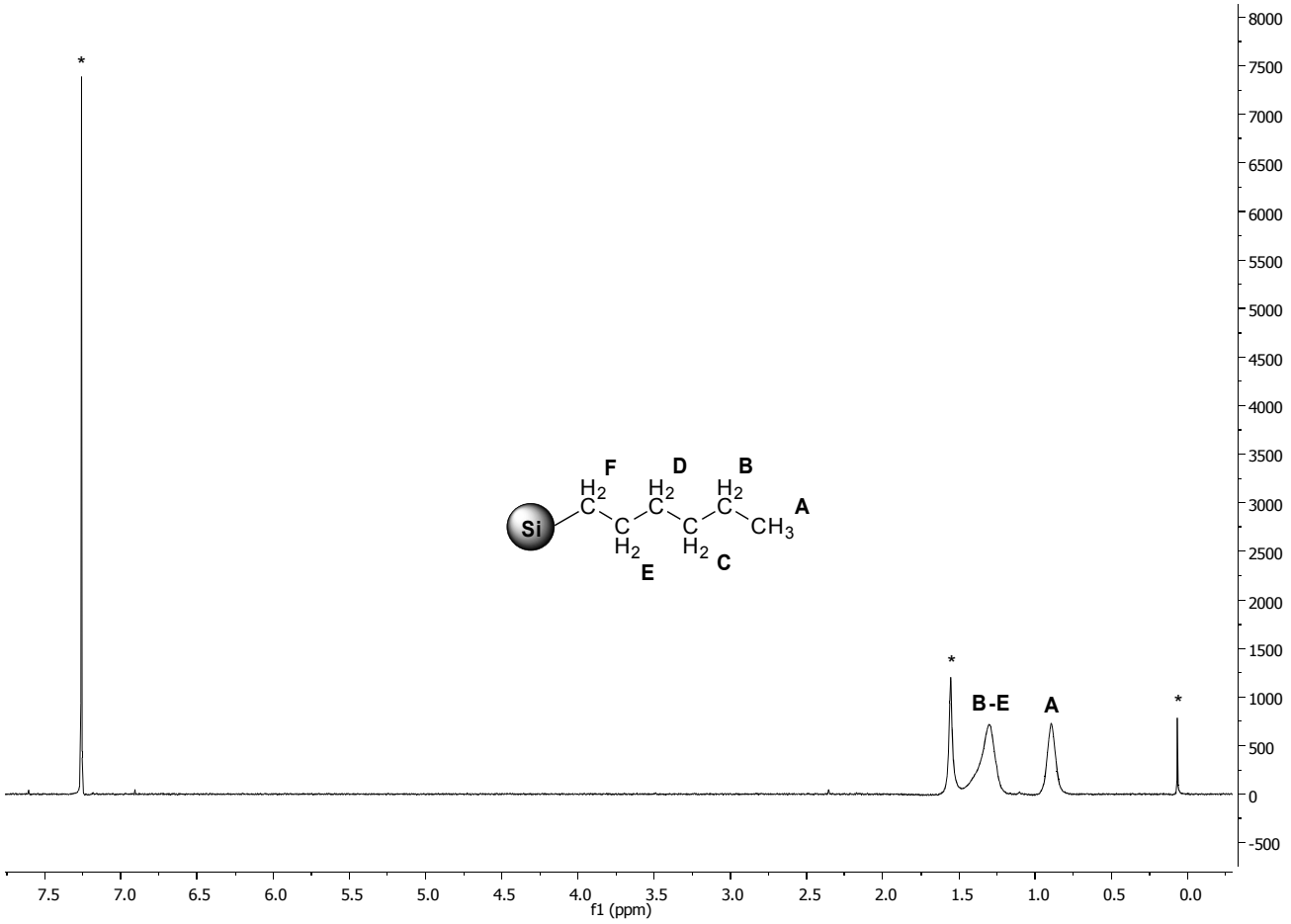

Figure S1: NMR spectrum of SiNCs functionalized with *n*-hexyllithium. Signals from the solvent are marked with an asterisk.

3.2 Fourier Transform Infrared Spectroscopy (FTIR)

A control experiment was conducted to rule out that the formation of Si–D groups is due to a proton/deuteron exchange *via* deprotonation of the SiNC surface. H-terminated SiNCs were treated with deuterated methanol, acidified with DCl, in the same manner as described above for the workup of SiNCs functionalized with organolithium reagents. No Si–D bands are visible which indicates that the Si-D surface groups are indeed formed via quenching of the Si–Li surface species (Figure S2).

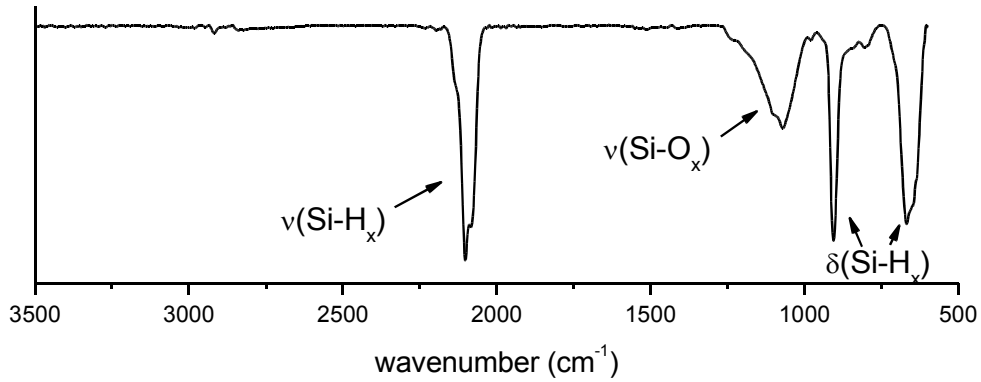

Figure S2. FTIR spectrum of H-terminated SiNCs treated with deuterated methanol and DCl.

SiNCs were reacted with hexylmagnesiumbromide analogous to the organolithium reagents. However the colloidal stabilization of the SiNCs was not as good as with hexyllithium so that the dispersion with the functionalized SiNCs was still turbid and could not be filtered through a 0.45 µm PTFE filter. Also the FTIR shows bands of the surface bound hexyl groups with a lesser intensity (Figure S3). This could be due to the in general higher reactivity of organolithium compounds compared to Grignard reagents.

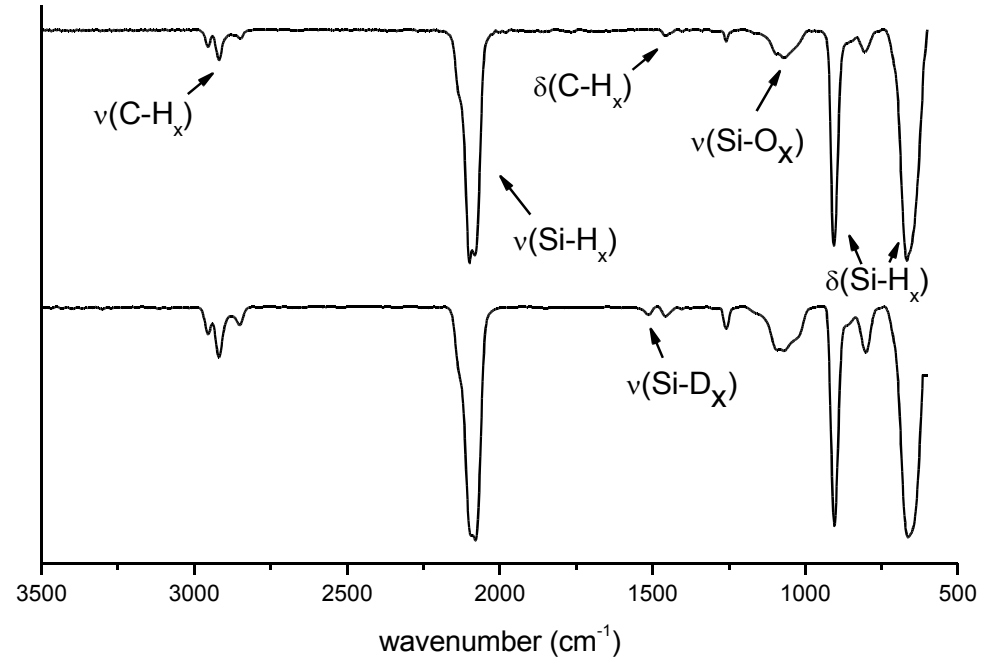

Figure S3. FTIR spectrum of SiNCs functionalized with hexylmagnesiumbromide.

3.3 Photoluminescence Spectra (PL)

SiNCs reacted with phenyllithium and quenched with 1-bromohexane or propylene oxide and SiNCs reacted first with phenyllithium and afterwards with dodecene also show PL maxima at 690 nm (Figure S4).

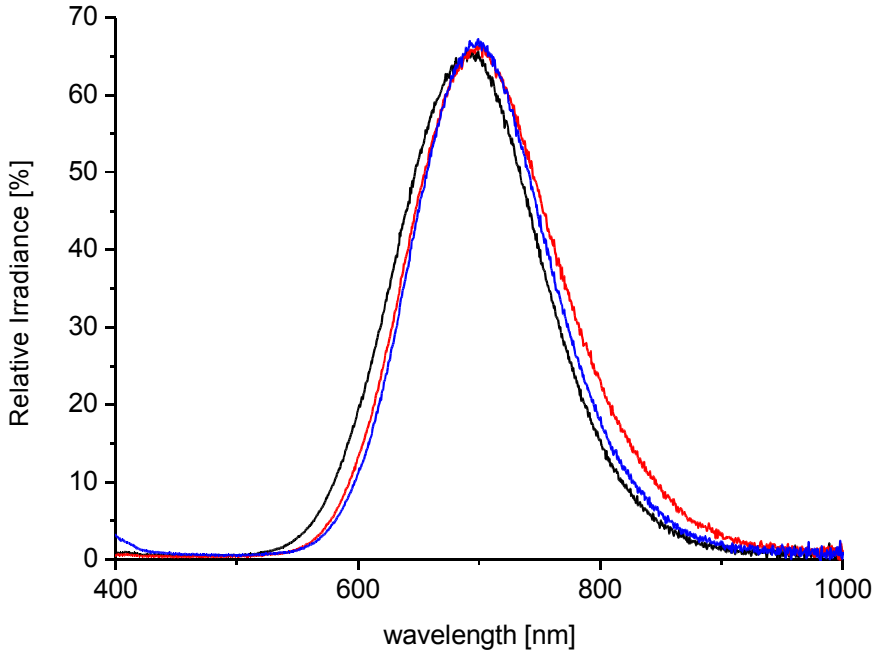

Figure S4. PL data of SiNCs functionalized with phenyllihtium and dodecene (black), phenyllihtium and 1-bromohexane (red) and phenyllithium and propylene oxide (blue) .

3.4 Thermogravimetric analysis (TGA)

To obtain a semiquantitative understanding of the amount of organic groups bound on the SiNCs, thermogravimetric (TG) analysis was performed of the SiNCs functionalized with organolithium reagents (Figure S5).

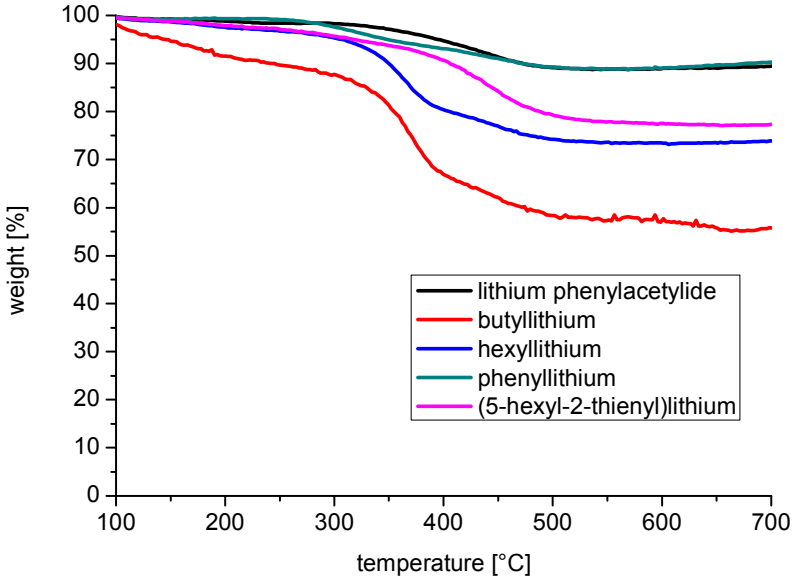

Figure S5. TG analysis of SiNCs functionalized with organolithium compounds.

The weightloss via TG was divided by the molecular weight of the bound surface groups to get comparable values (Table S1). The data suggests that the coverage with the aromatic organolithium reagents is similar for each compound. However the coverage with the aliphatic organolithium reagent hexyllithium is higher by a factor of around 2-2.5 and for the smaller butyllithium by a factor of 4-5. It can be assumed therefore that sterical issues are the main factor for the difference in surface coverage.

Table S1. TG data from SiNCs functionalized with organolithium compounds

Reagent	Weightloss [%]	Molecular weight [g/mol]	Weightloss/Molecular weight
n-butyllithium	38.0	57.1	0.67
n-hexyllithium	27.4	85.2	0.32
(5-hexyl-2-thienyl)lithium	23.8	167.3	0.14
lithiumphenylacetylide	11.8	101.1	0.12
phenyllithium	12.1	77.1	0.16

3.5 Dynamic light scattering (DLS)

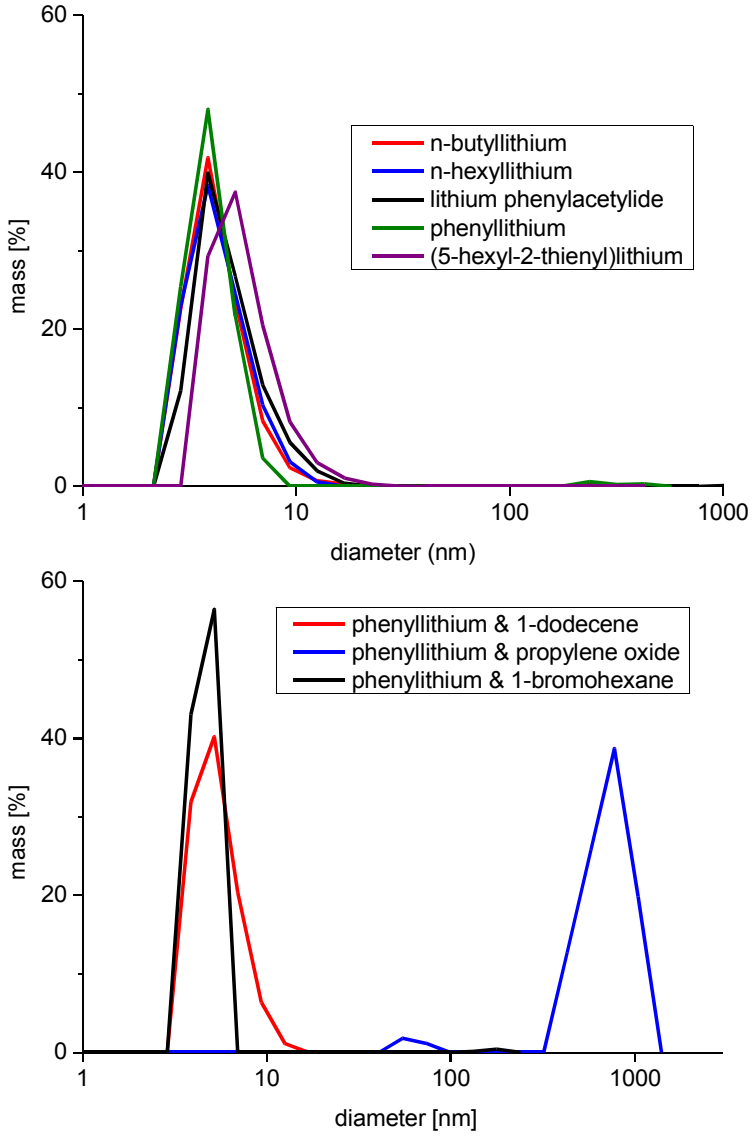

Figure S6: DLS data of the SiNCs functionalized with n-butyllithium, n-hexyllithium, lithium phenylacetylide, phenyllithium and (5-hexyl-2-thienyl)lithium (top) and SiNCs reacted with phenyllithium and 1-dodecene, propylene oxide and 1-bromohexane in a second step (bottom).

3.6 High Resolution Transmission Electron Microscopy (HR-TEM)

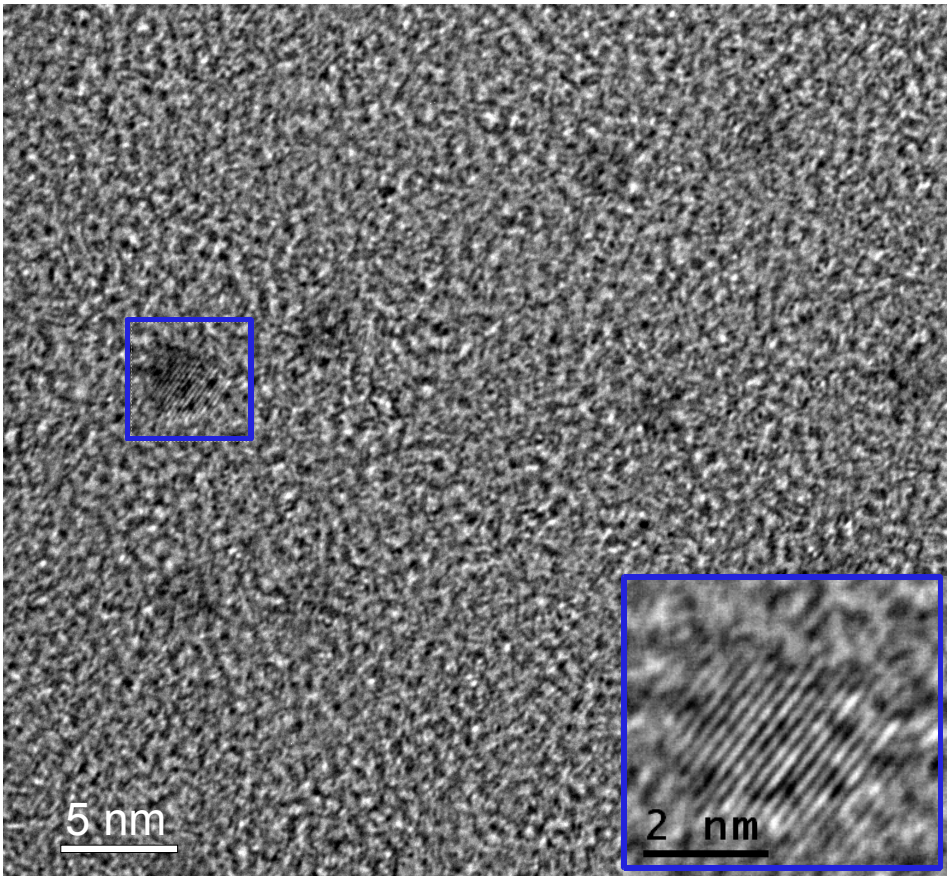

Figure S7: HR-TEM picture of SiNCs functionalized with *n*-hexyllithium. The lattice fringes of the crystals are clearly visible (blue box).

Literature

[1] H. M. Bank, M. E. Cifuentes, E. M. Theresa, *United States Pat.* **1991**, *5.010.159*.

[2] C. Xia, X. Fan, J. Locklin, R. C. Advincula, *Org. Lett.* **2002**, *4*, 2067–2070.

[3] F. Hua, M. T. Swihart, E. Ruckenstein, *Langmuir* **2005**, *21*, 6054–62.

[4] J. M. J. Paulusse, M. W. F. Nielen, H. Zuilhof, *Chem. Mater.* **2012**, 4311–4318.

[5] N. Shirahata, M. R. Linford, S. Furumi, L. Pei, Y. Sakka, R. J. Gates, M. C. Asplund, *Chem. Commun. (Camb).* **2009**, 4684–6.

[6] J. H. Ahire, Q. Wang, P. R. Coxon, G. Malhotra, R. Brydson, R. Chen, Y. Chao, *ACS Appl. Mater. Interfaces* **2012**, *4*, 3285–92.

8 Photoluminescent Silicon Nanocrystal-Polymer Hybrid Materials *via* Surface Initiated Reversible Addition-Fragmentation Chain Transfer (RAFT) Polymerization

Status	Published online: April 7, 2015
Journal	Nanoscale, 2015, Volume 7, 7811-7818.
Publisher	RSC Publishing
DOI	10.1039/c5nr00561b
Authors	Ignaz M. D. Höhlein, Patrick D. L. Werz, Jonathan G. C. Veinot, Bernhard Rieger

Content

A promising approach to combine the properties of SiNCs and polymers is to merge them in core-shell hybrid materials. In this article a procedure is described to obtain SiNCs coated with defined polymer shells *via* surface initiated RAFT polymerization. In the first step, chlorosilane terminated SiNCs are functionalized with a novel RAFT reagent bearing a hydroxy moiety. This is followed by a polymerization step which gives polymer grafted particles and free polymer in solution. Ultracentrifugation is applied to separate the grafted SiNCs. The polymerization was found to proceed in a living manner on the SiNCs and yielded particles with narrow size dispersions. A variety of monomers were successfully applied for the reaction.

Nanoscale

PAPER

View Article Online
View Journal

Cite this: DOI: 10.1039/c5nr00561b

Photoluminescent silicon nanocrystal-polymer hybrid materials *via* surface initiated reversible addition–fragmentation chain transfer (RAFT) polymerization

Ignaz M. D. Höhlein,†[a] Patrick D. L. Werz,†[a] Jonathan G. C. Veinot[b] and Bernhard Rieger*[a]

Received 25th January 2015,
Accepted 23rd March 2015

DOI: 10.1039/c5nr00561b

www.rsc.org/nanoscale

Silicon-polymer core–shell hybrid materials are obtained *via* surface initiated reversible addition–fragmentation chain transfer (RAFT) polymerization from photoluminescent silicon nanocrystals (SiNCs). Polymer grafted SiNCs and free polymers in solution are separated using ultracentrifugation. The polymerization on the surface proceeds in a living manner which is confirmed *via* GPC, DLS and TGA measurements. This method was applied to various other monomers. The obtained materials all show bright red photoluminescence originating from the SiNC core.

1. Introduction

Semiconductor nanoparticles within the size range of their exciton Bohr radius, also referred to as quantum dots (QD), are an intriguing class of materials. The properties of QD differ substantially from their bulk counterparts. For instance, the energy of their band gap is dependent on the particle size. Therefore fluorescence and absorption wavelengths can be tuned by the dimensions of the QD. Numerous applications including light emitting diodes (LEDs),[1] solar cells,[2,3] sensing materials[4] or photoluminescent biological markers[5] have been realized, which take advantage of this behaviour. II–VI and III–V semiconductor nanoparticles such as CdSe and InP are among the most commonly used QDs, synthesis and properties of these materials have been intensively investigated. However heavy metal induced cytotoxicity and high cost limit the applicability of these QDs in industry. Silicon as group IV semiconductor offers a promising alternative since it is comparably non-toxic and abundantly available.[6] Silicon nanocrystals (SiNCs) have therefore gained much attention recently and great progress has been made in the synthesis of well-defined SiNCs[7–10] that have found use in various applications.[11–14]

Nevertheless, there are some obstacles that need to be considered when handling SiNCs. They tend to agglomerate in solvents and the silicon is easily oxidized under ambient conditions by water and air due to the high surface area. Therefore the SiNC surface needs to be passivated to render the particles useful. In most cases, this is achieved by the formation of organic monolayers, either by hydrosilylation of alkenes[10,15,16] or the reaction with nucleophiles.[17–19] Another approach is to coat SiNCs with polymers. This method has the advantage that the favourable properties of polymers, such as versatile post-polymerization modification, high resistance against chemicals[20] or stimulus-responsive behaviour,[21] can be paired with the characteristics of SiNCs to obtain tailored hybrid materials. However reports on defined SiNC-polymer hybrid materials are scarce to this day.[20–24] Therefore to find new ways to functionalize SiNCs with polymers in a controlled way is an attractive target.

Reversible addition–fragmentation chain transfer (RAFT) polymerization offers a tool to synthesize a great variety of polymers with narrow size distributions.[25] This is achieved by a RAFT reagent, bearing a thiocarbonyl group that reversibly traps chain radicals and therefore mediates the polymerization. When the RAFT reagent is anchored on a substrate, highly uniform polymer structures can be grown from its surface. A great variety of materials including carbon nanotubes,[26] cotton,[27] cellulose,[28] CdSe nanoparticles,[29] gold nanorods[30] and silica particles[31] have been functionalized by this method. However to the best of our knowledge no reports exist so far that combine surface initiated RAFT polymerization and SiNCs.

In the following work, we present an approach to functionalize photoluminescent SiNCs by surface initiated RAFT polymerization with polystyrene. The polymerization on the surface proceeds in a very controlled, living manner. We

[a]Wacker-Lehrstuhl für Makromolekulare Chemie, Technische Universität München, Lichtenbergstraße 4, 85747 Garching, Germany. E-mail: rieger@tum.de
[b]Department of Chemistry, University of Alberta, Edmonton, Alberta T6G 2G2, Canada
† These authors contributed equally to this work.

demonstrate that ultracentrifugation is a useful and straightforward tool to separate grafted SiNCs from unbound polymers in solution.

When casted into films, the SiNC hybrid materials are highly stable against oxidation. Finally we show that the polymerization method can be applied to various other monomers.

2. Results and discussion

Synthesis of SiNCs with a surface bound RAFT reagent (SiNC-HMT)

The SiNCs used in this work are prepared *via* thermal disproportion of polymeric hydrogen silsesquioxane (HSQ) in a slightly reducing atmosphere ($N_2 : H_2$, 95 : 5) at 1100 °C. Under these conditions, SiNCs with an average diameter of around 3 nm are formed incorporated in a SiO_2 matrix (Scheme 1A). Subsequently the SiO_2 is removed with an HF–water–ethanol solution giving freestanding, hydride terminated SiNCs that show no residual oxide in the FTIR spectrum (Fig. 1 A). In the

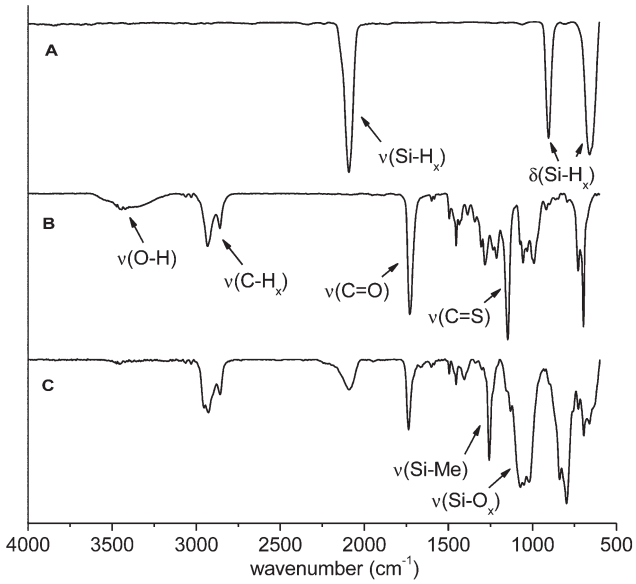

Fig. 1 FTIR spectra of A: etched, hydride terminated SiNCs, B: RAFT reagent HMT and C: HMT bound on SiNC-ClDMVS.

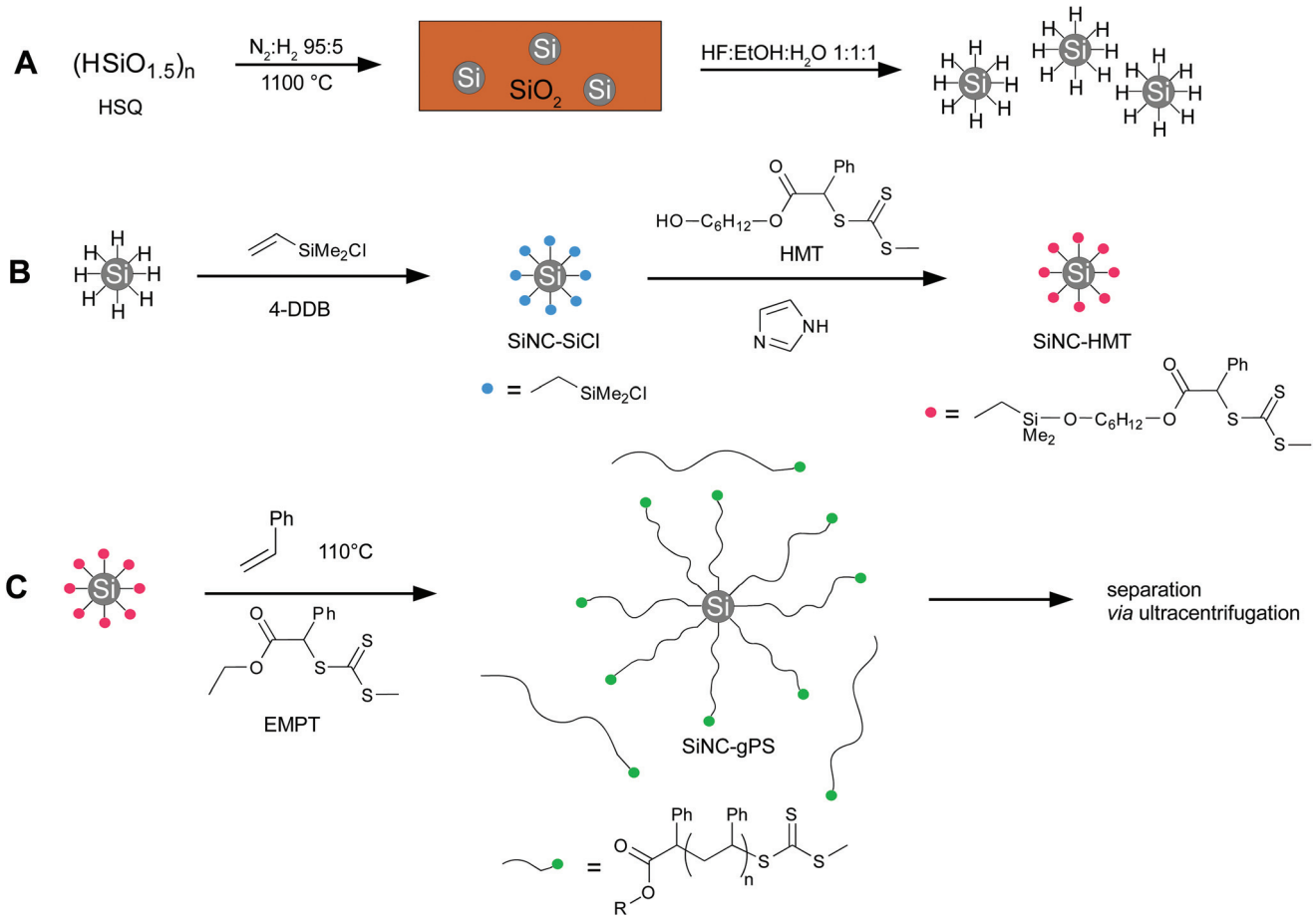

Scheme 1 A: Formation of hydride terminated SiNCs, B: hydrosilylation of SiNCs with vinyl(dimethyl)chlorosilane (SiNC-SiCl), initiated by 4-decylbenzene diazonium tetrafluoroborate (4-DDB) and subsequent fixation of the RAFT reagent HMT on the SiNCs (SiNC-HMT). C: Surface initiated RAFT polymerization from SiNC-HMT with styrene giving polystyrene grafted SiNCs (SiNC-gPS) and the free polymer which are separated *via* ultracentrifugation.

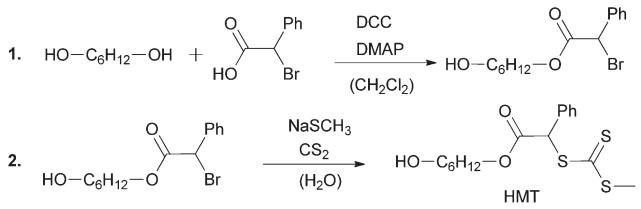

Scheme 2 Two-step synthesis of the RAFT reagent HMT.

next step, the SiNCs are hydrosilylated with chloro(dimethyl)-vinylsilane (ClDMVS), initiated by 4-decylbenzene diazonium tetrafluoroborate (4-DDB). By this way, SiNCs with a reactive chlorosilane surface (SiNC-SiCl) are formed which react under mild conditions with nucleophiles.[32]

The RAFT reagent was synthesized in a two-step reaction (Scheme 2). First, hexane-1,6-diol was acylated using α-bromo-phenylacetic acid and *N*,*N*′-dicyclohexylcarbodiimide (DCC) to yield 6-hydroxyhexyl 2-bromo-2-phenylacetate. In the second step, reaction with sodium methyl trithiocarbonate, formed *in situ* from sodium thiomethoxide and carbon disulfide, gives the RAFT reagent 6-hydroxyhexyl 3-(methylthio)-2-phenyl-3-thioxopropanoate (HMT).

To fixate the RAFT reagent on the SiNCs, HMT was added to a dispersion of SiNC-SiCl in toluene and then stirred overnight (Scheme 1B). The reaction is accelerated by a small amount of imidazole which acts as a base to trap the released HCl as well as the nucleophilic catalyst. Purification of the HMT functionalized SiNCs (SiNC-HMT) was performed *via* several precipitation/centrifugation steps from toluene with acetonitrile. The FTIR spectrum now shows the distinctive IR bands from HMT but lacking the O–H band at 3300 cm^{-1} since it is consumed during the formation of a silyl ether, which is apparent by the strong Si–O band around 1100 cm^{-1} (Fig. 1B and C). Also the Si–Me signal from the vinyldimethyl-silane surface groups can be found at 1260 cm^{-1}. Residual hydride is visible at 2100 cm^{-1} which is expected since the surface coverage cannot be complete due to steric hindrance.

Surface-initiated RAFT polymerization from SiNC-HMT

The polymerization was first performed with styrene. SiNC–HMT was dispersed in styrene and free RAFT reagent, ethyl 3-(methylthio)-2-phenyl-3-thioxopropanoate (EMPT) was then added (Scheme 1C). This is necessary to have enough RAFT reagents in the system to control the polymerization and obtain narrow size distributions of the polymers. The polymerization was performed at 110 °C which is a sufficient temperature for the self-initiation of styrene, so no additional radical initiator is needed. The reaction shows first order kinetic behaviour, which is expected for a living polymerization (Fig. 2).

Since the polymer formation is not restricted to the SiNC surface, in addition to grafted polymers free polymer chains are also formed in solution. Gel permeation chromatography (GPC) measurements of the crude polymerization product therefore show two species (Fig. 3A). The fraction which is

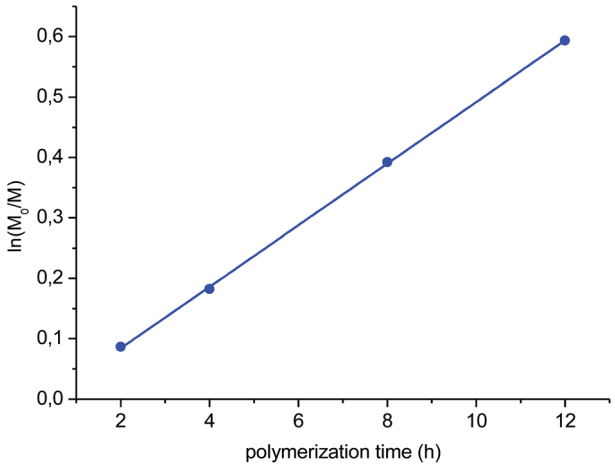

Fig. 2 Kinetic measurement of styrene polymerization in the presence of EMPT and SiNC-HMT. $\ln(M_0/M)$ is plotted against the polymerization time with M_0 being the monomer concentration at time 0 and M the concentration at time t. The concentrations were determined by ^{1}H NMR measurements.

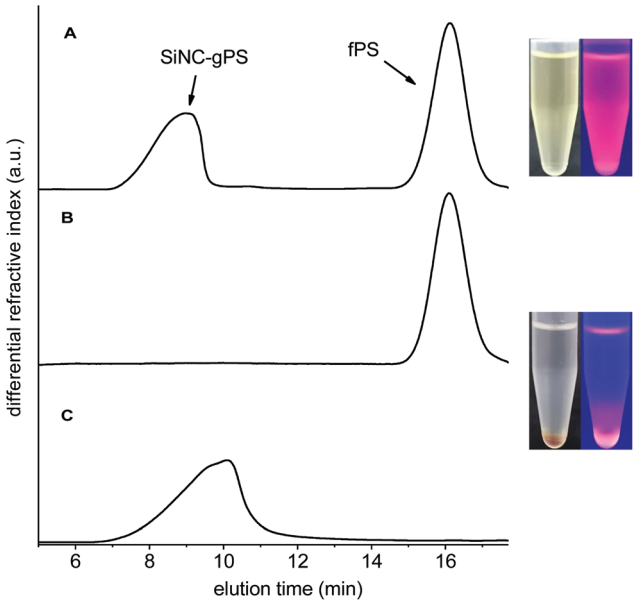

Fig. 3 GPC measurements of A: mixture of SiNC-gPS and fPS after polymerization for 2 h. B: fPS obtained from the supernatant of the ultracentrifugation. C: SiNC-gPS after 3 ultracentrifugation cycles. On the right side the centrifugation vials are depicted, under daylight (left) and irradiated by 365 nm UV-light (right). The sedimented SiNC-gPS are clearly visible after 8 h centrifugation at 200 000*g*.

eluted first has a broader signal and higher molecular weight than the second one with longer retention times. The first species is expected to be the SiNC grafted with polystyrene (SiNC-gPS) whereas the second ones are free polystyrene chains (fPS).

Ultracentrifugation has proven to be a versatile tool for the size separation of SiNCs.[33,34] Therefore, to isolate SiNC-gPS

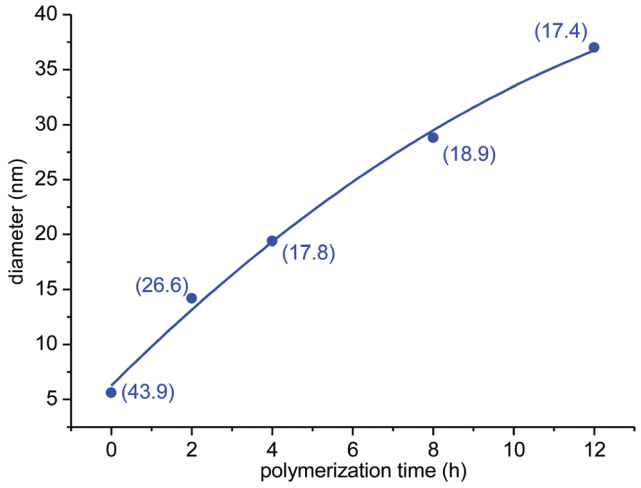

Fig. 4 DLS data of SiNC-HMT (0 h) and SiNC-gPS after 2, 4, 8 and 12 h polymerization time. The dispersities of the samples are given in brackets next to the data points as %PD.

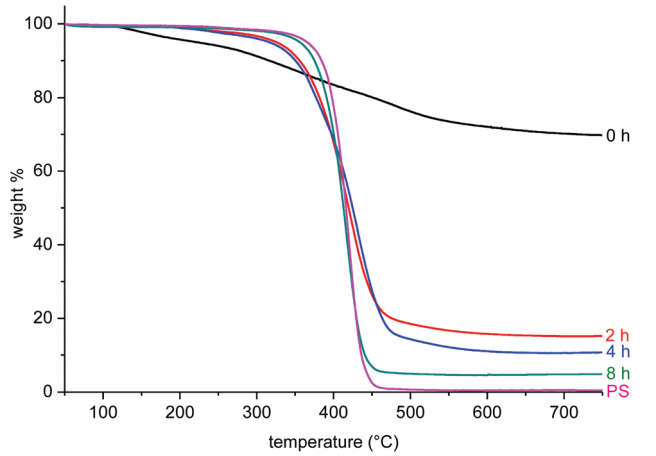

Fig. 5 TGA data of SiNC-HMT (0 h), SiNC-gPS after 2, 4 and 8 h polymerization time and polystyrene (PS).

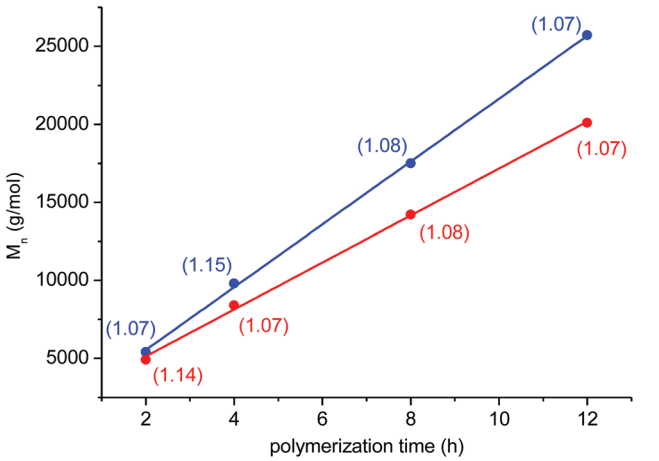

Fig. 6 Molecular masses and PDIs of PS grafted on SiNCs (blue) and PS which is formed in solution (red). The respective PDIs of the measurements are found in brackets next to the data points.

from fPS, ultracentrifugation was performed. The SiNC-gPS/fPS mixture was dispersed in THF and centrifuged at 200 000*g* for 8 h. Under these conditions, sedimentation of the SiNC-gPS is observed in contrast with the fPS which remains in the supernatant. With this method, a complete separation is achieved when the centrifugation was repeated for at least three times, which was confirmed by GPC measurements (Fig. 3B and C).

To determine the size of the separated SiNC-gPS, dynamic light scattering (DLS) measurements of dilute THF dispersions were done (Fig. 4). A steady increase of the hydrodynamic diameter is observed from 5.6 nm for the SiNC-HMT at 0 h to 37 nm after 12 h polymerization time. The size distribution is comparably narrow with around 18% PD after 4, 8 and 12 h polymerization times. For shorter reaction times, the dispersity is found to be higher, which could be due to particle interactions.

Additionally, thermogravimetric analysis (TGA) of the purified SiNC-gPS was performed (Fig. 5). As expected, an increasing weight loss is observed with progressing polymerization time.

TEM measurements of the SiNC-gPS were also done. However, due to the low electron density of the SiNC core and the comparably thick polymer coating, no satisfactory results could be obtained.

To obtain a closer insight into the polymer bound on the SiNCs, the polystyrene chains of the separated SiNC-gPS were cleaved from the SiNCs and compared to the free polymer in solution. This was achieved by dispersing the SiNC-gPS in THF with a small amount of concentrated aqueous ammonia solution, since under these conditions, the SiNC core gets dissolved. Both the cleaved polymer and the free polymer show linear growth and possess narrow PDIs (Fig. 6). The polymer chains bound on the SiNCs have slightly higher molecular weights than the ones formed in solution. This behaviour has been observed before with surface initiated RAFT polymerizations.[31]

The polymer on the SiNCs can behave as an effective protective layer for the silicon core against oxidation. This is demonstrated with glass capillaries coated by a thin film SiNC-gPS (Fig. 7A) or SiNCs that are hydrosilylated with only a monolayer of 1-dodecene (Fig. 7B) respectively. When immersed into aqueous KOH (5 M), the photoluminescence of dodecyl terminated SiNCs disappears and an immediate gas evolution is observed due to the dissolution of silicon. The SiNC-gPS coating however emits bright photoluminescence even after a week.

To show the broad applicability of this polymerization method, monomers hexyl acrylate (HAC), methyl methacrylate (MMA), *N*-isopropylacrylamide (NIPAM) and 4-vinylbenzyl chloride polymerized on the SiNCs (Fig. 8).

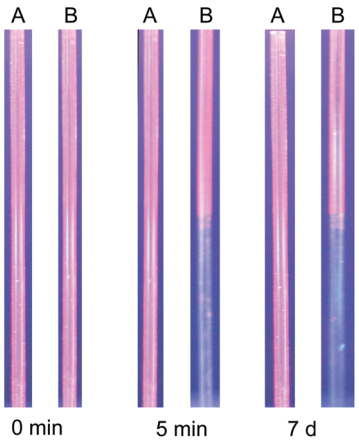

Fig. 7 Glass capillaries under 365 nm UV radiation, coated with A: SiNC-gPS (12 h polymerization time) and B: SiNCs hydrosilylated with 1-dodecene. The capillaries were half-immersed into 5 M aqueous KOH. 1-Dodecene functionalized SiNCs are dissolved by KOH, apparent by the disappearance of the photoluminescence, whereas SiNC-gPS are stable for more than a week under the given conditions.

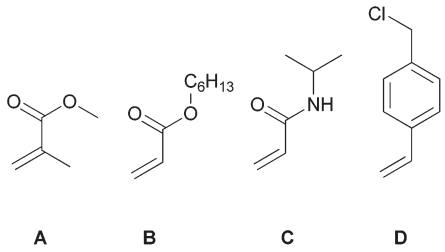

Fig. 8 Additional monomers used for the grafting on SiNCs. A: methyl methacrylate (MMA), B: hexyl acrylate (HAC), C: *N*-isopropylacrylamide (NIPAM), D: 4-vinylbenzyl chloride (4-VBCl).

Grafting was successful in every case as well as the separation of free polymers from functionalized particles *via* ultracentrifugation. GPC and DLS data of the obtained materials are given in Table 1.

The photoluminescence of the SiNC core does not change by the polymer grafted on the surface. In every case the PL maximum is around 700 nm. The only exception is for particles functionalized with NIPAM. In this case the photoluminescence is slightly blue-shifted to 670 nm and a less intense second maximum is observed around 450 nm. This could be due to interactions with the amine functionalities of the PNIPAM chains since amines are known to cause a blue shift in the PL of SiNCs (Fig. 9).[35]

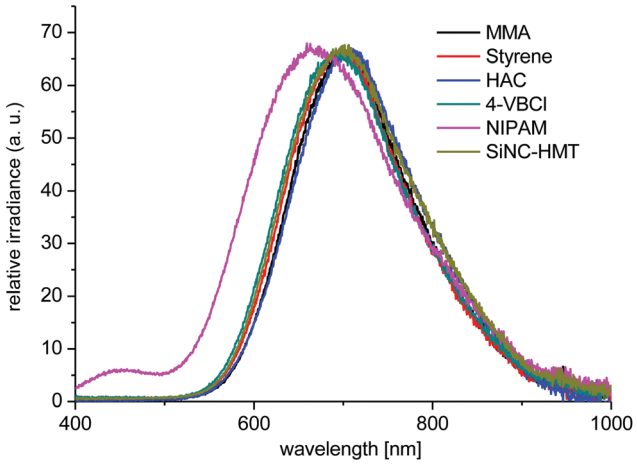

Fig. 9 PL spectra of SiNCs-HMT grafted with MMA, styrene, HAC, 4-VBCl, NIPAM and ungrafted SiNC-HMT.

3. Experimental

General information

All reactions were carried out under an argon atmosphere using standard Schlenk or glovebox techniques. Unless otherwise stated, all chemicals were purchased from Sigma-Aldrich, Acros Organics or ABCR and used as received. Toluene, dichloromethane, tetrahydrofuran and ether were dried using an MBraun SPS-800 solvent purification system. Styrene, 4-vinylbenzyl chloride, methyl methacrylate and hexyl acrylate were passed through a neutral alumina column and *N*-isopropylacrylamide was recrystallized from hexane–toluene (9 : 1) prior to use. Fourier transform infrared (FTIR) spectra were recorded with a Bruker Vertex 70 FTIR using a Platinum ATR from Bruker. Nuclear magnetic resonance (NMR) spectra were

Table 1 GPC and DLS data for SiNCs grafted with styrene, MMA, HAC, NIPAM and 4-VBCl

Monomer	Polymerization time (h)	Monomer conversion (%)	M_n grafted polymer (g mol^{-1})	PDI grafted polymer	M_n free polymer (g mol^{-1})	PDI free polymer	Hydrodynamic diameter (nm)	Dispersity (%PD)
Styrene	2	8	5400	1.07	4900	1.14	14.2	26.6
Styrene	4	17	9900	1.15	8400	1.07	19.4	17.8
Styrene	8	32	17 500	1.08	14 300	1.08	28.8	18.9
Styrene	12	45	25 700	1.07	20 100	1.07	37.0	17.4
MMA	7.5	25	50 800	1.12	28 900	1.18	38.0	32.7
HAC	5	29	46 400	1.09	42 100	1.05	30.6	47.3
NIPAM	23	24	24 700	1.24	18 600	1.11	23.8	55.4
4-VBCl	26	28	49 100	1.38	36 700	1.28	38.4	26.1

recorded on a Bruker ARX-300 in deuterated chloroform at 300 K. Dynamic light scattering measurements were made with a DynaPro NanoStar from Wyatt with toluene as the solvent. The DynaPro NanoStar possesses one 90° angle and was used in batch mode with a quartz cuvette. Photoluminescence (PL) spectra were recorded with an Avantes AvaSpec 2048 using a Prizmatix (LED current controller) as a light source. TGA measurements were carried out on a Texas Instruments TGA-Q5000 with a heating rate of 10 K min^{-1} under an argon atmosphere. GPC was measured on a Varian LC-920 equipped with two PL PolarGel columns with THF or DMF as the eluent. Absolute molecular weights were determined online by multiangle light scattering (MALS) analysis using a Wyatt Dawn Heleos II in combination with a Wyatt Optilab rEX as the concentration source. Ultracentrifugation was performed with a Sorvall MX 150+ micro-ultracentrifuge from Thermo Scientific with a 255-A2 2058 rotor.

Synthetic procedures

Synthesis of RAFT reagent HMT. First step: α-bromophenylacetic acid (5.38 g, 25.0 mmol, 1.0 eq.), 1,6-hexanediol (11.82 g, 100 mmol, 4.0 eq.) and DMAP (0.27 g, 2.25 mmol) were dissolved in 750 mL dry dichloromethane. The mixture was cooled to 15 °C in an ice/water bath and then DCC (5.67 g, 27.5 mmol, 1.1 eq.) dissolved in 40 mL dry dichloromethane was added dropwise to the solution over a period of 90 min. The reaction was stirred overnight at room temperature. The resulting precipitate was removed by filtration and the solvent was removed under reduced pressure. The crude product was purified by column chromatography with silica gel using a mixture of *n*-hexane and ethyl acetate (2 : 1) as an eluent to yield the desired product as a transparent liquid (5.85 g, 74% yield). ^{1}H NMR (300 MHz, $CDCl_3$) δ [ppm] = 7.58–7.50 (m, 2H, Ar*H*), 7.41–7.32 (m, 3H, Ar*H*), 5.34 (s, 1H, PhC*H*Br), 4.18 (td, J = 6.5, 1.8 Hz, 2H, CH_2OCO), 3.62 (t, J = 6.5 Hz, 2H, HOCH_2), 1.77–1.15 (m, 8H, CH_2). ^{13}C NMR (75 MHz, $CDCl_3$) δ [ppm] = 168.5, 136.0, 129.4, 128.9 (2C), 128.8 (2C), 66.5, 62.9, 47.1, 32.7, 28.5, 25.6, 25.4. EA calculated for $C_{14}H_{19}BrO_3$: C, 53.35; H 6.08. Found C, 53.67; H 6.16.

Second step: carbon disulfide (4.35 g, 57.1 mmol, 6.0 eq.) was added to a mixture of sodium thiomethoxide (3.34 g, 47.6 mmol, 5.0 eq.) in water (15 mL) at room temperature. The biphasic reaction was vigorously stirred for 2 h and then 6-hydroxyhexyl-2-bromophenylacetate (3.00 g, 9.52 mmol, 1.0 eq.) was added dropwise over a period of 15 min. The reaction mixture was heated to 60 °C for 6 h. Then the reaction mixture was extracted with dichloromethane (2 × 30 mL). The combined organic layers were washed with brine (3 × 50 mL), dried over anhydrous sodium sulfate and the solvent removed under reduced pressure. The crude product was purified by column chromatography with silica gel using a mixture of ethyl acetate and *n*-hexane (3 : 2) as an eluent to yield the desired product as a yellow liquid (2.03 g, 60% yield). ^{1}H NMR (300 MHz, $CDCl_3$) δ [ppm] = 7.47–7.41 (m, 2H, Ar*H*), 7.40–7.33 (m, 3H, Ar*H*), 5.81 (s, 1H, PhC*H*S), 4.31–4.04 (m, 2H, CH_2OCO), 3.63 (t, J = 6.5 Hz, 2H, HOCH_2), 2.75 (s, 3H, SCH_3), 1.72–1.22 (m, 8H, CH_2). ^{13}C NMR (75 MHz, $CDCl_3$) δ [ppm] = 222.7, 169.1, 133.3, 129.1 (2C), 129.0, 128.9 (2C), 66.3, 62.9, 58.4, 32.7, 28.5, 25.7, 25.4, 20.4. EA calculated for $C_{16}H_{22}O_3S_3$: C, 53.60; H, 6.19. Found: C, 53.31; H, 6.29.

Synthesis of free RAFT reagent EMPT. EMPT was synthesized following the literature procedure.[31]

Preparation of hydride terminated SiNCs. SiNCs for this work were prepared following the literature procedure.[32]

Synthesis of SiNC-HMT. Hydride terminated SiNCs obtained from etching of 500 mg SiNC/SiO_2 composite were dispersed in a solution of toluene (1.5 mL) and chloro(dimethyl)vinylsilane (0.5 mL, 3.7 mmol). The yellow dispersion was degased by three freeze–pump–thaw cycles and the hydrosilylation reaction was initiated with 4-decylbenzene diazonium tetrafluoroborate (4-DDB) (5 mg, 15.5 μmol). After 4 h, the solvent was removed and the obtained SiNC-SiCl were dispersed in 1.7 mL toluene, and HMT (50 mg 140 μmol) dissolved in 0.3 mL of toluene was added followed by imidazole (5.0 mg, 70 μmol). The mixture was stirred overnight and subsequently precipitated with acetonitrile and centrifuged. The precipitate was redispersed in a small amount of toluene, again precipitated with acetonitrile, centrifuged and then freeze dried from benzene.

Preparation of SiNC-gPS. SiNC-HMT (10 mg) was dispersed in styrene (2.0 mL, 17.5 mmol, 1000 eq.) along with free RAFT reagent EMPT (5.0 mg, 1 eq.). The clear yellow solution was degased by three freeze–pump–thaw cycles and heated to 110 °C. After the predetermined polymerization time, the mixture was precipitated from methanol and the resulting SiNC–gPS/fPS mixture was freeze-dried from methanol. To separate SiNC-gPS from fPS, 20–30 mg of the mixture was dissolved in 1.5 mL THF and centrifuged for 8 h at 200 000*g* (54 900 rpm). The colourless supernatant containing fPS was removed and the yellow SiNC-gPS fraction was redispersed in THF. The centrifugation/redispersion step was repeated at least 2 more times until no fPS could be detected *via* GPC.

Preparation of SiNC grafted with other monomers. SiNC-HMT (10 mg) was dispersed in the respective monomers MMA, HAC or 4-VBCl (17.5 mmol, 1000 eq.) with EMPT (5 mg, 17.5 μmol, 1 eq.) and AIBN (0.57 mg, 3.5 μmol, 0.2 eq.). For NIPAM (988 mg, 8.73 mmol, 500 eq.) a solution in THF (2 mL) was used. The mixtures were degassed *via* three freeze–pump–thaw cycles and heated to 60 °C. After the predetermined polymerization time, the grafted SiNCs were precipitated from methanol in the case of 4-VBCl or from pentane for MMA, HAC and NIPAM. Separation from grafted SiNCs and free polymers was performed with styrene as described above *via* ultracentrifugation.

Liberation of grafted polymer from SiNCs. SiNCs grafted with polymer (10 mg) were dispersed in THF (1 mL) and a small amount of concentrated aqueous ammonia was added. The mixture was ultrasonicated for 30 min and stirred overnight. Afterwards, THF and ammonia are evaporated and the obtained free polymer is dissolved in THF (styrene, MMA, HAC and 4-VBCl) or DMF (NIPAM) for GPC analysis.

Coating of glass capillaries. 1-Dodecene functionalized SiNCs were prepared following the literature procedure.[36] The respective SiNCs (5 mg) were dispersed in CH_2Cl_2 (0.1 mL) and a small amount of the dispersion was filled into a glass capillary (diameter 1 mm) *via* capillary rise. The capillary was gently shaken while allowing the solvent to evaporate to form a homogeneous SiNC film on the inside of the capillary.

4. Conclusions

In summary, we present an approach to synthesize defined photoluminescent SiNC-polymer hybrid materials *via* surface initiated RAFT polymerization of styrene. The reaction proceeds in a living manner and particles with narrow size distributions are obtained. We show that ultracentrifugation is a versatile tool to separate functionalized SiNCs from the dissolved free polymer. Films of the grafted SiNCs show high stability against oxidation. The grafting process was applied to various other monomers.

Acknowledgements

Prof. J. G. C. Veinot acknowledges funding from the Natural Sciences and Engineering Research Council of Canada (NSERC), Canada Foundation for Innovation (CFI), Alberta Science and Research Investment Program (ASRIP), and University of Alberta Department of Chemistry. I. M. D. Höhlein is grateful for scholarships from the Fonds der Chemischen Industrie (FCI).

Notes and references

1 Q. Sun, Y. A. Wang, L. S. Li, D. Wang, T. Zhu, J. Xu, C. Yang and Y. Li, *Nat. Photonics*, 2007, **1**, 717–722.
2 Y. Zhou, M. Eck and M. Krüger, *Energy Environ. Sci.*, 2010, **3**, 1851.
3 S. Ren, L.-Y. Chang, S.-K. Lim, J. Zhao, M. Smith, N. Zhao, V. Bulović, M. Bawendi and S. Gradecak, *Nano Lett.*, 2011, **11**, 3998–4002.
4 A. Y. Nazzal, L. Qu, X. Peng and M. Xiao, *Nano Lett.*, 2003, **3**, 819–822.
5 X. Michalet, F. F. Pinaud, L. a. Bentolila, J. M. Tsay, S. Doose, J. J. Li, G. Sundaresan, a M. Wu, S. S. Gambhir and S. Weiss, *Science*, 2005, **307**, 538–544.
6 J. Liu, F. Erogbogbo, K.-T. Yong, L. Ye, J. Liu, R. Hu, H. Chen, Y. Hu, Y. Yang, J. Yang, *et al.*, *ACS Nano*, 2013, **7**, 7303–7310.
7 X. Li, Y. He, S. S. Talukdar and M. T. Swihart, *Langmuir*, 2003, **19**, 8490–8496.
8 C. M. Hessel, E. J. Henderson and J. G. C. Veinot, *Chem. Mater.*, 2006, **18**, 6139–6146.
9 J. M. Lauerhaas and M. J. Sailor, *Science*, 1993, **261**, 1567–1568.
10 R. D. Tilley, J. H. Warner, K. Yamamoto, I. Matsui and H. Fujimori, *Chem. Commun.*, 2005, 1833–1835.
11 S. Niesar, W. Fabian, N. Petermann, D. Herrmann, E. Riedle, H. Wiggers, M. S. Brandt and M. Stutzmann, *Green Chem.*, 2011, **1**, 339–350.
12 F. Maier-Flaig, J. Rinck, M. Stephan, T. Bocksrocker, M. Bruns, C. Kübel, A. K. Powell, G. A. Ozin and U. Lemmer, *Nano Lett.*, 2013, **13**, 475–480.
13 C. M. Gonzalez, M. Iqbal, M. Dasog, D. G. Piercey, R. Lockwood, T. M. Klapötke and J. G. C. Veinot, *Nanoscale*, 2014, **6**, 2608–2612.
14 Y. Zhong, F. Peng, F. Bao, S. Wang, X. Ji, L. Yang, Y. Su, S.-T. Lee and Y. He, *J. Am. Chem. Soc.*, 2013, **135**, 8350–8356.
15 J. A. Kelly and J. G. C. Veinot, *ACS Nano*, 2010, **4**, 4645–4656.
16 T. K. Purkait, M. Iqbal, M. H. Wahl, K. Gottschling, C. M. Gonzalez, M. A. Islam and J. G. C. Veinot, *J. Am. Chem. Soc.*, 2014, **136**, 17914–17917.
17 I. M. D. Höhlein, A. Angı, R. Sinelnikov, J. G. C. Veinot and B. Rieger, *Chem. – Eur. J.*, 2015, **21**, 2755–2758.
18 C. Yang, R. A. Bley, S. M. Kauzlarich and H. W. H. Lee, *J. Am. Chem. Soc.*, 1999, **121**, 5191–5195.
19 R. D. Tilley and K. Yamamoto, *Adv. Mater.*, 2006, **18**, 2053–2056.
20 Z. Yang, M. Dasog, A. R. Dobbie, R. Lockwood, Y. Zhi, A. Meldrum and and J. G. C. Veinot, *Adv. Funct. Mater.*, 2014, **24**, 1345–1353.
21 J. Kehrle, I. M. D. Höhlein, Z. Yang, A.-R. Jochem, T. Helbich, T. Kraus, J. G. C. Veinot and B. Rieger, *Angew. Chem., Int. Ed.*, 2014, **53**, 12494–12497.
22 C. M. Hessel, M. R. Rasch, J. L. Hueso, B. W. Goodfellow, V. a. Akhavan, P. Puvanakrishnan, J. W. Tunnel and B. a. Korgel, *Small*, 2010, **6**, 2026–2034.
23 M. X. Dung, J.-K. Choi and H.-D. Jeong, *ACS Appl. Mater. Interfaces*, 2013, **5**, 2400–2409.
24 F. Erogbogbo, K. Yong, I. Roy, R. Hu, W. Law, W. Zhao, H. Ding, F. Wu, R. Kumar, M. T. Swihart, *et al.*, *ACS Nano*, 2011, **5**, 413–423.
25 J. Chiefari, Y. K. B. Chong, F. Ercole, J. Krstina, J. Jeffery, T. P. T. Le, R. T. A. Mayadunne, G. F. Meijs, C. L. Moad, G. Moad, *et al.*, *Macromolecules*, 1998, **9297**, 5559–5562.
26 J. Cui, W. Wang, Y. You, C. Liu and P. Wang, *Polymer*, 2004, **45**, 8717–8721.
27 P. Takolpuckdee, J. Westwood and D. M. Lewis, *Macromolecules*, 2004, **37**, 2709–2717.
28 D. Roy and J. T. Guthrie, *Macromolecules*, 2005, **38**, 10363–10372.
29 H. Skaff and T. Emrick, *Angew. Chem., Int. Ed.*, 2004, **43**, 5383–5386.
30 J. W. Hotchkiss, A. B. Lowe and S. G. Boyes, *Chem. Mater.*, 2007, **19**, 6–13.
31 K. Ohno, Y. Ma, Y. Huang, C. Mori, Y. Yahata, Y. Tsujii, T. Maschmeyer and J. Moraes, *Macromolecules*, 2011, **44**, 8944–8953.

32 I. M. D. Höhlein, J. Kehrle, T. K. Purkait, J. G. C. Veinot and B. Rieger, *Nanoscale*, 2015, **7**, 914–918.
33 J. B. Miller, A. R. Van Sickle, R. J. Anthony, D. M. Kroll, U. R. Kortshagen and E. K. Hobbie, *ACS Nano*, 2012, **6**, 7389–7396.
34 M. L. Mastronardi, F. Hennrich, E. J. Henderson, F. Maier-Flaig, C. Blum, J. Reichenbach, U. Lemmer, C. Kübel, D. Wang, M. M. Kappes and G. A. Ozin, *J. Am. Chem. Soc.*, 2011, **133**, 11928–11931.
35 M. Dasog, G. B. De Los Reyes, L. V. Titova, F. A. Hegmann and J. G. C. Veinot, *ACS Nano*, 2014, **8**, 9636–9648.
36 I. M. D. Höhlein, J. Kehrle, T. Helbich, Z. Yang, J. G. C. Veinot and B. Rieger, *Chem. – Eur. J.*, 2014, **20**, 4212–4216.

9 Summary and Outlook

In the first project of the PhD-thesis, diazonium salts were established as efficient radical initiators for the hydrosilylation of SiNCs with alkenes and alkynes (Scheme 9.1). The reaction proceeds under very mild conditions and with short reaction times. Novel diazonium compounds, highly soluble in nonpolar organic solvents were synthesized for this purpose.

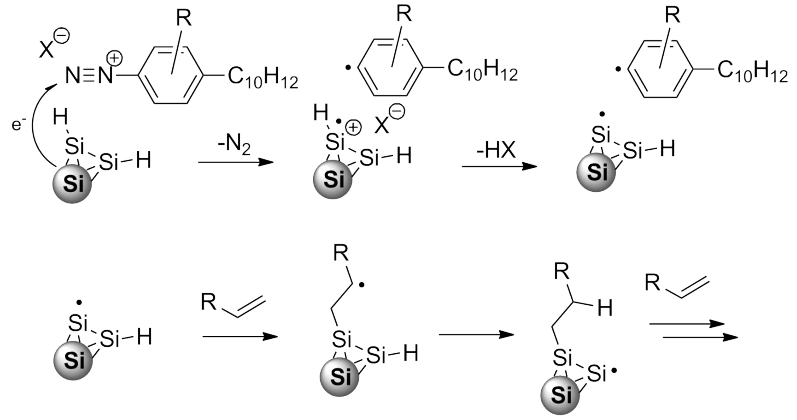

Scheme 9.1: Reaction scheme for the diazonium salt initiated hydrosilylation reaction of SiNCs.[121]

The next project took advantage of the diazonium initiated hydrosilylation to react hydride terminated SiNCs with chlorodimethyl(vinyl)silane. By this way, SiNCs with chlorosilane surface groups were obtained (Scheme 9.2). These particles are highly reactive towards nucleophiles and allow the functionalization with alcohols, silanols and organolithium reagents while widely retaining their photoluminescence properties. As a side reaction, it was observed that organolithium reagents can directly react with the silicon surface of the particles.

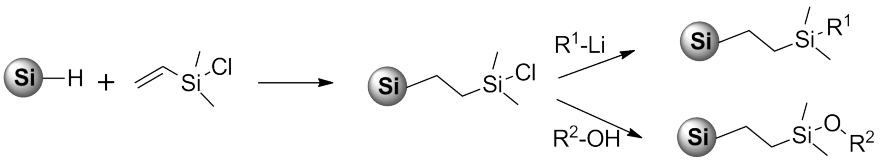

Scheme 9.2: Chlorosilanes as reactive binding layer for nucleophiles on hydride terminated SiNCs.[122]

The finding that organolithium reagents react with the surface of SiNCs was further investigated in the third project. Hydride terminated SiNCs were reacted with several organolithium compounds. The reaction is proposed to proceed *via* breaking of Si–Si bonds and formation of a Si–Li surface species (Scheme 9.3). SiNCs with mixed surfaces are obtained when the Si–Li group is quenched with electrophiles. Si–H groups are not consumed in the reaction, this allows even further functionalization by hydrosilylation.

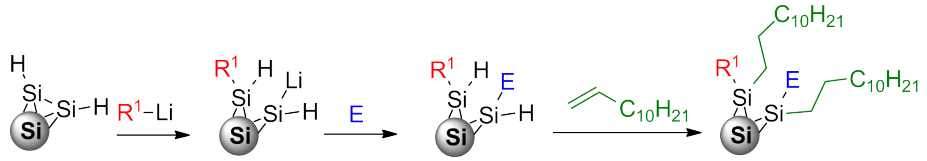

Scheme 9.3: Reactivity of organolithium reagents towards hydride terminated SiNCs and subsequent quenching with electrophiles (E) and hydrosilylation of residual Si–H groups. [123]

In the last project, a novel RAFT reagent was bound on chlorosilane terminated SiNCs. This allowed the polymerization of various monomers from the SiNC surface (Scheme 9.4). The polymerization proceeds in a living manner and defined core-shell particles were obtained. Ultracentrifugation was found to be a suitable tool to purify the functionalized SiNCs from unbound polymer. The particles show high stability against oxidation in contrast to conventional hydrosilylated SiNCs. It is the first report in literature of freestanding photoluminescent SiNCs with a defined polymer shell.

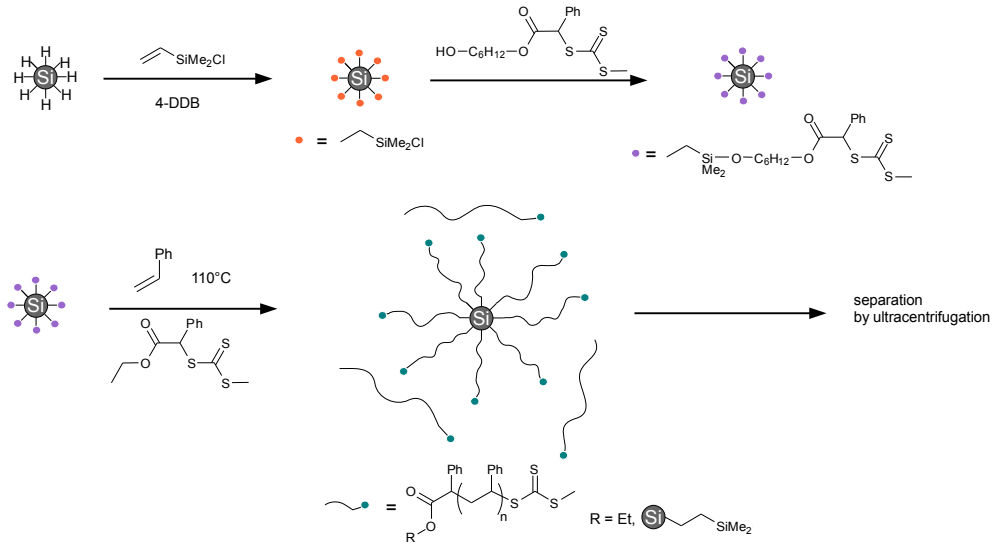

Scheme 9.4: Reaction scheme for the RAFT polymerization of styrene on SiNCs with subsequent purification *via* ultracentrifugation.

The chemistry presented in this PhD thesis paves the way for following chemical approaches to functionalize the surface of nanomaterials. Since the diazonium salt initated hydrosilylation has proven itself as a valuable tool for the reaction with hydride terminated SiNCs, it would be interesting if this approach can also be used for other nanomaterials such as silicon nanosheets or germanium nanocrystals.

SiNCs with a chlorosilane surface could be suitable for reaction with silanol terminated polysiloxanes. In this process stable Si–O–Si bonds are formed and novel hybrid materials would be obtained with photoluminescent SiNCs covalently attached to a siloxane matrix. This could be of use in gas sensoring applications since polysiloxanes are highly gas permeable. [124]

The organolithium chemistry offers the opportunity to functionalize SiNCs with conjugated organic molecules, oligomers and polymers. Of great interest is the question how the electronic and optical properties of SiNCs change with such a treatment since a photoluminescence shift has already been observed at the reaction with lithiated phenylacetylene. [122, 123] It is possible that conjugated organic surface groups could enhance the exchange of charge carriers from or to the particles and therefore improve their properties in applications such as solar cells.

The RAFT polymerization process on SiNCs could be transferred to other surface initiated polymerization methods like atom transfer radical polymerization (ATRP) or nitroxide mediated polymerization (NMP), therefore increasing the monomer spectrum. Also more complex polymer structures could be created, such as block copolymers. Of special interest would be polar, water soluble polymers since the defined sizes of the obtained core-shell particles are advantageous for biomedical applications.

10 Publications beyond the Scope of this Thesis

The paper "Thermoresponsive and Photoluminescent Hybrid Silicon Nanoparticles by Surface-Initiated Group Transfer Polymerization of Diethyl Vinylphosphonate" is based on previous work of our group about surface-initiated group transfer polymerization on bulk silicon surfaces.[125] We were able to transfer this approach to photoluminescent SiNCs to obtain polymer coated, water dispersible, thermoresponsive SiNC agglomerates.

A side project during my PhD was a cooperation with Prof. Katharina Krischer from the physics department at TU Munich. Diazopyridines were electrochemically grafted on a silicon surface to obtain a material which should supposedly be active for electrochemical CO_2 reduction. This behavior could not be observed, however the pyridine grafting on the silicon surface significantly lowered the overpotential for hydrogen evolution. These results were published in the paper "Activation of Silicon Surfaces for H_2 Evolution by Electrografting of Pyridine Molecules".

During my master thesis with Prof. Bernhard Rieger in 2012, I worked on the polymerization of fluorinated alkenes, such as trifluoropropene, with zirconocene catalysts. Polymerization attempts were not successful, however we observed a catalytic C-F activation of the fluorinated compounds and a subsequent reaction with the aromatic solvents. These findings were published in "Catalytic C–F Activation via Cationic Group IV Metallocenes".

The publication "A Robust Route towards Functionalized Pyrrolizidines as Precursors for *Daphniphyllum* Alkaloids" is a result of parts of the work during my bachelor thesis at Prof. Dirk Trauners Chair at the Ludwig-Maximilians-University, Munich in 2010.

10.1 Thermoresponsive and Photoluminescent Hybrid Silicon Nanoparticles by Surface-Initiated Group Transfer Polymerization of Diethyl Vinylphosphonate

Status	Published online: September 08, 2014
Journal	Angewandte Chemie, 2014, Volume 53, 12494-12497.
Publisher	Wiley-Blackwell
DOI	10.1002/anie.201405946
Authors	Julian Kehrle, Ignaz M. D. Höhlein, Zhenyu Yang, Aljosha-Rakim Jochem, Tobias Helbich, Tobias Kraus, Jonathan G. C. Veinot, Bernhard Rieger

abstract

We present a method to combine the functional features of poly(diethyl vinylphosphonate) (PDEVP) and photoluminescent silicon nanocrystals. The polymer–particle hybrids were synthesized in three steps through surfaceinitiated group transfer polymerization using $Cp_2YCH_2TMS(thf)$ as a catalyst. This pathway of particle modification renders the nanoparticle surface stable against oxidation. Although SiNC properties are known to be sensitive toward transition metals, the hybrid particles exhibit red photoluminescence in water. The temperature-dependent coiling of PDEVP results in a change of the hydrodynamic radius of the hybrid particles in water. To the best of our knowledge, this is the first example of controlled catalytic polymerization reactions on a silicon nanocrystal surface.

10.2 Activation of silicon surfaces for H_2 evolution by electrografting of pyridine molecules

Status	Published online: July 16, 2014
Journal	Surface Science, 2015, Volume 631, 185-189.
Publisher	Elsevier
DOI	10.1016/j.susc.2014.07.007
Authors	Qi Li, Konrad Schönleber, Patrick Zeller, Ignaz M. D. Höhlein, Bernhard Rieger, Joost Wintterlin, Katharina Krischer

abstract

In this work we describe an electrografting procedure for the preparation of pyridine-functionalized Si(111) surfaces, and we demonstrate that this modified surface reduces the overpotential for the hydrogen evolution reaction by about 400 mV compared to the H-terminated Si surface. Thus, evidence is presented that the functionalized Si surface has a catalytic activity for an inner sphere electrochemical reaction and might be an attractive alternative to metal or metal oxide cluster-covered semiconductors in photoelectrochemical devices converting solar energy into chemical energy.

10.3 Catalytic C–F activation via cationic group IV metallocenes

Status	Published online: December 16, 2014
Journal	Journal of Organometallic Chemistry, 2015, Volume 778, 21-28.
Publisher	Elsevier
DOI	10.1016/j.jorganchem.2014.12.011
Authors	Dominik Lanzinger, Ignaz M. D. Höhlein, Sebastian B. Weiß, Bernhard Rieger

abstract

The catalytic cleavage of sp^3 C–F bonds of 3,3,3-trifluoropropene (TFP) can be performed using cationic group IV metallocenes and an excess of triisobutylaluminum. The isobutyl adduct 1,1-difluoro-5-methyl-hex-1-ene (DFMH) as well as 3,3-(difluoroallyl)aromates (DFAArs) are formed in different ratios, depending on reaction conditions. The Friedel–Crafts type reaction of TFP and the aromatic solvent represents a new catalytic route toward DFAArs with different substituents (especially electron donors), such as alkyl groups. In-situ FTIR and ^{19}F NMR spectroscopy were used to gain closer insight into the different defluorination reactions. The influence of the central metal, the ligand structure, the aromatic solvent and the concentration of the reactants was investigated and mechanistic conclusions were drawn.

10.4 A Robust Route towards Functionalized Pyrrolizidines as Precursors for *Daphniphyllum* Alkaloids

Status	Published online: February 02, 2014
Journal	Synlett, 2014, Volume 25, 741-745.
Publisher	Thieme Medical Publishers
DOI	10.1055/s-0033-1340677
Authors	Michael Pangerl, Ignaz M. D. Höhlein, Dirk Trauner

abstract

A diastereoselective Fráter-Seebach-type alkylation provides access to a highly functionalized pyrrolizidine, which could serve as a key building block for the total synthesis of Daphniphyllum alkaloids, such as oldhamine A.

Bibliography

[1] *Nanotechnology: A Realistic Market Assessment - Overview*, NAN031F, bccResearch, **2014**, 2.

[2] H. S. Mansur, *Wiley Interdiscip. Rev.: Nanomed. Nanobiotechnol.* **2010**, *2*, 113–129.

[3] A. D. Yoffe, *Adv. Phys.* **2001**, *50*, 1–208.

[4] D. L. Klein, R. Roth, A. K. L. Lim, A. P. Alivisatos, P. L. McEuen, *Nature* **1997**, *389*, 699–701.

[5] M. C. Schlamp, X. G. Peng, A. P. Alivisatos, *J. Appl. Phys.* **1997**, *82*, 5837–5842.

[6] W. U. Huynh, J. J. Dittmer, A. P. Alivisatos, *J. Appl. Phys.* **2002**, *295*, 2425-2427.

[7] L. S. Li, A. P. Alivisatos, *Adv. Mater.* **2003**, *15*, 408–411.

[8] B. Dubertret, P. Skourides, D. J. Norris, V. Noireaux, A. H. Brivanlou, A. Libchaber, *Science* **2002**, *298*, 1759–1762.

[9] K. Bourzac, *Nature* **2013**, *493*, 283–129.

[10] J. G. C. Veinot, *Chem. Comm.* **2006**, 4160–4168.

[11] X. Cheng, S. B. Lowe, P. J. Reece, J. J. Gooding, *Chem. Soc. Rev.* **2014**, *20*, 2680–2700.

[12] F. Maier-Flaig, J. Rinck, M. Stephan, T. Bocksrocker, M. Bruns, C. Kübel, A. K. Powell, G. A. Ozin, , U. Lemmer, *Nano Lett.* **2013**, *13*, 475–480.

[13] X. H. Liu, L. Zhong, S. Huang, S. X. Mao, T. Zhu, J. Y. Huang, *ACS Nano* **2012**, *6*, 1522–1531.

[14] C. Liu, Z. C. Holman, U. R. Kortshagen, *Nano Lett.* **2009**, *9*, 449-452.

[15] S. K. Bux, R. G. Blair, P. K. Gogna, H. Lee, G. Chen, M. S. Dresselhaus, R. B. Kaner, J. P. Fleurial, *Adv. Funct. Mater.* **2009**, *19*, 2445–2452.

[16] C. M. Gonzalez, M. Iqbal, M. Dasog, P. D. G., R. Lockwood, T. M. Klapötke, Veinot, *Nanoscale* **2014**, *6*, 2608–2612.

[17] F. Erogbogbo, K. Yong, I. Roy, W. L. Rui Hu, W. Zhao, H. Ding, F. Wu, R. Kumar, M. T. Swihart, P. N. Prasad, *ACS nano* **2010**, *5*, 413–423.

[18] R. Freeman, I. Willner, *Chem. Soc. Rev.* **2012**, *41*, 4067–4085.

[19] J. M. Costa-Fernandez, R. Pereiro, A. Sanz-Medel, *Trends Anal. Chem.* **2006**, *25*, 207–218.

[20] I. N. Germanenko, S. Li, M. S. El-Shall, *J. Phys. Chem.* **2001**, *105*, 59-66.

[21] X. Zhang, X. Chen, S. Kai, H. Wang, J. Yang, F. Wu, Z. Chen, *Anal. Chem.* **2015**, DOI: 10.1021/ac504520g.

[22] K. Jackowska, P. Krysinski, *Anal. Bioanal. Chem.* **2013**, *405*, 3753–3771.

[23] A. Jäger-Waldau, *PV Status Report 2013*, European Commission, DG Joint Research Centre, **2013**, 25.

[24] W. Shockley, H. J. Queisser, *J. Appl. Phys.* **1961**, *32*, 510–519.

[25] E. Cho, S. Park, X. Hao, D. Song, G. Conibeer, S. Park, M. A. Green, *Nanotechnology* **2008**, *19*, 245201.

[26] A. De Vos, *J. Phys. D: Appl. Phys* **1980**, *13*, 839.

[27] *http://www.nrel.gov/ncpv/images/efficiency_chart.jpg*, NREL National Renewable Energy Laboratory, accessed 04.02.2015.

[28] R. J. Ellingson, M. C. Beard, J. C. Johnson, P. R. Yu, O. I. Micic, A. J. Nozik, A. Shabaev, A. L. Efros, *Nano Lett.* **2005**, *5*, 865-871.

[29] R. D. Schaller, M. Sykora, S. Jeong, V. I. Klimov, *J. Phys. Chem. B* **2006**, *5*, 865-871.

[30] M. C. Beard, K. P. Knutsen, P. Yu, J. M. Luther, Q. Song, W. K. Metzger, R. J. Ellingson, A. J. Nozik, *Nano Lett.* **2007**, *7*, 2506-2512.

[31] E. Klampaftis, D. Rossand, K. R. McIntosh, B. S. Richards, *Sol. Energ. Mat. Sol. Cells* **2009**, *93*, 1182–1194.

[32] J. Kelly, J. G. C. Veinot, *ACS Nano* **2010**, *4*, 4645–4656.

[33] X. Pi, L. Zhang, D. Yang, *J. Phys. Chem. C* **2012**, *116*, 21240–21243.

[34] K. Cheng, R. Anthony, U. R. Kortshagen, R. J. Holmes, *Nano Lett.* **2010**, *10*, 1154–1157.

[35] D. P. Puzzo, E. J. Henderson, M. G. Helander, Z. Wang, G. A. Ozin, Z. Lu, *Nano Lett.* **2011**, *11*, 1585–1590.

[36] K. Cheng, R. Anthony, U. R. Kortshagen, , R. J. Holmes, *Nano Lett.* **2011**, *11*, 1952–1956.

[37] R. J. Anthony, K. Cheng, Z. C. Holman, R. J. Holmes, U. R. Kortshagen, *Nano Lett.* **2012**, *12*, 2822–2825.

[38] F. Maier-Flaig, J. Rinck, M. Stephan, T. Bocksrocker, M. Bruns, C. Kübel, A. K. Powell, G. A. Ozin, U. Lemmer, *Nano Lett.* **2013**, *13*, 475–480.

[39] B. S. Mashford, M. Stevenson, Z. Popovic, C. Hamilton, Z. Zhou, C. Breen, J. Steckel, V. Bulovic, M. Bawendi, S. Coe-Sullivan, P. T. Kazlas, *Nature Photonics* **2013**, *7*, 407–412.

[40] P. Pust, V. Weiler, C. Hecht, A. Tücks, A. S. Wochnik, A.-K. Henß, D. Wiechert, C. Scheu, P. J. Schmidt, W. Schnick, *Nat. Mat.* **2012**, *13*, 891–896.

[41] U. Rensch-Genger, M. Grabolle, S. N. Cavaliere-Jaricot, T. Roland Nann, *Nature Methods* **2008**, *5*, 763–775.

[42] M. A. Walling, J. A. Novak, J. R. E. Shepard, *Int. J. Mol. Sci.* **2009**, *10*, 441–491.

[43] C. Kirchner, T. Liedl, S. Kudera, T. Pellegrino, A. Muñoz Javier, H. Gaub, S. Stolzle, N. Fertig, W. Parak, *Nano Lett.* **2005**, *5*, 331–338.

[44] Z. F. Li, E. Ruckenstein, *Nano Lett.* **2004**, *4*, 1463–1467.

[45] R. D. Tilley, K. Yamamoto, *Adv. Mater.* **2006**, *18*, 2053–2056.

[46] B. A. Manhat, A. L. Brown, L. A. Black, J. B. A. Ross, K. Fichter, T. Vu, E. Richman, A. M. Goforth, *Chem. Mater.* **2011**, *23*, 2407–2418.

[47] E. J. Henderson, A. J. Shuhendler, P. Prasad, V. Baumann, F. Maier-Flaig, D. O. Faulkner, U. Lemmer, X. Y. Wu, G. A. Ozin, *small* **2011**, *7*, 2507–2516.

[48] F. Erogbogbo, K. Yong, I. Roy, G. Xu, P. N. Prasad, M. T. Swihart, *ACS Nano.* **2008**, *2*, 873–878.

[49] F. Erogbogbo, C. A. Tien, C. W. Chang, K. T. Yong, W. C. Law, H. Ding, I. Roy, M. T. Swihart, P. N. Prasad, *Bioconjugate Chem.* **2011**, *22*, 1081–1088.

[50] Z. Xu, D. Wang, M. Guan, X. Liu, Y. Yang, D. Wei, C. Zhao, H. Zhang, *Bioconjugate Chem.* **2012**, *4*, 3424–3431.

[51] J. Heitmann, *Grössenkontrollierte Herstellung von Silizium-Nanokristallen und ihre Charakterisierung*, Martin-Luther-Universität, Halle/Wittenberg, **2003**, 45.

[52] D. S. English, L. E. Pell, Z. Yu, P. F. Barbara, B. a. Korgel, *Nano Lett.* **2002**, *2*, 681–685.

[53] D. C. Hannah, J. Yang, P. Podsiadlo, M. K. Chan, A. Demortière, D. J. Gosztola, V. B. Prakapenka, G. C. Schatz, U. Kortshagen, , R. D. Schaller, *Nano Lett.* **2012**, *12*, 4200–4205.

[54] M. V. Wolkin, J. Jorne, P. M. Fauchet, G. Allan, C. Delerue, *Phys. Rev. Lett.* **1999**, *82*, 198.

[55] M. Dasog, G. B. De Los Reyes, L. V. Titova, F. A. Hegmann, J. G. C. Veinot, *ACS nano* **2014**, *8*, 9636–9648.

[56] J. Fuzell, A. Thibert, T. Atkins, M. M. Dasog, E. Busby, J. G. C. Veinot, S. Kauzlarich, D. S. M. Larsen, *J. Phys. Chem. Lett.* **2013**, *4*, 3806–3812.

[57] V. Švrček, J.-L. Rehspringer, E. Gaffet, A. Slaoui, J.-C. Muller, *Journal of Crystal Growth* **2005**, *275*, 589–597.

[58] T. D. Shen, C. C. Koch, T. L. McCormick, R. J. Nemanich, J. Y. Huang, J. G. Huang, *J. Mater. Res.* **1995**, *10*, 139.

[59] T. D. Shen, I. Shmagin, C. C. Koch, R. M. Kolbas, Y. Fahmy, L. Bergmann, R. J. Nemanich, M. T. McClure, Z. Sitar, M. X. Quan, *Phys. Rev. B* **1997**, *55*, 761.

[60] L. T. Canham, *Applied Physics Letters* **1990**, *57*, 1046.

[61] V. Lehmann, U. Gösele, *Applied Physics Letters* **1991**, *58*, 856.

[62] J. L. Heinrich, C. L. Curns, G. M. Credo, K. L. Kavanagh, M. J. Sailor, *Science* **1992**, *255*, 66–68.

[63] R. A. Bley, S. M. Kauzlarich, J. E. Davis, H. W. H. Lee, *Chem. Mater.* **1996**, *8*, 1881–1888.

[64] G. Belomoin, J. Therrien, a. Smith, S. Rao, R. Twesten, S. Chaieb, M. H. Nayfeh, L. Wagner, L. Mitas, *Applied Physics Letters* **2002**, *80*, 841.

[65] W. Cannon, S. Danforth, J. Flint, J. Haggerty, R. Marra, *J. Am. Ceram. Soc.* **1981**, *65*, 324–330.

[66] W. R. Cannon, S. C. Danforth, J. S. Haggerty, R. A. Marra, *J. Am. Ceram. Soc.* **1981**, *65*, 330–335.

[67] F. Huisken, B. Kohn, V. Paillard, *Appl. Phys. Lett.* **1999**, *74*, 3776.

[68] L. E. Brus, P. F. Szajowski, W. L. Wilson, T. D. Harris, S. Schuppler, P. H. Citrin, *J. Am. Chem. Soc* **1995**, *117*, 2915–2922.

[69] X. Li, Y. He, S. S. Talukdar, M. T. Swihart, *Langmuir* **2003**, *19*, 8490–8496.

[70] U. Kortshagen, *J. Phys. D. Appl. Phys.* **2009**, *42*, 113001.

[71] M. T. Swihart, *J. Phys. Chem. A.* **2000**, *104*, 6083.

[72] V. a. Schweigert, I. V. Schweigert, *J. Phys. D. Appl. Phys.* **1996**, *29*, 655–659.

[73] S. K. Friedlander, *Smoke, Dust and Haze - Fundamentals of Aerosol Dynamics*, 2., Oxford University Press, Oxford, **2000**, 338.

[74] L. Mangolini, E. Thimsen, U. Kortshagen, *Nano Lett.* **2005**, *5*, 655–9.

[75] G. Viera, M. Mikikian, E. Bertran, P. R. I. Cabarrocas, L. Boufendi, *J. Appl. Phys.* **2002**, *92*, 4684.

[76] M. Otobe, T. Kanai, T. Ifuku, H. Yajima, S. Oda, *J. Non-Cryst. Solids* **1996**, *198*, 875-878.

[77] J. D. Holmes, K. J. Ziegler, R. C. Doty, L. E. Pell, K. P. Johnston, B. A. Korgel, *J. Am. Chem. Soc* **2001**, *123*, 3743–3748.

[78] J. R. Heath, *Science* **1992**, *258*, 1131–1133.

[79] R. K. Baldwin, K. A. Pettigrew, E. Ratai, M. P. Augustine, S. M. Kauzlarich, *Chem. Comm.* **2002**, 1822–1823.

[80] N. Arul Dhas, C. P. Raj, A. Gedanken, *Chem. Mater* **1998**, 3278–3281.

[81] J. P. Wilcoxon, G. A. Samara, P. N. Provencio, *Phys. Rev. B: Condens. Matter Mater. Phys.* **1999**, *60*, 2704–2714.

[82] J. Wang, S. Sun, F. Peng, L. Cao, L. Sun, *Chem. Commun* **2011**, *47*, 4941–4943.

[83] X. Y. Cheng, R. Gondosiswanto, S. Ciampi, P. J. Reece, J. J. Gooding, *Chem. Commun* **2012**, *49*, 11874–11876.

[84] X. Cheng, S. B. Lowe, P. J. Reece, J. J. Gooding, *Chem. Soc. Rev.* **2014**, *43*, 2680–2700.

[85] R. A. Bley, S. M. Kauzlarich, *J. Am. Chem. Soc.* **1996**, *118*, 12461–12462.

[86] K. A. Pettigrew, Q. Liu, P. P. Power, S. M. Kauzlarich, *Chem. Mater.* **2003**, *15*, 4005–4011.

[87] E.-C. Cho, S. Park, X. Hao, D. Song, G. Conibeer, S.-C. Park, M. Green, *Nanotechnology* **2008**, *19*, 245201.

[88] I. Antonova, M. Gulyaev, E. Savir, J. Jedrzejewski, I. Balberg, *Phys. Rev. B* **2008**, *77*, 125318.

[89] C.-Y. Hsiao, C.-F. Shih, S.-H. Chen, W.-T. Jiang, *Thin Solid Films* **2011**, *519*, 5086-5089.

[90] H. M. Bank, M. E. Cifuentes, E. M. Theresa, *United States Pat.* **1991**, 5.010.159.

[91] J. Hummel, K. Endo, W. W. Lee, M. Mills, S. Q. Wang, *Low-Dielectric Constant Materials V*, The Materials Research Society, Warrendale PA, **1999**, Vol. 565.

[92] C. M. Hessel, E. J. Henderson, J. G. C. Veinot, *Chem. Mater.* **2006**, *18*, 6139-6146.

[93] C.-C. Yang, W.-C.Chen, *J. Mater. Chem.* **2002**, *12*, 1138-1141.

[94] C. M. Hessel, D. Reid, M. G. Panthani, M. R. Rasch, B. W. Goodfellow, J. Wei, H. Fujii, V. Akhavan, B. A. Korgel, *Chem. Mater.* **2012**, *24*, 393–401.

[95] Z. Yang, A. R. Dobbie, K. Cui, J. G. C. Veinot, *J. Am. Chem. Soc.* **2012**, *134*, 13958-13961.

[96] B. Marciniec, *Hydrosilylation*, 1, Springer, Dordrecht, **2009**, 3 ff.

[97] J. Buriak, *Chem. Rev.* **2002**, *102*, 1271-1308.

[98] J. Nelles, D. Sendor, A. Ebbers, F. M. Petrat, H. Wiggers, C. Schulz, S. Ulrich, *Colloid. Polym. Sci.* **2007**, *285*, 729-736.

[99] M. P. Stewart, J. M. Buriak, *J. Am. Chem. Soc.* **2001**, *123*, 7821–7830.

[100] J. Kelly, A. M. Shukaliak, M. D. Fleischauer, J. G. C. Veinot, *J. Am. Chem. Soc.* **2011**, *133*, 9564-9571.

[101] Q.-Y. Sun, L. C. P. M. De Smet, B. van Lagen, M. Giesbers, P. C. Thüne, J. van Engelenburg, F. A. de Wolf, H. Zuilhof, E. J. R. Sudhölter, *J. Am. Chem. Soc.* **2005**, *127*, 2514–2523.

[102] J. Cornelisse, *Chem. Rev.* **1993**, *93*, 615–669.

[103] Z. Yang, M. Dasog, A. R. Dobbie, R. Lockwood, Y. Zhi, A. Meldrum, J. G. C. Veinot, *Adv. Funct. Mater.* **2013**, *24*, 1345–1353.

[104] M. Dasog, Z. Yang, S. Regli, T. M. Atkins, A. Faramus, M. P. Singh, E. Muthuswamy, S. M. Kauzlarich, R. D. Tilley, J. G. C. Veinot, *ACS nano* **2013**, *7*, 2676–2785.

[105] S. Content, W. C. Trogler, M. J. Sailor, *Chem. Eur. J.* **2000**, *6*, 2205–2213.

[106] J. L. Speier, J. A. Webster, G. H. Barnes, *J. Am. Chem. Soc.* **1957**, *79*, 974–979.

[107] R. D. Tilley, J. H. Warner, K. Yamamoto, I. Matsuib, H. Fujimoric, *Chem. Comm.* **2005**, 1833–1835.

[108] J. H. Warner, A. Hoshino, K. Yamamoto, R. D. Tilley, *Angew. Chem. Int. Ed.* **2005**, *44*, 4550–4554.

[109] Z. Yang, M. H. Wahl, J. G. Veinot, *Can. J. Chem.* **2014**, *92*, 951–957.

[110] J. M. Holland, M. P. Stewart, M. J. Allen, J. M. Buriak, *J. Solid State Chem.* **1999**, *147*, 251–258.

[111] J. M. Buriak, M. P. Stewart, T. W. Geders, M. J. Allen, H. C. Choi, J. Smith, D. Raftery, L. T. Canham, *J. Am. Chem. Soc.* **1999**, *121*, 11491–11502.

[112] T. K. Purkait, M. Iqbal, M. H. Wahl, K. Gottschling, C. M. Gonzalez, M. A. Islam, J. G. C. Veinot, *J. Am. Chem. Soc.* **2014**, *136*, 17914–17917.

[113] L. Mangolini, U. Kortshagen, *Adv. Mater.* **2007**, *19*, 2513–2519.

[114] B. N. Jariwala, O. S. Dewey, P. Stradins, C. V. Ciobanu, S. Agarwal, *ACS Appl. Mater. Interfaces* **2011**, *3*, 3033–3041.

[115] C. S. Yang, R. A. Bley, S. M. Kauzlarich, H. W. H. Lee, G. R. Delgado, *J. Am. Chem. Soc.* **1999**, *121*, 5191–5195.

[116] E. Rogozhina, G. Belomoin, A. Smith, L. Abuhassan, N. Barry, O. Akcakir, P. V. Braun, M. H. Nayfeh, *Appl. Phys. Lett.* **2001**, *78*, 3711–3713.

[117] Y. Zhai, M. Dasog, R. B. Snitynsky, T. K. Purkait, M. Aghajamali, A. H. Hahn, C. B. Sturdy, T. L. Lowaryab, J. G. C. Veinot, *J. Mater. Chem. B* **2014**, *2*, 8427–8433.

[118] J. Zou, R. K. Baldwin, K. A. Pettigrew, S. M. Kauzlarich, *Nano Lett.* **2004**, *4*, 1181–1186.

[119] A. Shiohara, S. Hanada, S. Prabakar, K. Fujioka, T. H. Lim, K. Yamamoto, P. T. Northcote, R. D. Tilley, *J. Am. Chem. Soc.* **2010**, *132*, 248–253.

[120] L. Ruizendaal, S. P. Pujari, V. Gevaerts, J. M. J. Paulusse, H. Zuilhof, *Chem. Asian J.* **2011**, *6*, 2776-2786.

[121] I. M. D. Höhlein, J. Kehrle, T. Helbich, Z. Yang, J. G. C. Veinot, B. Rieger, *Chem. Eur. J.* **2014**, *15*, 4212–4216.

[122] I. M. D. Höhlein, J. Kehrle, T. K. Purkait, J. G. C. Veinot, B. Rieger, *Nanoscale* **2015**, *7*, 914-918.

[123] I. M. D. Höhlein, A. Angı, R. Sinelnikov, J. G. C. Veinot, B. Rieger, *Chem. Eur. J.* **2015**, *22*, 2775-2758.

[124] H. Moretto, M. Schulze, G. Wagner, *"Silicones" Ullmann's Encyclopedia of Industrial Chemistry*, Wiley-VCH Verlag GmbH & Co. KGaA, Weinheim, **2012**, 698 ff.

[125] N. Zhang, S. Salzinger, F. Deubel, R. Jordan, B. Rieger, *J. Am Chem. Soc.* **2012**, *134*, 7333–7336.